



NTNU – Trondheim
Norwegian University of
Science and Technology

Stability Analysis of Small Hydro Power Plants

Model Verification and Analysis of the
Impacts of the Voltage Regulation System

Ida Larsen Loen

Master of Energy and Environmental Engineering

Submission date: Januar 2014

Supervisor: Kjetil Uhlen, ELKRAFT

Co-supervisor: Trond Toftevaag, ELKRAFT

Norwegian University of Science and Technology
Department of Electric Power Engineering

Preface

This thesis is submitted in partial fulfillment of the requirements for the degree of Master of Science (M.Sc.) at the Norwegian University of Science and Technology (NTNU) in Trondheim. It is weighted with 30 credits on the final diploma.

My supervisor has been Professor Kjetil Uhlen to whom I would like to express my gratitude for his guidance and encouragement throughout the work presented in this report. Great thanks also go to Dinh Thuc Duon for valuable help with the simulation tools, for providing a very useful MATLAB code, and for assistance in the laboratory. Furthermore a great thanks is owed to Professor Trond Toftevaag for valuable information and advices.

Abstract

This master thesis concerns stability problems and protection related to small hydro distributed generation. Behavior related to the voltage regulator and the excitation limiters is the main focus in this report. The report consists of two main parts. Part one concerns laboratory studies with focus on the characteristics of the laboratory model, and system modeling and validation. In the other part of the thesis, the validated model is used to study the effect of the excitation limiters and their influence on the system response and performance. These studies are useful to obtain knowledge considering operation close to the power system limits.

The laboratory model considered in this thesis is a motor-generator set in the NTNU/SINTEF renewable energy laboratory, representing a small hydro power plant. The characteristics of this model are studied through laboratory measurements, and the system is modeled in Simulink and validated by laboratory testing. The final simulation model of the laboratory system has a response very similar to the actual model. The response of the simulation model has some deviations from the laboratory model, but these are considered small and it is concluded that the model is valid for further studies of excitation limiters for these master thesis.

Studies and measurements in the laboratory have given important information about the model and its characteristics and performance. The motor drive operating as a turbine governing system for the laboratory model does not seem to give a realistic representation of a hydraulic turbine governing system. The motor drive responds fast and efficient to disturbances, and contributes greatly to a well damped system with a high stability margin. The motor drive should respond more slowly to give a more realistic representation of the relatively slow response of hydro turbine governors. The excitation system parameters have a great influence on the behavior of the synchronous generator in the laboratory model. The details concerning the excitation system structure are partly unknown, which makes it challenging to find the exact parameters for the voltage regulator implemented in the Simulink model. The parameters found through studying the simulated response seems to be satisfying, as the voltage response of the simulation model is regulated similarly as for the laboratory model. For the cases evaluated in this report, the laboratory model seems to have better small signal stability characteristics when operating underexcited. Whether the stability margin is higher for under- or overexcited operation seems to depend on the characteristics of the generator.

The dynamic field current limiters implemented in the simulation model seem to be a close representation of the excitation limiters in the laboratory model. The limiters, controlled by PI controllers are activated as the field current has exceeded a given limit for a certain amount of time. The field current response in field current limiting operation mode depends on the proportional- and integral gain of the PI controller. It is shown that changes of these parameters affect the response significantly. Further studies are needed to draw any conclusions if, and for which cases, this can provoke instability when the field current limiters are activated.

Sammendrag

Denne masteroppgaven omhandler stabilitets problemer og vern relatert til distribusjonsnett med lokal kraftproduksjon. Stabilitetsproblemer relatert til spenningsregulering og feltstrømbegrensere er hovedfokus i denne oppgaven. Oppgaven består hovedsakelig av to deler. Den første delen omhandler studier i laboratorium, og implementering av en simuleringsmodell, med fokus på modell validering. I den andre delen av oppgaven blir den validerte simuleringsmodellen benyttet til studier av feltstrømbegrensere og deres innvirkning på systemets respons og ytelse, for å få kjennskap til hvordan systemet opererer nær sin stabilitetsgrense.

Laboratoriet for fornybar energi, tilhørende NTNU/SINTEF, består blant annet av en motor-generator modell som representerer et lite vannkraftverk. Denne modellen er implementert i Simulink og validert ved hjelp av målinger i laboratoriet. Den endelige simuleringsmodellen av systemet, viser en respons veldig nær responsen til laboratorium modellen. Simuleringsmodellen viser enkelte avvik, men disse betraktes som små, og modellen anses som godkjent for videre studier i denne oppgaven av magnetiseringssystem og feltstrømbegrensere.

Studier og målinger i laboratoriet har avdekket flere viktige egenskaper ved laboratorium modellen. Motordriften som representerer turbin og turbin regulator for laboratorium modellen, ser ikke ut til å være en realistisk representasjon av en vannturbin. Denne responderer fort ved forstyrrelser i systemet og bidrar effektivt til god demping og økt stabilitetsmargin. For å gjengi den relativt trege responsen til en vannturbinregulator, skulle motordriften ideelt sett hatt en tregere respons. Oppbygningen og parameterne i spenningsregulatoren har stor innvirkning på responsen til synkrongeneratoren i laboratorium modellen. Oppbygningen av magnetiseringssystemet er ikke kjent i detalj, noe som gjør det utfordrende å bestemme nøyaktige parametere for spenningsregulatoren. Parameterne som er funnet ved å studere responsen til simuleringsmodellen ser ut til å være tilfredsstillende, ettersom spenningsresponsen er regulert relativt likt som for laboratorium modellen. For tilfellene som er evaluert i denne oppgaven ser laboratorium modellen ut til å ha bedre småsignal stabilitets egenskaper når den opererer undermagnetisert. Om stabilitetsmarginen er høyere når generatoren opererer under- eller over magnetisert ser ut til å avhenge av generatorens egenskaper og parametere, og varierer derfor for ulike systemer.

De dynamiske feltstrømbegrensere som er implementert i simuleringsmodellen ser ut til å være en god representasjon for begrensere i laboratorium modellen. Feltstrømbegrensere som reguleres av PI regulatorer aktiveres dersom feltstrømmen er lavere enn sin nedre grense eller overstiger sin øvre grense. Feltstrøm responsen i feltstrømbegrensende modus avhenger av proporsjonal- og integral forsterkningen i PI regulatoren. Det er tydelig at endring av disse parameterne påvirker responsen i stor grad. Videre studier er nødvendig for å trekke noen konklusjon om, og eventuelt for hvilke tilfeller, aktivering av feltstrømbegrensere kan forårsake stabilitetsproblemer for systemet.

List of symbols

Symbol	Explanation	Unit
D_d	Damping coefficient	Nms
E_{fd}	Output field voltage from field-generator	V
E_f	Field voltage	V
E'	Transient excitation voltage	V
f_s	Synchronous frequency	Hz
H	Inertia constant	W/Vas
I_f	Field current	A
J	Moment of inertia	Kgm ²
P(PID)	Voltage regulator gain (proportional gain)	-
D(PID)	Derivate gain, PID-regulator	-
I(PID)	Integral gain, PID-regulator	-
n_r	Rotor rotational speed	rpm
n_s	Synchronous speed	rpm
p	Number of poles	-
P	Active power	W
P_D	Damping power	W
P_e	Electrical power	W
P_m	Mechanical power	W
Q	Reactive power	VAr
S	Apparent power	VA
T_{d0}'	d-axis transient open-loop time constant	s
T_{d0}''	d-axis subtransient open-loop time constant	s
T_{q0}''	q-axis subtransient open-loop time constant	s
T_d'	d-axis transient short-circuit time constant	s
T_d''	d-axis subtransient short-circuit time constant	s
T_q''	q-axis subtransient short-circuit time constant	s
V_{REF}	Reference voltage, voltage regulator	V
V_s	Grid voltage	V
ω_m	Rotor rotational speed	rad/s
ω_{sm}	Rotor rotational speed equal to synchronous speed	rad/s
ω	Rotor speed	rpm
x_d	d-axis synchronous reactance	p.u
x_d'	d-axis transient reactance	p.u
x_d''	d-axis subtransient reactance	p.u
x_q	q-axis synchronous reactance	p.u
x_q'	q-axis transient reactance	p.u
x_q''	q-axis subtransient reactance	p.u
r_a	Armature resistance	p.u
x_l	Leakage reactance	p.u
L_a	Armature inductance	H
\mathcal{R}	Reluctance	H ⁻¹
A	Area	m ²
N_a	Number of armature windings	-
N_ϕ	Number of field windings	-

Abbreviations

Abbreviation	
AVR	Automatic voltage regulator
DG	Distribution generator
FCL	Field current limiting
GOV	Turbine governor
HV	High voltage
MV	Medium voltage
LV	Low voltage
OC	Open circuit
OEL	Over excitation limiter
PMU	Phasor measurement unit
PSS	Power system stabilizer
SC	Short circuit
UEL	Under excitation limiter

Table of contents

Preface.....	i
Abstract	iii
Sammendrag.....	v
List of symbols	vii
Abbreviations	ix
List of Figures	xiii
List of Tables.....	xvii
1 Introduction	1
1.1 Background	1
1.2 Objectives	1
1.3 Approach	1
1.4 Outline	2
2 Synchronous generator	3
2.1 General	3
2.1.1 dq0-transformation	5
2.1.2 Equivalent reactance and time constants	5
2.1.3 Equivalent circuit and phasor diagram	7
3 Turbine governing system	9
4 Excitation system	10
4.1 Exciter and Automatic Voltage Regulator	10
4.2 IEEE standard AC8B.....	12
4.3 Excitation Limiters	13
4.3.1 Overexcitation limiter.....	14
4.3.2 Underexcitation limiter.....	14
5 Power System Stability	16
5.1 Transient stability (Large disturbances)	17
5.2 Small signal stability (small disturbances)	19
5.2.1 Linear system analyses	19
5.2.2 Effect of the AVR on power system stability.....	21
5.2.3 Effect of the field current limiters on power system stability	23
6 System description	25
6.1 Small hydro power plant model	25
6.2 The distribution generator power plant model	26

6.3	Turbine governing system	27
6.4	Excitation system	28
7	Model validation.....	31
7.1	Laboratory testing.....	31
7.1.1	Model setup and test scenarios	31
7.1.2	Laboratory test results	32
7.2	Simulations	40
7.2.1	Simulation model.....	40
7.2.2	Simulation results	44
7.3	Sensitivity analysis	52
7.4	Comparison	53
8	Excitation limiters studies	55
8.1	Laboratory testing.....	55
8.1.1	Setup/case description	55
8.1.2	Laboratory test results	55
8.2	Simulations	57
8.2.1	Simulation model and setup	58
8.2.2	Simulation results	58
9	Discussion	65
9.1	Model validation.....	65
9.1.1	Generator model	65
9.1.2	Excitation system.....	66
9.1.3	Turbine governing system	67
9.1.4	Underexcited operation	67
9.1.5	Laboratory measurements – excitation system studies.....	67
9.1.6	Simulink power system module as simulation program.....	68
9.2	Excitation limiters stability studies	68
10	Conclusions and Recommendations for Further Work	69
10.1	Main conclusions.....	69
10.1.1	Model validation.....	69
10.1.2	Excitation limiter studies	69
10.2	Recommendations for further work.....	70
	Bibliography	71
	Appendix	73

List of Figures

Figure 1: Block diagram of a typical power generation unit, including excitation and turbine governing system. Based on [6]	3
Figure 2: Simplified two pole salient-pole machine [10]	4
Figure 3: Three sets of fictitious perpendicular windings representing the synchronous generator [6]..	5
Figure 4: Armature flux paths in a) subtransient state, b) transient state, c) steady-state [6].....	6
Figure 5: Per phase equivalent, representing a generator connected to a strong grid.	7
Figure 6: Phasor diagram of a synchronous generator connected to a strong grid.....	8
Figure 7: Functional block diagram of hydraulic turbine governing system.....	9
Figure 8: Typical excitation systems (a) Synchronous generator with rotating rectifier. (b) controlled rectifier fed from the generator terminals. Figure based on [6].....	10
Figure 9: Block diagram of the excitation and AVR system with Power System Stabilizer (PSS) based on [6].	11
Figure 10: Alternator-rectifier excitation system. Type AC8B. IEEE [11].....	12
Figure 11: Generator capability diagram. [13]	13
Figure 12: Classification of power system stability [18].....	16
Figure 13: Synchronous machine connected to infinite bus.....	17
Figure 14: Acceleration and deceleration areas: (a) stable case, short clearing time; (b) unstable case, long clearing time. [6]	18
Figure 15: Block diagram representation of the small signal linearized performance of the single line generator- infinite bus system, including Automatic voltage regulator and excitation system [20]	20
Figure 16: Components determining the phase shift between $\Delta\delta$ ($\Delta\omega$) and $\Delta E'q$ (ΔE_f).	22
Figure 17: Phasor diagram demonstrating the phase shift between the excitation emf components. ...	22
Figure 18: Sensitivity analysis, eigenvalues for increasing regulator gain 0-100.	23
Figure 19: Example of the influence of the field current limiter on the steady state power angle characteristic [6]	24
Figure 20: Single line diagram of the Renewable Energy laboratory showing the main units.	25
Figure 21: Laboratory model of the distribution generating unit, including the induction motor and frequency converter representing the turbine governing unit.....	28
Figure 22: Simple turbine governor equivalent diagram.....	28
Figure 23: Simplified block diagram of excitation system HPC 185, based on figure from [5]. V_{ref} : voltage reference value, V_{term} : measured generator terminal voltage, I_f : field current, EFD: AVR output field voltage.....	29
Figure 24: Three-phase thyristor converter for static excitation.	29
Figure 25: Per phase equivalent of laboratory system network.....	31
Figure 26: Active power output response of generator initially producing $P=10kW$, subjected to a small disturbance represented by increased system impedance. (a) Not at torque limit, (b) At torque limit	33
Figure 27: System response following a small disturbance, of the system initially operating at $P=5kW$, $Q=5kVAr$. (a) Generator output voltage (b) Generator output current	34
Figure 28: Output power response following a small disturbance, of the system initially operating at $P=5kW$, $Q=5kVAr$. (a) Active power, (b) Reactive power.....	34
Figure 29: Field voltage response following a small disturbance, for the system initially operating at $P=5kW$, $Q=5kVAr$	35

Figure 30: Generator output voltage response following a small disturbance, of the system initially operating at $P=5\text{kW}$, $Q=-5\text{kVAr}$.	36
Figure 31: Generator output current response following a small disturbance, of the system initially operating at $P=5\text{kW}$, $Q=-5\text{kVAr}$.	36
Figure 32: Active power response following a small disturbance, of the system initially operating at $P=5\text{kW}$, $Q=-5\text{kVAr}$.	36
Figure 33: Reactive power response following a small disturbance, of the system initially operating at $P=5\text{kW}$, $Q=-5\text{kVAr}$.	36
Figure 34: AVR output field voltage response following a small disturbance, of the system initially operating at $P=5\text{kW}$, $Q=-5\text{kVAr}$.	37
Figure 35: Field voltage response, Laboratory model case 3	38
Figure 36: Generator output voltage response following a small disturbance, $K_{pr}(\text{AVR})=110$	38
Figure 37: Generator output current response following a small disturbance, $K_{pr}(\text{AVR})=110$	38
Figure 38: Active power response following a small disturbance, of the system	39
Figure 39: Reactive power response following a small disturbance, of the system	39
Figure 40: Case 4. Voltage response following a 200ms short circuit	39
Figure 41: Case 4. Active power response, following a 200ms short circuit.	39
Figure 42: Case 4. AVR field voltage response following a 200ms short circuit	40
Figure 43: Electrical model of the synchronous generator. d, q , d and q axis quantity; R, s , rotor and stator quantity; l, m , leakage and magnetizing inductance; f, k , field and damper winding quantity. [22]	41
Figure 44: Per phase equivalent diagram for the simulation model.	42
Figure 45: Simulink model of the simplified turbine governing system	43
Figure 46: AVR/excitation system simulation model	44
Figure 47: Simulated field voltage response following a small disturbance, for the system initially operating at $P=5\text{kW}$, $Q=5\text{kVAr}$. AVR $P=55$, $I=120$.	45
Figure 48: Simulated field voltage response following a small disturbance, for the system initially operating at $P=5\text{kW}$, $Q=5\text{kVAr}$. AVR $P=20$, $I=43$.	46
Figure 49: Case 1. Generator output rms (a) phase to ground voltage and (b) current, zoomed in to show the oscillations following a small disturbance represented by a sudden increase in the external system impedance.	47
Figure 50: Case 1. Generator output (a) active and (b) reactive power, zoomed in to show the oscillations following a small disturbance represented by a sudden increase in the external system impedance.	47
Figure 51: Case 2. Generator output rms (a) phase to ground voltage and (b) current, zoomed in to show the oscillations following a small disturbance represented by a sudden increase in the external system impedance.	48
Figure 52: Case 2. Generator output (a) active and (b) reactive power, zoomed in to show the oscillations following a small disturbance represented by a sudden increase in the external system impedance.	49
Figure 53: Field voltage case 2.	49
Figure 54: Case 3. Generator output rms (a) phase to ground voltage and (b) current, zoomed in to show the oscillations following a small disturbance represented by a sudden increase in the external system impedance.	50
Figure 55: Case 3. Generator output (a) active and (b) reactive power, zoomed in to show the oscillations following a small disturbance represented by a sudden increase in the external system impedance.	51
Figure 56: AVR field voltage	51

Figure 57: AVR field voltage, high AVR gain → unstable response	52
Figure 58: Case 1. Generator output voltage Case 1 (a) laboratory model (b) Simulation model	53
Figure 59: Case 2. Generator output voltage (a) laboratory model (b) Simulation model	54
Figure 60: Case 3. Generator output voltage (a) laboratory model (b) Simulation model	54
Figure 61: AVR output field voltage, at field current limiting operation.....	56
Figure 62: Generator output voltage, during FCL operation.....	56
Figure 63: Generator output reactive power FCL operation.	56
Figure 64: AVR output field voltage, returning from field current limiting operation of regular AVR action	57
Figure 65: Generator output voltage, returning from FCL operation to regular AVR operation.	57
Figure 66: Generator output reactive power, returning from FCL operation to regular AVR operation.	57
Figure 67: Simulink model of the excitation system.....	58
Figure 68: Upper field current limit, output from OEL PI controller.....	59
Figure 69: Field current, limited by the OEL	59
Figure 70: Field voltage without limiter action	60
Figure 71: Field voltage with active limiters.....	60
Figure 72: Upper field current limit, output from OEL PI controller, adjusted parameters	61
Figure 73: Field current, limited by the OEL, adjusted parameters	61
Figure 74: Field voltage, FCL operation, adjusted PI controller parameters	62
Figure 75: Reactive power, FCL operation, adjusted PI controller parameters	62
Figure 76: Upper field current limit, output from OEL PI controller, out of FCL mode by increasing system impedance.....	62
Figure 77: Field current, out of FCL mode by increasing system impedance.....	63
Figure 78: AVR field voltage, out of FCL mode by increasing system impedance.....	63
Figure 79: Reactive power, out of FCL mode by increasing system impedance	63
Figure 80: Sensitivity analysis, increasing Inertia constant 0.5-5. [1]	65
Figure 81: Examples of phasor diagrams of a system with (a) Low AVR gain (b) High AVR gain	66

List of Tables

Table 1: Ratings of the laboratory model [4]	26
Table 2: Synchronous generator data (small hydro power model).....	27
Table 3: AVR parameters, laboratory model	32
Table 4: Test scenarios for model validation.	32
Table 5: Operation situation, laboratory model, case 1	33
Table 6: Operation situation, laboratory model, case 2.....	35
Table 7: Operation situation, laboratory model, case 3.....	37
Table 8: Operation situation, laboratory model, case 4.....	39
Table 9: Network parameters	42
Table 10: Generator parameters	42
Table 11: Governor settings	43
Table 12: AVR settings	44
Table 13: Generator operating situation, simulation case 1	45
Table 14: Generator operating situation, simulation case 1, adjusted AVR parameters	46
Table 15: Generator operating situation, simulation case 2	48
Table 16: Generator operating situation, simulation case 3	50
Table 17: Laboratory model, excitation system parameters.....	55
Table 18: Line inductance, simulation model	58
Table 19: Field current limiter PI controller parameters as given in [5].	59
Table 20: Adjusted field current limiter PI controller parameters.....	61

1 Introduction

1.1 Background

The expectations and requirements for safe, continuous and high quality power supply have increased significantly over the last years. At the same time the energy consumption increases, and the power system is challenged to operate close to its maximum production limits. This requires a stable and safe power system and brings new concerns about power system stability and protection.

Several small hydro power plants have experienced problems related to power system stability the last years, e.g. at Kurås fossen power plant, and Breieva power plant. These two cases has been analyzed in earlier reports [1] [2] [3], but the exact reasons for the problems are still unknown.

1.2 Objectives

This master thesis considers concerns about stability and protection related to small distributed hydro power generation. Stability problems related to the voltage regulator and the excitation limiters is the main focus in this report. The report consists of two main parts. Part one concerns laboratory studies with focus on model validation. Part two is mainly a study of excitation limiters and their influence on the system response and performance to obtain knowledge considering operation close to the stability limits.

The renewable energy laboratory at NTNU is described in the report “Distribution Network Laboratory Model” by Astrid Petterteig at SINTEF [4]. It includes a model of a small hydro power plant, consisting of a motor-generator set, equipped with a generator excitation and control unit and a frequency converter for induction motor control. This is an interesting model for future stability studies of the synchronous generator unit including the excitation system. To use the model for these kinds of studies, and to create comparable simulation models, it is useful to know the characteristics of the model, and its response to different kinds of system changes and disturbances.

The small hydro power plant model includes a digital excitation system, equipped with several protective and limiting functions. These limiting functions includes over- and under excitation limiters. From earlier studies (e.g. [2][5]) there are indications that excitation limiter functions for certain voltage regulators (e.g. the HPC 185) can have a negative impact on the stability of the generator at certain operational states.

1.3 Approach

The main purpose of this thesis is to study the characteristics of the small hydro power plant laboratory model, and to use this model for validation of a simulation model. This simulation model will be used to study how the field current limiters of the excitation system of synchronous generators can influence the system response and the damping and stability of the system. The study will include simulations and measurements in the laboratory, where the voltage regulator is implemented in simple test systems.

This thesis consists of two main parts. Part one will focus on validation of the simulation model. This validation will be done by modeling the simplified power system in the renewable energy laboratory at NTNU, and comparing the simulation results with measurements done in the laboratory. The aim of this work is to create a simulation model for the small hydro power plant model in the laboratory, as well as validating the simulation model for use in further stability studies in part two. The simulation

model will be a simplified network model, with main focus on the generator model and the excitation system, including the excitation limiters. MATLAB/Simulink PowerSystems will be used for simulations.

The other part of the thesis concerns the excitation system including the voltage regulator, and how the interaction between the AVR function and the excitation limiters can affect the system response and stability. These studies will be done mainly by simulations. Measurements in the laboratory will be done to support the results and conclusions.

1.4 Outline

Chapter 2-5 is a presentation of the theoretical background considered relevant for the studies done in this master thesis. This theoretical part starts by presenting some general aspects considering the synchronous generator in chapter 2. This is followed by chapter 3 and 4, presenting the turbine governing system and the excitation system, including the excitation limiters. Chapter 5 is a short presentation of power system stability, with focus on rotor angle stability and how the excitation system and voltage regulation can affect the damping of the power system.

Chapter 6 gives a description of the small hydro power plant laboratory model studied in this master thesis. This part is mainly a presentation of the distribution generator power plant model, including the turbine governing system and the excitation system.

Chapter 7 concerns model validation. In chapter 7.1 the laboratory tests are described, presenting the different test scenarios and the test results. Chapter 7.2 describes the corresponding simulation model and the results of the simulations. A brief sensitivity analysis and a comparison of the results will be included in chapter 7.3 and 7.4.

Chapter 8 is a study of the excitation limiters, including laboratory testing and simulations using the model validated in the previous parts.

Chapter 9 is a final discussion of the results obtained from these studies, while the main conclusions and recommendations for further work is presented in chapter 10.

2 Synchronous generator

The first chapters of this report present the aspects concerning the synchronous generator in small distributed hydro power generation, which are considered important background information for this master thesis.

Figure 1 shows the total generating unit, including the excitation system and the turbine governing system, which will be described in the following chapters.

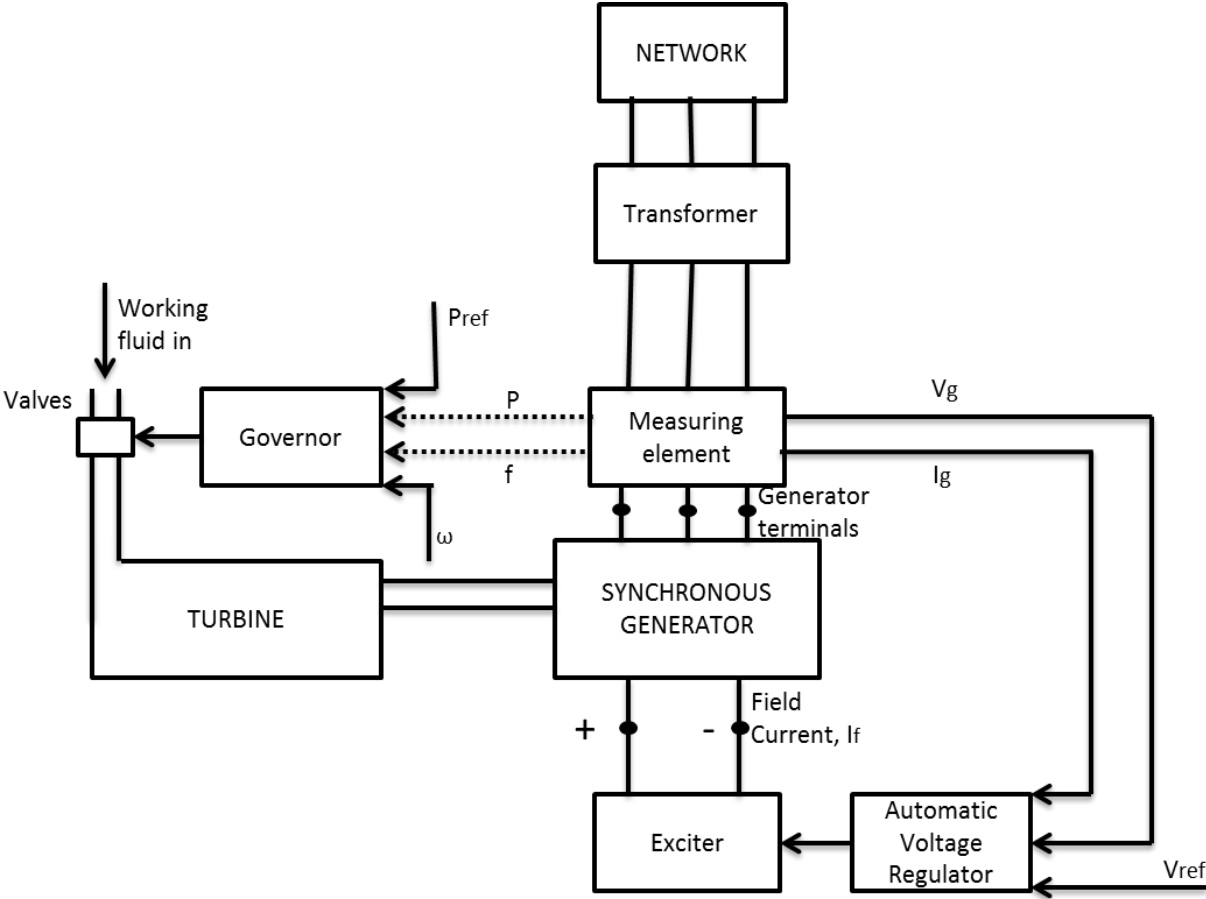


Figure 1: Block diagram of a typical power generation unit, including excitation and turbine governing system. Based on [6]

2.1 General

Information concerning the synchronous generator presented in this part of the report is mainly found from [6] [7] [8] and [9].

In the synchronous generator, the rotor turns at the same speed as the produced magnetic field. The mechanical speed of the rotor is related to the stator electrical frequency by the following equation Where P is the number of poles on the rotor, f_{se} is the stator electrical frequency in Hz and n_m is the rotational speed of the magnetic field in rpm.

$$f_{se} = \frac{n_m P}{120} \tag{2.1}$$

As derived in [8] the generated voltage is directly proportional to the flux in the machine, ϕ , and the rotational speed ω , as shown in the following equation, where K is a constant representing the construction of the machine.

$$E_A = K\phi\omega \quad (2.2)$$

The synchronous generator consists of a stator with three-phase armature winding wound on it, and a rotor with a DC field winding. The rotor also has additional damper windings, to add damping to the mechanical oscillations of the rotor. The generator can be a round-rotor machine, or a salient-pole machine. In this report the focus will be on the salient-pole synchronous generator, which is shown in figure 2.

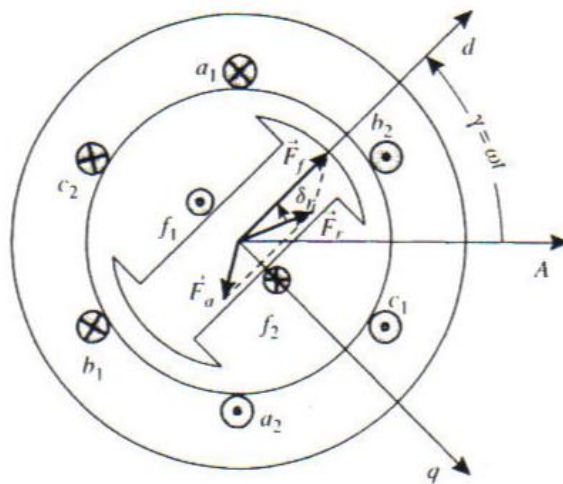


Figure 2: Simplified two pole salient-pole machine [10]

In the salient pole synchronous machine the width of the air gap varies around the generator with the narrowest gap along the d-axis and the widest along the q-axis.

The reluctance \mathfrak{R} is proportional to the length of the air gap. Increasing the air gap length gives a higher reluctance value, which gives a lower inductance and a lower value of the air gap reactance [6] [7]. The air gap length in the rotor affects the reactance values of the generator. The relation between the air gap length and the air-gap reactance is shown in the following equations, where L_a is the air-gap inductance and \mathfrak{R} is the air gap reluctance.

$$X_a = \omega L_a \quad (2.3)$$

$$L_a = \frac{1.5 N_a N_\phi}{\mathfrak{R}} \quad (2.4)$$

$$\mathfrak{R} = \frac{l}{\mu A} \quad (2.5)$$

2.1.1 dq0-transformation

For the synchronous machine, all the machine windings are transferred into rotor reference frame. This transformation is called Park Transformation, or direct-quadrature-zero, dq0, transformation, and is used to simplify the analysis. By applying this transformation to the three phase system, the three ac components are reduced to two dc components. The park transformation for the currents is given by the following matrix equation.

$$\begin{bmatrix} i_0 \\ i_d \\ i_q \end{bmatrix} = \begin{bmatrix} \beta_0 & \beta_0 & \beta_0 \\ \beta_d & \beta_d \cos\left(\gamma - \frac{2}{3}\pi\right) & \beta_d \cos\left(\gamma + \frac{2}{3}\pi\right) \\ \beta_q & \beta_q \sin\left(\gamma - \frac{2}{3}\pi\right) & \beta_q \sin\left(\gamma + \frac{2}{3}\pi\right) \end{bmatrix} * \begin{bmatrix} i_A \\ i_B \\ i_C \end{bmatrix} \quad (2.6)$$

Where β_0 , β_d , and β_q are non-zero coefficients. A similar transformation can be defined for the stator voltage and flux linkages. [6] The dq0-transformed windings are shown in figure 2.

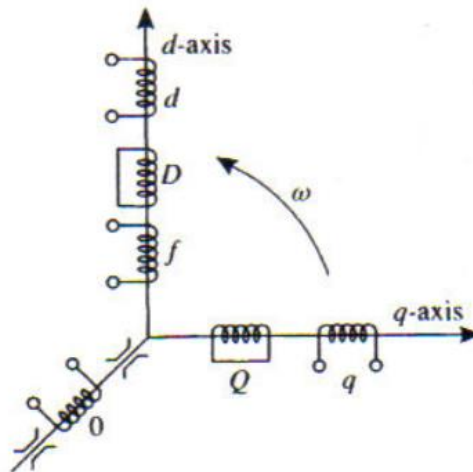


Figure 3: Three sets of fictitious perpendicular windings representing the synchronous generator [6]

The windings D and Q correspond to the rotor damper windings in d- and q- axes direction respectively, while f represents the rotor field windings. d and q are fictitious and represents the effect of the stator winding in the rotor.

2.1.2 Equivalent reactance and time constants

When a fault occurs, additional currents are induced in the rotor windings of the synchronous generator which force the armature flux to take a different path than it would in steady state. The period during and after the fault, is divided into three different stages. Figure 4 shows how the flux path changes for the different states.

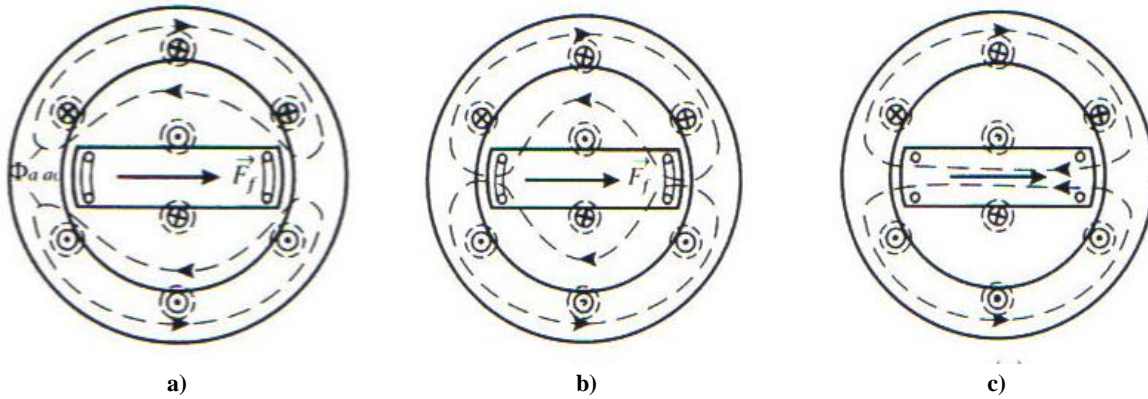


Figure 4: Armature flux paths in a) subtransient state, b) transient state, c) steady-state [6]

Immediately after the fault, the generator is said to be in subtransient state. In this state currents are induced in the rotor field and damper windings. To keep the rotor flux linkage constant, the armature reaction flux is forced out of the rotor as shown in figure 4a. The currents decay with time, and allow the armature reaction flux into the rotor. The current in the damper windings decay the fastest as the damper windings have the highest resistance. In transient state the armature reaction flux is allowed through the damper windings but still not through the rotor field windings as shown in figure 4b. When the current in the field winding has decayed sufficiently, the armature reaction flux can enter the whole rotor and the generator has returned to its steady state.

The synchronous generator equivalent reactance corresponding to the flux path depends on the state of the generator. The machine reactance is a combination of the air gap reactance, the armature leakage reactance, and the reactance corresponding to the flux path around damper- and field windings.

X_1	corresponds to the path that the armature leakage flux takes around the stator windings and is referred to as the armature leakage reactance.
X_{ad}	corresponds to the flux path across the air gap in d-axis direction, and is referred to as the armature reaction reactance.
X_{aq}	corresponds to the flux path across the air gap in q-axis direction, and is referred to as the armature reaction reactance.
X_D	corresponds to the flux path around the damper winding in d-axis direction.
X_Q	corresponds to the flux path around the damper winding in q-axis direction.
X_f	corresponds to the flux path around the field winding.
X_d	direct-axis synchronous reactance
X_d'	direct-axis transient reactance
X_d''	direct-axis sub-transient reactance
X_q	quadrature-axis synchronous reactance
X_q'	quadrature-axis transient reactance
X_q''	quadrature-axis sub-transient reactance

The equivalent reactance of the synchronous generator in the different states, depend on the armature leakage reactance, the air gap reactance, and the reactance corresponding to the flux path around field- and damper windings.

2.1.3 Equivalent circuit and phasor diagram

The equivalent circuit and the phasor diagram are important tools to understand and study the power system stability phenomena. This part describes the phasor diagram of a generator connected to a strong grid. The equivalent per phase circuit is shown in Figure 5.

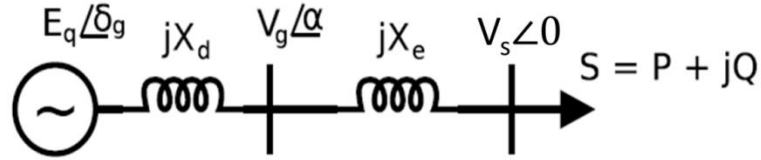


Figure 5: Per phase equivalent, representing a generator connected to a strong grid.

The current I can be found from the active and reactive power delivered to the grid, and the grid voltage. Given an infinite grid with voltage 1pu, the current can be expressed as

$$I = P - jQ \quad (2.7)$$

Knowing the current, the infinite grid voltage, and the q-axis synchronous reactance, the induced q-axis synchronous voltage can be found.

$$E_q = V_s + jX_q I \quad (2.8)$$

The angles φ and δ are the angles of I and E_q respectively, relative to V_s . The angle δ is necessary to locate the q-axis.

$$\varphi = \tan^{-1} \frac{-Im(I)}{Re(I)} \quad (2.9)$$

$$\delta = \tan^{-1} \frac{Im(E_q)}{Re(E_q)} \quad (2.10)$$

The d- and q-axis components of the terminal voltage and current can now be found, from the generator voltage V_g , the angles δ and φ , and the current I

$$V_q = |V_g| \cos \delta_g \quad (2.11)$$

$$V_d = -|V_g| \sin \delta_g \quad (2.12)$$

$$I_d = -|I| \sin(\delta_g + \varphi) \quad (2.13)$$

$$I_q = |I| \cos(\delta_g + \varphi) \quad (2.14)$$

Knowing the d-axis component of the current I_d and the d-axis reactances, the induced voltages E_q and E'_q in steady state and transient state respectively, can be found as follows

$$E_q = V_s \cos \delta_g - jX_d I_d \quad (2.15)$$

$$E'_q = V_s \cos \delta_g - jX'_d I_d \tag{2.16}$$

$$\omega = 2\pi f \tag{2.17}$$

These values describes the operating situation of the generator, and can be expressed as a phasor diagram as shown in Figure 6.

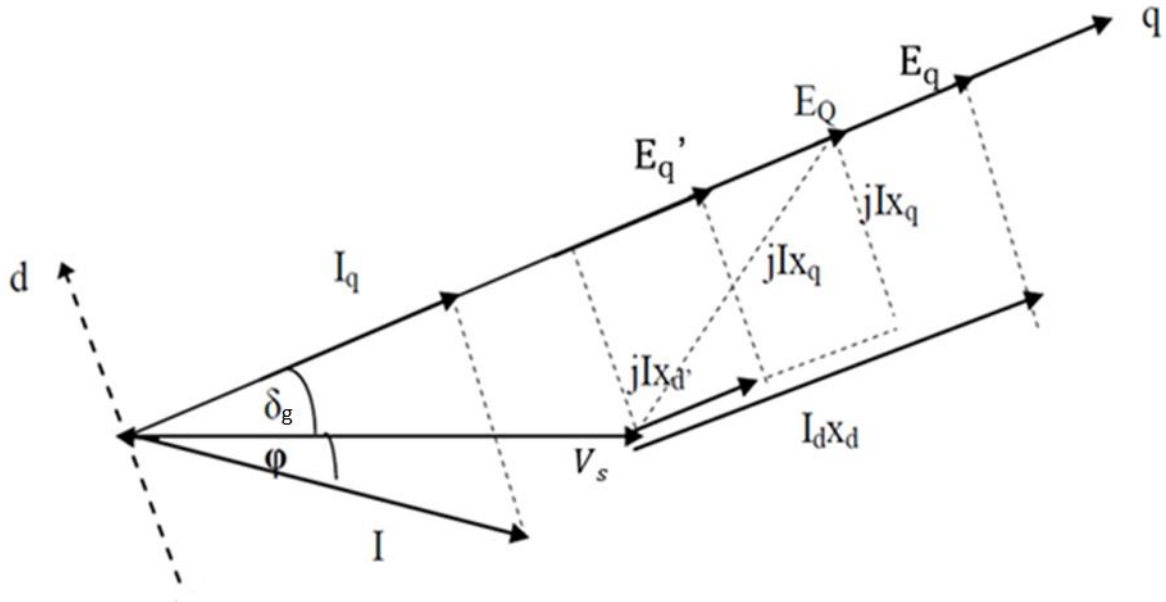


Figure 6: Phasor diagram of a synchronous generator connected to a strong grid

3 Turbine governing system

The turbine governing system is the part of the power system which controls the input to the turbine in order to control the generator speed and hence the active power response to load variations. The turbine governing system makes the machine able to start, reach its operational speed and operate with the required power output. The turbine governing system controls the mechanical input power, so that the power input is reduced as the speed increases, and increased if the speed reduces. This way the balance between the input and output power is maintained. The synchronous generator is normally driven by steam- gas- or hydro turbines equipped with a turbine governing system.

The laboratory model considered in this report is a model of a small hydro power plant. A functional diagram of a standard hydraulic turbine governing system is shown in Figure 7.

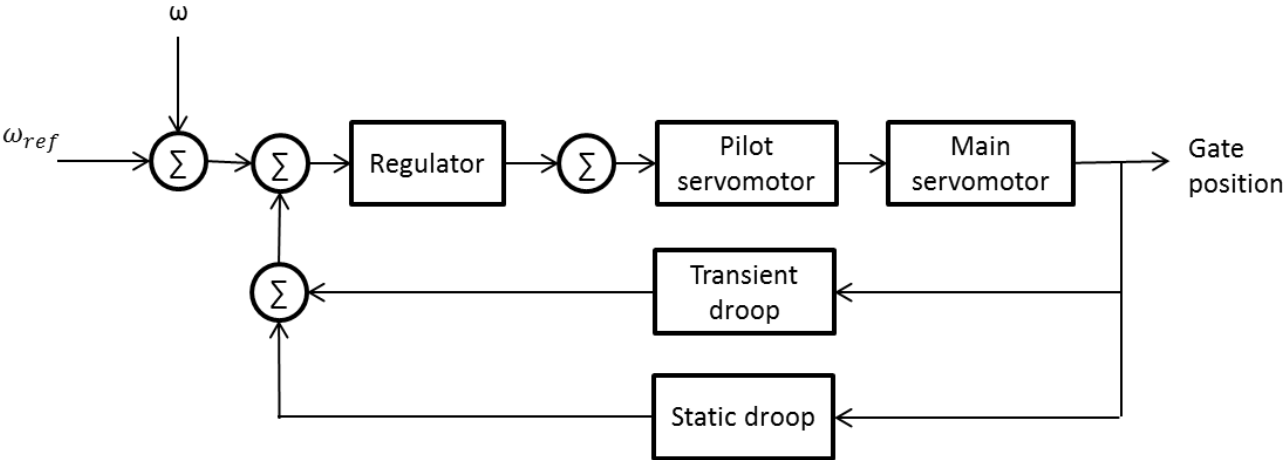


Figure 7: Functional block diagram of hydraulic turbine governing system.

The main difference between the hydro turbine governing system and the gas- and steam turbine governing systems, is that a higher force is required to move the control gate, as the water pressure and the frictional forces are high. To provide this force two servomotors are use as shown in the figure. The feedback loop including the transient droop, allows the water flow to catch up to the changes in the gate position. These factors make the hydro turbine governing systems relatively slow. The turbine governing system model considered in this master thesis is described in part 6.3.

4 Excitation system

The excitation system mainly consists of an exciter and an automatic voltage regulator (AVR). It supplies field current to the generator, and includes control-, regulating- and protective functions. The excitation system should supply and automatically adjust the field current of the generator to maintain the terminal voltage as the output varies. In addition, it should be able to respond to transient disturbances, to enhance transient stability. [9]

The excitation system should fulfill the following requirements [9]:

- Meet specified response criteria
- Provide limiting and protective functions as required to prevent damage to itself, the generator and other equipment.
- Meet specified requirements for operating flexibility.
- Meet the desired reliability and availability, by incorporating the necessary level of redundancy and internal fault detection and isolation capability.

4.1 Exciter and Automatic Voltage Regulator

The exciter supplies DC field current to the generator field winding. There are different kinds of exciters, which can be classified as rotating or static. Figure 8 shows two typical systems, where figure (a) is rotating and (b) is a static exciter system using static thyristor converter.

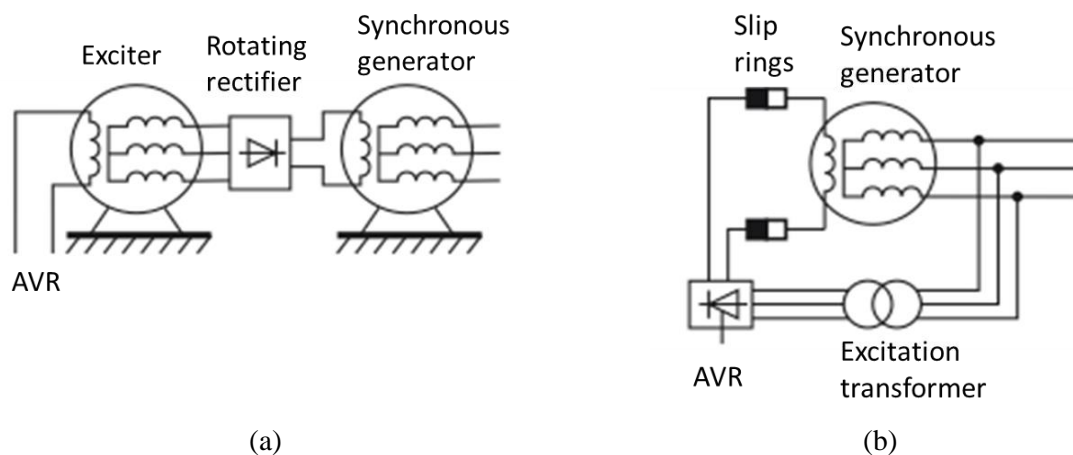


Figure 8: Typical excitation systems (a) Synchronous generator with rotating rectifier. (b) controlled rectifier fed from the generator terminals. Figure based on [6]

Today the static exciter is the most common source of excitation for high power generators. In these exciters the thyristor rectifier is controlled directly by a voltage regulator. For the static exciters slip rings are necessary to feed current to the rotor of the main generator. The excitation system implemented in the small hydro power plant laboratory model considered in this report, is a rotating rectifier as shown in Figure 8a.

The AVR regulates the generator terminal voltage by controlling the amount of current supplied to the generator field winding by the exciter. Figure 9 shows the block diagram of an excitation- and AVR system, including limiters and protective functions, load compensation and power system stabilizer (PSS). [6]

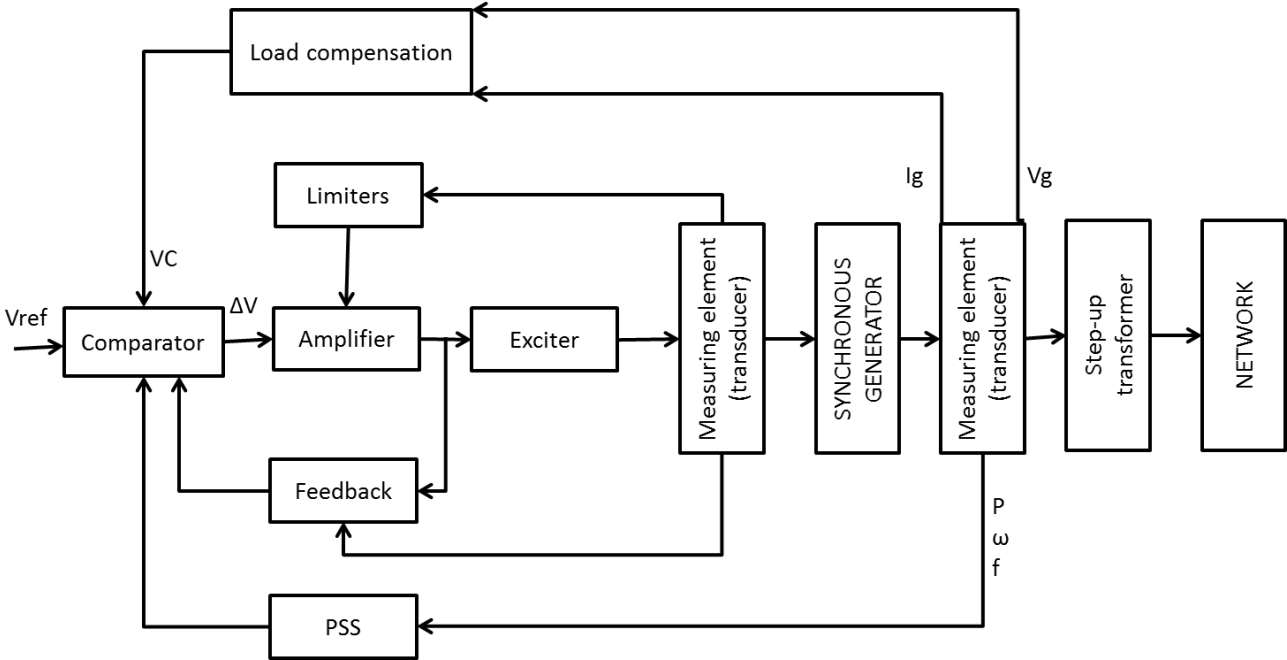


Figure 9: Block diagram of the excitation and AVR system with Power System Stabilizer (PSS) based on [6].

As shown in Figure 9, the modern excitation system is more than the exciter and AVR. It normally includes numerous control, limiting and protective functions.

The power system stabilizer (PSS) is included in some excitation systems to add damping power to the system, to improve the dynamic performance and enhance small-signal stability. Load compensation is sometimes used to shift the point where constant voltage is maintained. The AVR normally controls the voltage at the stator terminals, but this way it can be controlled at another point in the system with the same effect on the generator voltage.

4.2 IEEE standard AC8B

The excitation system included in the laboratory model is a Basler DECS-200 digital excitation control system. This is an IEEE standard 421.4 AC8B excitation system model. [11]. A block diagram of the IEEE AC8B excitation system, described in IEEE standard 421.5 is shown in Figure 10.

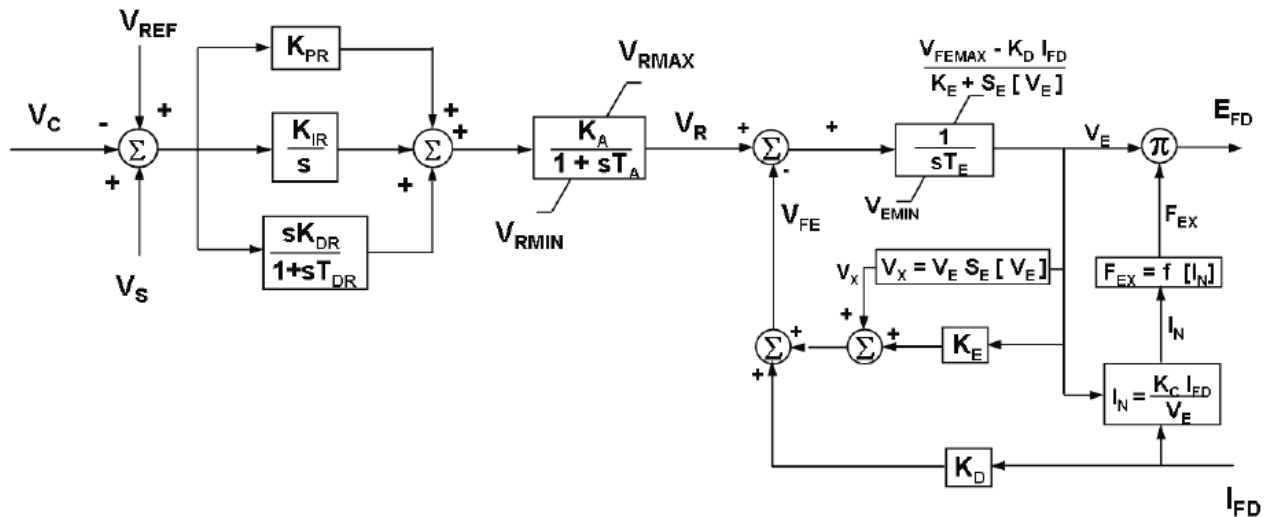


Figure 10: Alternator-rectifier excitation system. Type AC8B. IEEE [11]

The AVR is represented by a PID regulator described by the proportional gain K_{PR} , the integral gain K_{IR} and the derivative gain and time constant K_{DR} and T_{DR} . T_E represents the excitation system time delay. To represent digital AVR feeding DC rotating exciters, the constants K_C and K_D are set to 0. [11].

Dynamic field current limiters are also included in the laboratory excitation system. These are controlled by PI controllers, which are activated when the field current exceeds a given limit.

The PID regulator shown in Figure 10 contains a proportional gain K_{PR} , an integral gain K_{IR} and a derivative gain and time constant K_{DR} and T_{DR} . The excitation limiters PI controllers consist of a proportional gain and an integral gain. The proportional gain amplifies the deviation between the reference and the measured value. A high proportional gain will give a faster system but can cause exaggerated controller action and lead to instability. The integral time T_I is the inverse of the integral gain. Hence a high integral gain will give a small integral time and the integrating function will have greater effect on the regulation process. The transient response of the system will be faster for higher values of TD, and the derivative function can raise the phase margin and hence the stability margin for the system. [12]

4.3 Excitation Limiters

To protect the AVR, exciter and generator from excessive voltages and currents, the excitation system includes several control, limiting and protective functions. These keep the AVR signal within given limits, to protect the amplifier from too high input signals, the exciter and generator against too high field current, and the generator against too high armature current and power angle.

The Synchronous generator is normally bounded by 6 different limiting functions, to protect the generator. Three of these functions represent the underexcitation limiter actions, while one represents the overexcitation limiter. In addition, the active power is limited by the turbine power rating, and the stator current has an upper thermal limit. The excitation limiters will be the main focus in this report. The limits valid for synchronous generators are illustrated in the generator capability diagram in Figure 11.

1. armature current limit
2. maximum rotor field current limit (OEL)
3. minimum rotor field current limit (UEL)
4. steady-state rotor-angle stability limit (UEL)
5. (stator core end-region heating limit (UEL))
6. maximum (and minimum) turbine power rating

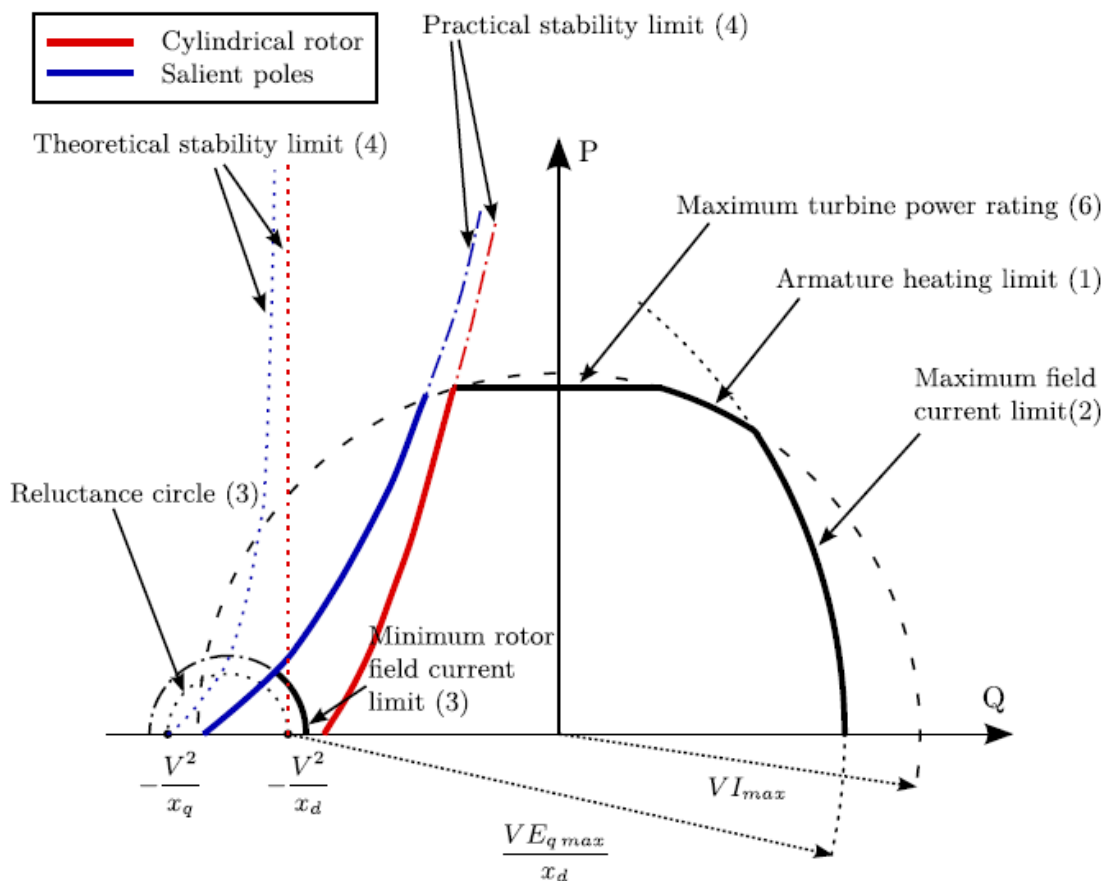


Figure 11: Generator capability diagram. [13]

4.3.1 Overexcitation limiter

The main aim of the overexcitation limiter is to protect the generator from overheating, by limiting the field current which is accepted over a longer period of time. In situations where the reactive power demand is high, the AVR will still attempt to keep a constant output power from the generator. In these situations the resulting field current may become high enough to cause overheating of the armature windings. The OEL should prevent too high field current levels, while at the same time allowing maximum field forcing for a shorter period to enhance power system stability.

The overexcitation limit can be expressed in terms of active and reactive power, P and Q, by the following equations, assuming $I_f \sim E_q$:

$$P = \frac{E_q V}{x_d} \sin \delta_g \quad (4.1)$$
$$Q = \frac{E_q V}{x_d} \cos \delta_g - \frac{V^2}{x_d}$$

Combining the two equations and applying the term $\sin^2 \delta_g + \cos^2 \delta_g = 1$ gives the following expression:

$$P^2 + \left(Q + \frac{V^2}{x_d} \right)^2 = \left(\frac{E_q V}{x_d} \right)^2 \quad (4.2)$$

This equation represents the black dashed circle in Figure 11, marked as armature heating limit (1).

The overexcitation condition is normally detected by measuring the field current (or the field voltage). The measured values are compared to a defined maximum level which represents the field winding temperature. When an overexcitation condition occurs, the OEL allows this overload to persist for a certain amount of time, before it takes action through the ac regulator and reduces the excitation. [9] [14]

The period the overexcitation is allowed to persist, is described by a time constant. This may be a fixed time period, or it can vary with the excitation level, as the generator can stand a lower excitation level for a longer period. As for the under excitation limiter, the output signal of the OEL may be implemented in the control system in different ways. It can have a fixed or varying maximum excitation level and time delay, and it can reduce the excitation set point to a safe value instantly or gradually. [9] [15] [16]

4.3.2 Underexcitation limiter

Most modern voltage regulators on large synchronous generators include underexcitation limiters to boost the excitation level when it is below a certain limit. The main intention of this limiter is to prevent operation at too low excitation levels. When the excitation is reduced to a level which is considered too low, the underexcitation limiter is meant to increase the field current to keep the excitation above this level.

As shown in the generator capability diagram in Figure 11, the UEL typically acts for three different reasons. [15]

- To keep the rotor field current at a sufficient level during underexcited operation, to prevent loss of field relay. (minimum rotor field current limit)
- To prevent insufficient excitation which could lead to loss of synchronism, or lower the stability level of the synchronous generator (Rotor-angle stability limit)
- To prevent overheating of the stator core end-region, caused by large amounts absorbed reactive power. (Stator core end-region heating limit)

The minimum rotor field current limit is illustrated by the dotted semi-circle to the left in Figure 11, called reluctance circle. The dash-dotted circle called rotor field current limit, is the same limit with a safety margin added. This circle is described by the power equation for a salient pole machine, with $E_q=0$, as the reluctance term makes it possible to produce some active power at zero field current.

$$P = \frac{E_q V}{x_d} \sin \delta_g + \frac{V^2}{2} \frac{x_d - x_q}{x_d x_q} \sin^2(2\delta_g) \quad (4.3)$$

$$Q = \frac{E_q V}{x_d} \cos \delta_g + \frac{V^2}{x_d} - V^2 \frac{x_d - x_q}{x_d x_q} \sin^2 \delta_g$$

These equations, with $E_q=0$ leads to the two points; $\frac{-V^2}{x_q}$ and $\frac{-V^2}{x_d}$, describing this limit.

The theoretical rotor angle stability limit is described by $\frac{\partial P}{\partial \delta_g} = 0$, from the previous equations this gives the following expression for the rotor angle

$$\cos \delta_g = \frac{1}{4} \left(-\frac{E_q x_q}{V(x_d - x_q)} \pm \sqrt{\left(\frac{E_q x_q}{V(x_d - x_q)} \right)^2 + 8} \right) \quad (4.4)$$

From this expression the corresponding P and Q values can be found, which is shown as the red dashed line in Figure 11.

During underexcited operation, the low field current causes an increase in the leakage flux, which leads to stator core end-region heating. At very low excitation levels this generated heat may cause problems. The stator core end-region heating limit describes the excitation level where these problems occur. This is normally not a problem for salient pole machines.

The control signal of the underexcitation limiter is derived from a combination of either voltage and current, or active and reactive power of the generator. The limits are determined by this signal exceeding a reference level. When this limit is crossed, the output of the UEL or becomes a part of the excitation control system. [9]

5 Power System Stability

Definitions of power system stability terms used in this report is the suggestions made by IEEE/CIGRE Joint Task Force on Stability terms and definitions defines power system stability, in [17]. They define power system stability as: *the ability of an electric power system, for a given initial operating condition, to regain a state of operating equilibrium after being subjected to a physical disturbance, with most system variables bounded so that practically the entire system remains intact.*

How the power system respond to a disturbance depends on the characteristics of the disturbance, and the power systems initial state. Load changes and different kinds of disturbances cause dynamic performances for the components in the power system. The disturbance is classified as small or large. A small disturbance may occur in form of a load change, and the system should be able to adjust to this change without any severe oscillations or loss of supply. Short-circuit on transmission lines, loss of large generator or loads, or loss of a tie between subsystems, are examples of large disturbances. The system must be able to survive such disturbances, without causing instability or breakdowns.

Figure 12 describes the classification of different power system stability problems. The studies described in this report will mainly concern rotor angle stability.

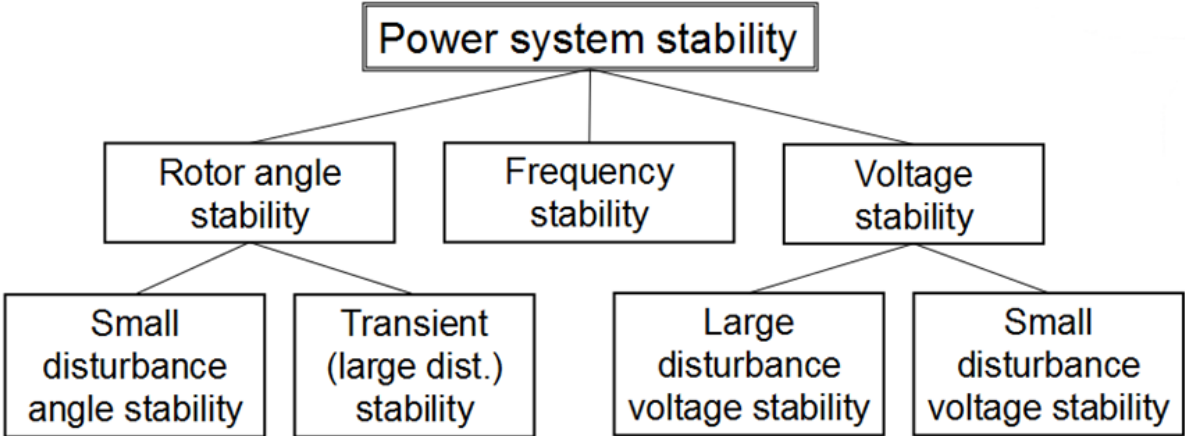


Figure 12: Classification of power system stability [18]

Rotor angle stability is the ability of interconnected synchronous machines of a power system to remain in synchronism. [9]

In steady state, the electrical power delivered by the generator is equal to the mechanical power supplied by the turbine. When the power system is subjected to a disturbance, the electrical power P_e changes fast, while the mechanical power P_m changes relatively slowly. This will lead to a temporary power imbalance and variation in the applied torque, which causes change in the rotor speed. This will also lead to a change in the relative rotor angle.

An important characteristic concerning rotor angle stability is how the power produced by the generator varies according to the rotor angle. For a synchronous machine connected to an infinite grid, as shown in Figure 13, the power-angle characteristic in steady state is given by equation 5.1.

$$P_e = P_{E_q} = \frac{E_q V_s}{x_d} \sin(\delta) \quad (5.1)$$

Where P_e is the electrical power produced by the generator, E_q is the internal induced voltage of the generator, V_s is the grid voltage, x_d is the sum of the synchronous reactance of the generator and the transformer and line reactances between the generator and the point of V_s , and δ is the rotor angle.

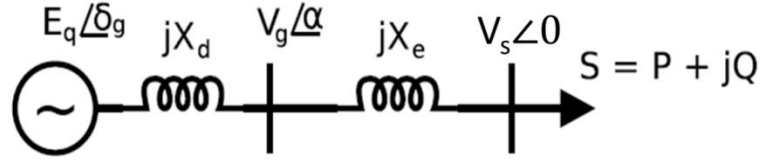


Figure 13: Synchronous machine connected to infinite bus

5.1 Transient stability (Large disturbances)

Transient stability is the ability of the power system to maintain in synchronism when subjected to a severe transient disturbance. [9] Examples of severe transient disturbances are loss of generations, loss of large loads and fault on transmission facilities.

As the mechanical torque changes relatively slowly and cannot balance out the transient variation in the electrical torque instantaneously, a transient disturbance will cause some oscillations. The change in the electrical torque following a load change or a disturbance can be divided into two different components, as shown in the following equation.

$$\Delta T_e = T_s \Delta \delta + T_D \Delta \omega \quad (5.2)$$

The first component called the “synchronizing torque” is in phase with the rotor angle change, while the second component called the “damping torque” is in phase with the speed change. [19] Lack of sufficient synchronizing torque will result in loss of synchronism. This is prevented if enough magnetic flux is developed when a transient change in the electrical torque occurs.

When the system is subjected to a sudden disturbance, additional currents will be induced in the rotor windings to maintain constant induced voltage, E' , as explained in 2.1. The rotor swings must therefore follow the transient power-angle curve.

$$P_e(\delta) = P_{E'_q}(\delta') \Big|_{x'_q=x_q} = \frac{E'_q V_s}{x'_d} \sin(\delta') - \frac{V_s^2 (x_d - x'_d)}{2 x_q x'_d} \sin(2\delta') \quad (5.3)$$

Assuming classical generator model, and ignoring saliency, this equation is simplified as follows.

$$P_e(\delta) = P_{E'_q}(\delta') \Big|_{x'_q \approx x'_d} = \frac{E'_q V_s}{x'_d} \sin(\delta'). \quad (5.4)$$

Figure 14 shows how the generator output power changes with respect to the rotor angle following a three-phase fault. Figure 14 a) shows the situation with a short clearing time, whereas figure b) shows the same case with a longer clearing time. This figure shows how the power system stability depends on the fault clearing time.

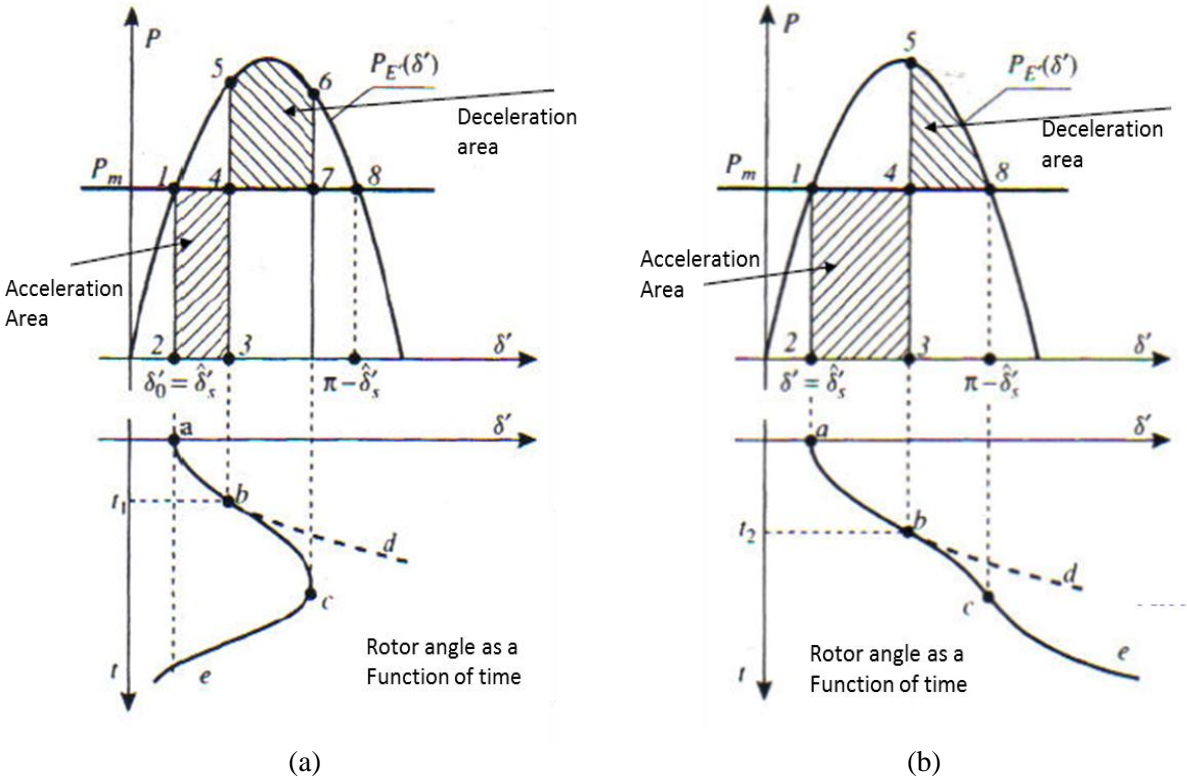


Figure 14: Acceleration and deceleration areas: (a) stable case, short clearing time; (b) unstable case, long clearing time. [6]

At point 1 in Figure 14 the electrical power is equal to the mechanical power and the system operates at steady state. As a three-phase fault occurs, the generator electrical output power drops to zero, as illustrated with point two in the figure. The electrical power stays at zero until the fault is cleared. During this period the mechanical power is higher than the electrical power, as the inertia keeps the rotor angle from changing instantaneously. This results in an acceleration torque which causes the rotor to accelerate until the fault is cleared. When the fault is cleared the power increases from point 3 to 4. At this point the acceleration torque is zero, but the rotor speed is now higher than the synchronous speed, so the rotor angle continues to increase. From this point the rotor decelerates, and if there is enough retarding torque, the generator will be transiently stable and move back towards its operating point as shown in Figure 14a). If not, the angle will continue to increase until the generator loses synchronism as shown in figure b).

The swing equation can be solved to see if the system is transiently stable, by telling if the rotor angle continues to increase or if it oscillates about an equilibrium position.

$$\frac{2H}{\omega_0} \frac{d^2\delta}{dt^2} = P_m - P_{max} \sin\delta \tag{5.5}$$

Where the rotor acceleration is equal to $\frac{d^2\delta}{dt^2}$ and H is the inertia constant defined as

$$H = \frac{0.5J\omega_{sm}^2}{S_n} \quad (5.6)$$

J is the moment of inertia in kgm^2 , S_n is the machine rating in VA, and ω_{sm} is the mechanical synchronous speed in rad/s. [6]

Another way to obtain this information is by the equal-area criteria. This criteria says that as long as the deceleration power, represented by the size of the deceleration area in Figure 14 is higher than the acceleration power, represented by the acceleration area, the system is transiently stable.

5.2 Small signal stability (small disturbances)

Small-signal stability is the ability of the power system to maintain synchronism during and after small-disturbances. [9] These disturbances are categorized by being small enough for the linearized system equations to be valid for system analysis. Small-disturbances may result in instability two different ways. It can cause the rotor angle to increase continually due to lack of synchronizing torque, or it can give rotor oscillations with increasing amplitude caused by insufficient damping torque.

5.2.1 Linear system analyses

Linear systems analysis can give important information about the system and how it behaves under different operating conditions. Figure 11 shows a block diagram of a general linearized model of a system where a synchronous generator, including excitation system and voltage regulator, is connected to an infinite bus through a transmission line. This model can be helpful for studying the systems small-signal stability and damping of oscillatory modes. Expressions for the constants shown in Figure 15 are given in appendix A1.

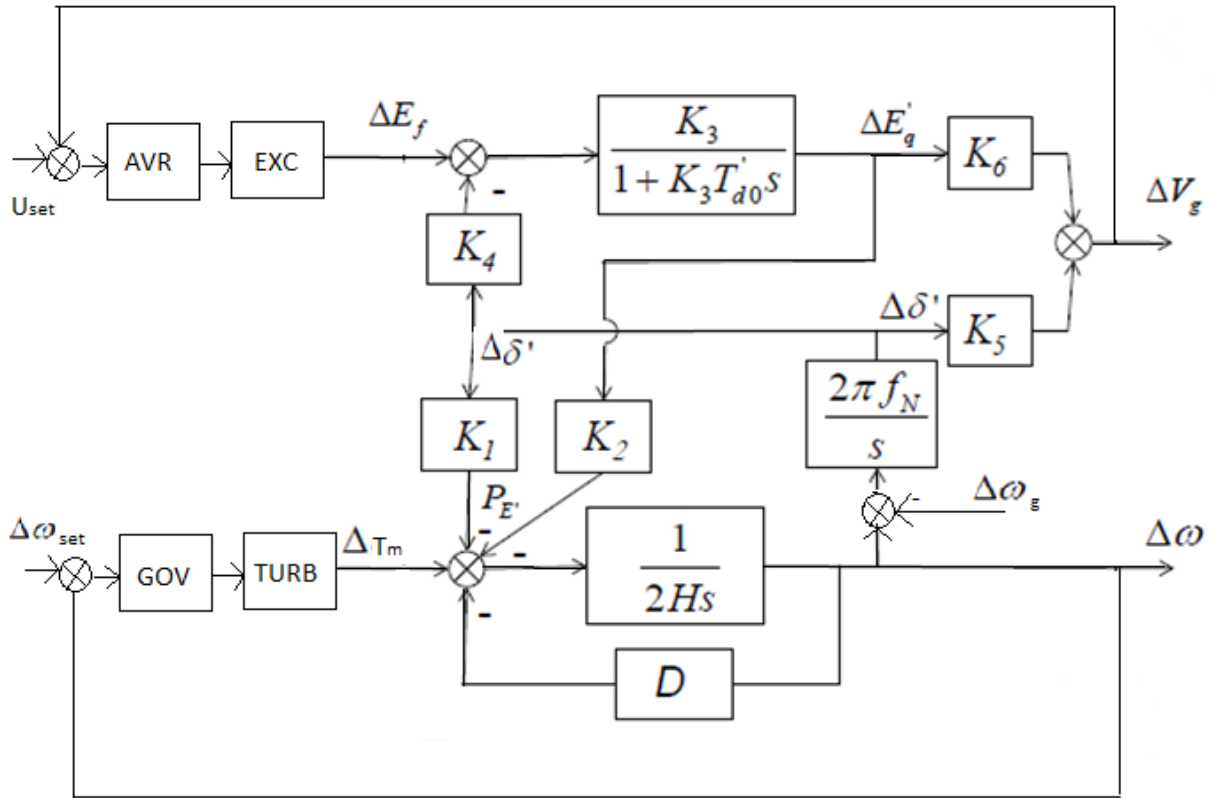


Figure 15: Block diagram representation of the small signal linearized performance of the single line generator-infinite bus system, including Automatic voltage regulator and excitation system [20]

The generator considered here is a simplified model, for which the power-angle characteristic is expressed through the transient induced internal voltage $\Delta E'_q$. The effect of the damper windings is represented by the damping constant D .

The stability of the system can be described by the location of the poles of the block diagram transfer function. The state of the system is the minimum amount of information needed to provide a complete description of the system behavior. This can be presented as a state space model as shown in equations 5.7 and 5.8.

$$\Delta \dot{\mathbf{x}} = \mathbf{A} \Delta \mathbf{x} + \mathbf{B} \Delta \mathbf{u} \quad (5.7)$$

$$\Delta \mathbf{y} = \mathbf{C} \Delta \mathbf{x} + \mathbf{D} \Delta \mathbf{u} \quad (5.8)$$

The A -matrix describes the dynamic characteristics of the system, while the B -matrix describes the inputs and disturbances the system is exposed to. The A and B matrix corresponding to the block diagram shown in Figure 15 are given in appendix A2.

The eigenvalues of the matrix A , are the values of s which satisfy the following equation

$$\det(s\mathbf{I} - \mathbf{A}) = 0 \quad (5.9)$$

The small signal stability of the system can be evaluated by the eigenvalues of the A-matrix for the linearized system, which are the roots of this characteristic equation. The eigenvalues may be real or complex. A damped mode has negative real part, while an unstable mode has a positive real part. The real part of the eigenvalue represents the damping, while the imaginary part describes the frequency of oscillation. An eigenvalue with positive real part gives an unstable system, as this represents oscillation of increasing amplitude. If all eigenvalues have negative real parts, this means the oscillations are damped and the system is stable. For the system to be asymptotic stable, all the eigenvalues need to have negative real parts. [12]

A real eigenvalue corresponds to a non-oscillatory mode. A negative real eigenvalue represents a decaying mode. A large magnitude of the eigenvalue means it has a faster decay. A positive real eigenvalue represents aperiodic instability. Complex eigenvalues occur in pairs, with positive and negative imaginary part. Each of these pairs corresponds to one oscillatory mode.

For a pair of eigenvalues

$$\lambda = \sigma \pm j\omega \quad (5.10)$$

The actual (damped) oscillation frequency, f , in Hz and the damping ratio, ζ , is given by the following expressions

$$f = \frac{\omega}{2\pi} \quad (5.11)$$

$$\zeta = \frac{-\sigma}{\sqrt{\sigma^2 + \omega^2}} \quad (5.12)$$

The damping ratio gives the decay rate of the oscillation amplitude.

The eigenvalues give a description of the response of the system. The eigenvalues are calculated based on the linearized system. The linearization is found as the tangential function of the power versus rotor angle characteristic.

5.2.2 Effect of the AVR on power system stability

The effect of the AVR in the transient period following a disturbance depends to a great extent on the excitation system time constant. If the time constant is large, the AVR is slow acting and will in principle not react during the transient period. In this case the AVR will not affect the stability limit other than the additional load it will add to the system. In the case of a short excitation system time delay, the AVR will react during the transient period and cause an increase in the steady state field current. This will affect the transient induced voltage $E' = E'_q$ ($E' = E'_q$ for the salient pole generator). The change of the transient induced voltage can be divided into two components, one caused by the rotor swings and the other by voltage regulation. This is shown in the following equations [6].

$$\Delta E'_q = \Delta E'_{q(\Delta\delta)} + \Delta E'_{q(\Delta E_f)} \quad (5.13)$$

$$\Delta E'_{q(\Delta\delta)} = -\frac{AB}{1 + BT'_{d0}S} \Delta\delta \quad (5.14)$$

$$\Delta E'_{q(\Delta E_f)} = +\frac{B}{1 + BT'_{d0}S} \Delta E_f \quad (5.15)$$

The component $\Delta E'_{q(\Delta\delta)}$, representing the change caused by rotor swing, is in phase with the speed deviation $\Delta\omega$ and will add damping to the system. The effect of the component $\Delta E'_{q(\Delta E_f)}$ depends on the phase shift of this component compared to the speed deviation. The block diagram in Figure 16 shows the components that affect the phase shift between these two components and which determines the sign of this damping component.

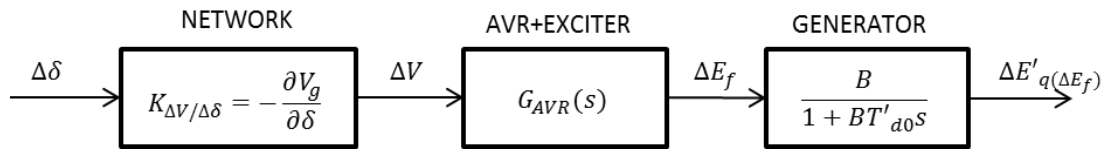


Figure 16: Components determining the phase shift between $\Delta\delta$ ($\Delta\omega$) and $\Delta E'_{q(\Delta E_f)}$.

The first block represents the network by the constant $K_{\Delta V/\Delta\delta}$ (which is a simplified, and negative, version of the linearization constant K_5 shown in Figure 15), this constant is normally positive which means that ΔV is in phase with the rotor angle change. The AVR/exciter block causes a phase shift between the field voltage change and ΔV , depending on the characteristics of the excitation system. The generator block adds a phase shift of approximately 90° , depending on the time constant T'_d . The minus sign in the expression of $\Delta E'_{q(\Delta\delta)}$ shows that this component leads ΔV , while the other component lags the voltage change. A phasor diagram of this situation is shown in Figure 17. Other systems and operating situations may lead to other phase shifts between the components. An inertia element will add an additional phase shift for ΔE_f and give a different phasor diagram.

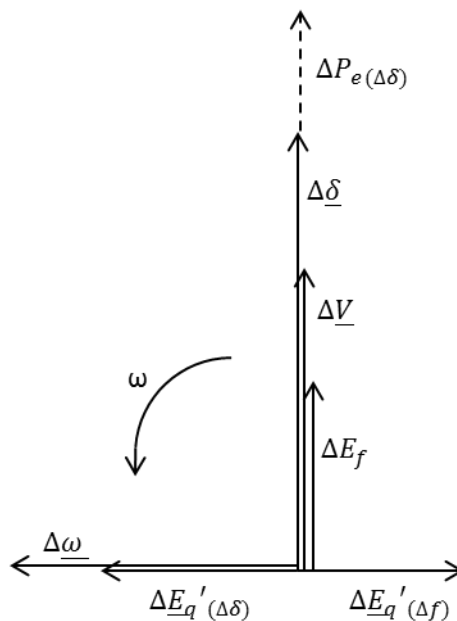


Figure 17: Phasor diagram demonstrating the phase shift between the excitation emf components.

As a part of the specialization project TET4520, performed at the Norwegian University of Science and Technology, spring 2013, an eigenvalue analysis was performed, considering the power system eigenvalues related to certain system parameters. Details about this power plant and the analysis are found in the project report [1]. The power system considered in this specialization project was Kuråsfossen power plant in Røros, where they were experiencing oscillations in active power in one of the synchronous generators. A sensitivity analysis was performed to investigate the influence certain parameters have on the stability of the system, including the AVR proportional gain.

The regulator gain is expected to have a significant effect on the stability of the system. A sensitivity analysis was done using MATLAB, where the eigenvalues was found corresponding to the voltage regulator gain which was increased from 0-100. For the original system the gain is set to 8. The result of this sensitivity analysis is shown in Figure 18, the complete results can be found in [1]. This is based on Kuråsossen power plant, and the values will be different for other cases, but the principle is expected to be the same.

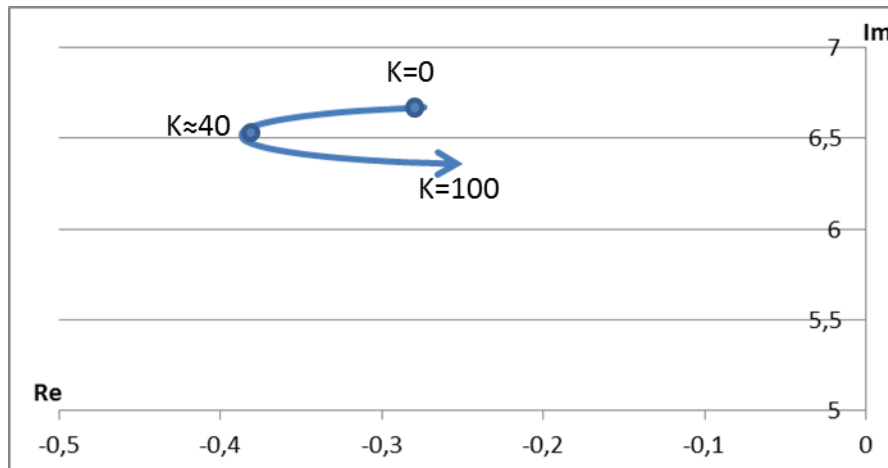


Figure 18: Sensitivity analysis, eigenvalues for increasing regulator gain 0-100.

Figure 18, shows how the eigenvalues of the system move, when the regulator gain is increasing from 0-100 in direction of the arrow. This shows that for high values of the gain, the damping of the mode decreases. In these cases the regulator causes the voltage to oscillate in counter phase to the rotor angle, which gives a negative contribution to the damping.

The influence of the regulator gain is also affected by the operating situation, the values of the linearization constants and reactance values. In a case where the linearization constants included in the feedback loop in Figure 15 are higher, the value of the regulator gain is expected to have a stronger influence on the damping of the system. If the product of these constants is negative, an increasing gain would lead to an increasing negative contribution to the damping, and a lower stability margin. To which extent the AVR influences the damping is therefore dependent on these linearization constants and the operating situation.

5.2.3 Effect of the field current limiters on power system stability

The field current limiters limits the field current, and thereby the field voltage E_f . During normal operation the AVR may change $E_q = E_f$ to keep the generator terminal voltage constant. If the field current reaches its upper limit and the overexcitation limiter is activated, the field current will not increase even though a load increase may cause a drop in the generator terminal voltage V_g . Figure 19 shows the power-angle curve for the system operating under field current limiting conditions, P_{EqMAX} , compared to regular operation shown as P_{Vg} . [6] [21]

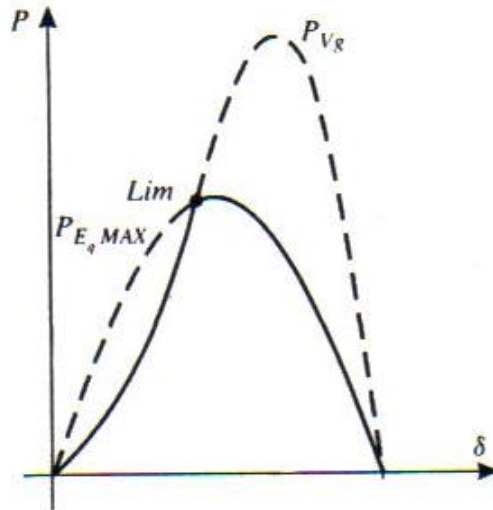


Figure 19: Example of the influence of the field current limiter on the steady state power angle characteristic [6]

The maximum value of the power P_{V_g} in the power angle curve depends on the external system reactance as well as the grid voltage and the generator terminal voltage. This relation is shown in the following equation.

$$P_{V_{gM}} = P_{V_g}(\delta) \Big|_{\delta=\delta_M} = \frac{V_g V_s}{X} \quad (5.16)$$

If the external system reactance is low, the power curve will have a high maximum value, and it is probable that the field current limiting function will be activated at a lower rotor angle than the one corresponding to the maximum power $P_{V_{gM}}$. This will change the power-angle relation, and can affect the system stability.

6 System description

The system studied in this report is the 17kVA motor-generator set in the renewable energy laboratory at NTNU/SINTEF. This laboratory model represents a small hydro power plant. Information about this model is found in the laboratory report [4].

6.1 Small hydro power plant model

The laboratory model representing a small hydro power plant, is built in the SINTEF/NTNU Renewable Energy Laboratory, and consists of:

- A HV/MV substation model with variable line inductance, transformer and two MV feeders with standard distribution network protection.
- A brushless synchronous generator with a DECS-200 digital excitation system,
- Turbine equivalent, induction motor, including a frequency converter for torque control.
- A flexible line equivalent with 6 line sections represented by π -equivalents with R, L and C. (Each line section is able to represent 2, 4 and 8km of 22kV overhead line with dimensions of 25 to 240mm².)

A single line diagram showing the main units of the SINTEF/NTNU Renewable Energy Laboratory is shown in Figure 20. The complete model is described in [4].

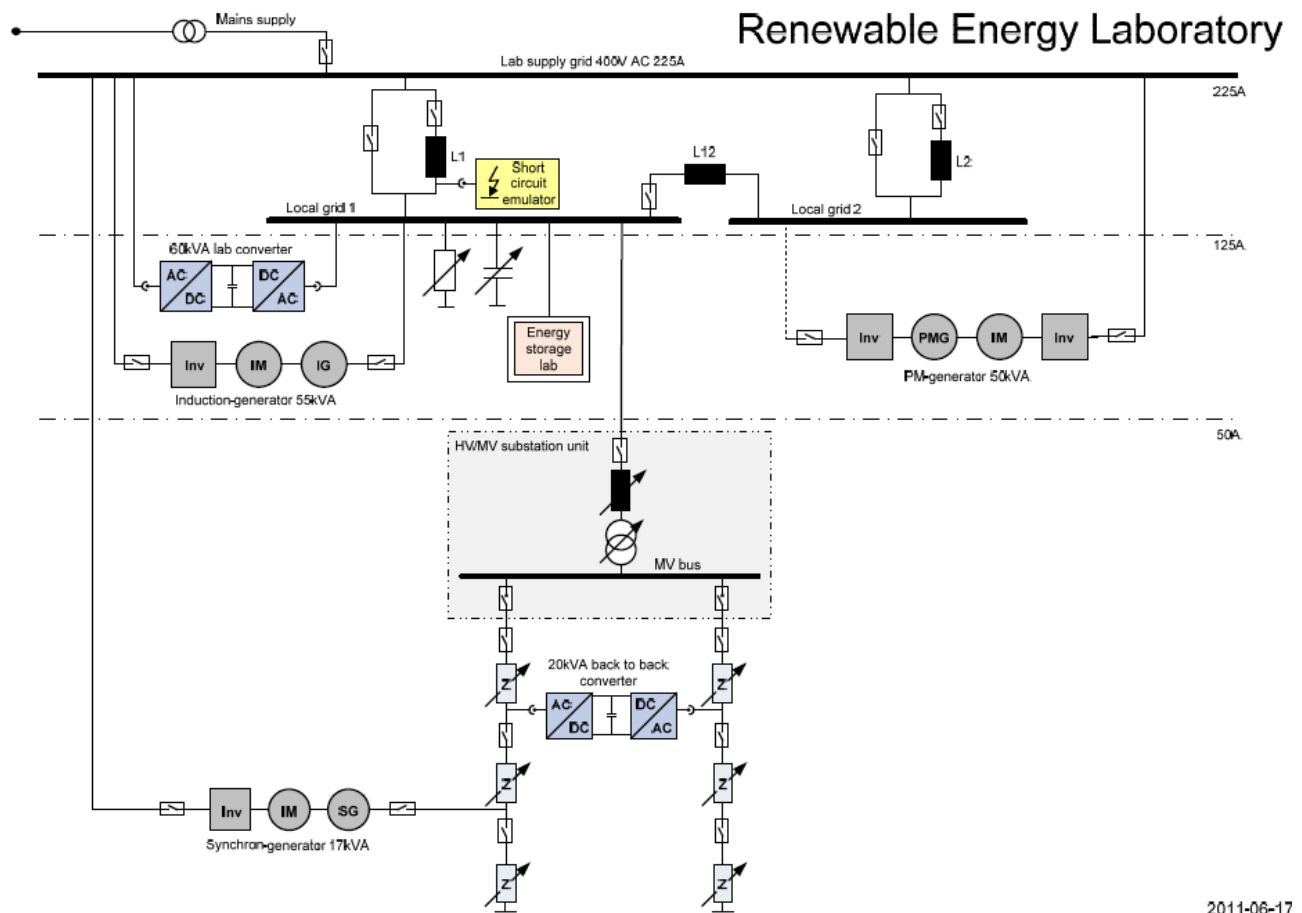


Figure 20: Single line diagram of the Renewable Energy laboratory showing the main units.

The network in the laboratory is down scaled compared to a real distribution network as follows:

Power:	1:1000
Voltage:	1:60
Current:	1:16.7
Line impedances:	1:3.6

The distribution generator (DG) unit model is a standard synchronous generator, with parameters close to those of a real small hydro power generator. Scaling factors are used to make the model comparable to a real system, as e.g. better damping due to increased losses in this generator compared to a real small hydro generator. The machine ratings are shown in Table 1.

Table 1: Ratings of the laboratory model [4]

Unit	Laboratory rating	Representing real network rating of:
HV network voltage	400 V	66 kV
HV short circuit capability	3.8 MVA (4 kA)	3.8 GVA
Maximum laboratory power supply	165 kVA	165 MVA
HV/MV transformer voltages	400/400 V	66/24 kV
Substation power rating	40 kVA	40 MVA
MV network voltage	400 V	24 kV
Short circuit current/power at HV bus	400-1200 A	300-900 MVA (66kV)
Short circuit current/power at MV bus	300-600 A	200-400 MVA (24kV)
Synchronous generator unit (DG) rating	17 kVA	17 MVA
MV line equivalent power rating	20-30 kVA	20-30 MVA

Ratings of the distribution network model can be found in appendix A5.

6.2 The distribution generator power plant model

The distribution generator power plant model consists of the following three units, as shown in Figure 20:

- Motor generator set (delivered by Bevi) with:
 - Brushless synchronous generator (17kVA Marelli type MJB 160 SA4)
 - Induction motor (18.5 kVA BEVI type 3D180M-4)
 - Extra fly wheel for changing the inertia (to be mounted on the shaft) -2 disks. Large disc approximately 0.35kgm^2 and small disc approximately 0.25kgm^2 . (The generator inertia is 0.11kgm^2 . motor inertia is assumed to be in the same range.)
- Generator excitation and control unit (delivered by Voith Hydro) with:
 - Basler DECS 200 digital excitation control system (incl. voltage control)
 - Deif Generator protective unit GPU
 - Additional over voltage protection unit
 - Manual or automatic synchronization
 - Data collection
- Frequency converter for induction motor control (delivered by Voith hydro)
 - A 22kW Siemens Micromaster 440 frequency converter, using encoder for motor speed measurement.

The frequency converter, controlling the motor torque, runs in vector control mode. The motor controller normally runs at speed control, with a speed regulator giving the torque reference signal. The maximum torque limit can be set on the generator control cabinet.

Table 2: Synchronous generator data (small hydro power model)

Ratings and parameters	Symbol	Values (at 50 Hz)
Serial no.	-	MW25667 10/09
Weight	-	Appr. 110kg
IO class	-	IP-23
Ambient temperature	-	40°C
Rated power	S_n	17kVA
Overload	S_{Max}	+10 for 1 hour
Rated Current	I_n	24.5 A
Short circuit current	I_{sc}	$3 \cdot I_n$
Rated voltage	U_n	400 V
Rated frequency	F_n	50 Hz
Rated power factor	$\cos\phi_n$	0.8
Number of poles	p	4
Rotation speed	n_n	1500 rpm
Over speed	-	2250 rpm
Direct axis synchronous reactance	X_d	2.5 pu
Direct axis transient reactance	X_d'	0.245 pu
Direct axis sub-transient reactance	X_d''	0.12 pu
Quadrature axis synchronous reactance	X_q	1.4 pu
Quadrature axis sub-transient reactance	X_q''	0.132 pu
Armature reactance	R_a	0.005 pu
Direct axis open-circuit transient time constant	T_{d0}'	0.4 s
Direct axis short-circuit transient time constant	T_d'	0.035 s
Direct axis short-circuit sub-transient time constant	T_d''	0.008 s
Inertia	J	0.109 kgm ²
Zero sequence reactance	X_0	0.016 pu
Negative sequence reactance	X_2	0.121 pu

6.3 Turbine governing system

In the laboratory model, the turbine and governing system is represented by a motor drive consisting of an induction motor and a frequency converter for torque control, as shown in Figure 21. It is not known exactly how this control works, but from tests done in the laboratory it seems to have a faster response than a regular hydraulic hydro turbine governing system.

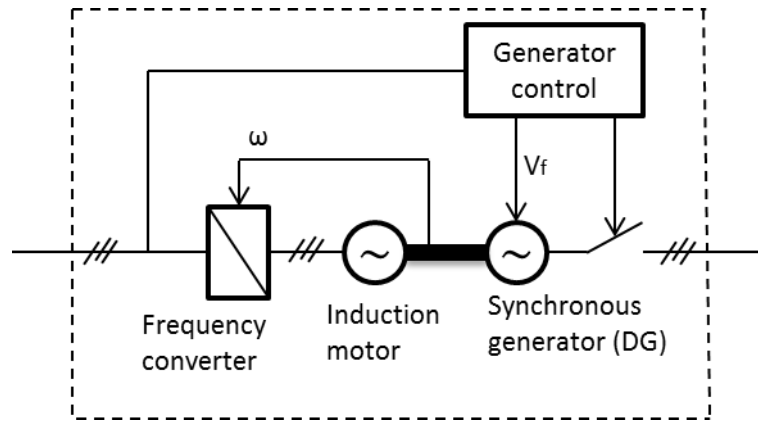


Figure 21: Laboratory model of the distribution generating unit, including the induction motor and frequency converter representing the turbine governing unit.

Figure 22 shows the equivalent block diagram of a simplified turbine governing system. This simplified model will be used for the simulations in part 6 and 7. Even though the laboratory model is a model of a small hydro power plant, the motor drive representing the governing system, seems to have a faster response than a regular hydro turbine. A simple turbine governor model, consisting of a gain and a time delay, gives a better representation of the laboratory model. A torque limiting block is also included in the simulation model of the turbine governing system. The laboratory model can be set to operate at its torque limit, which can be recreated in the simulation. This will be further discussed in the following parts of the report.

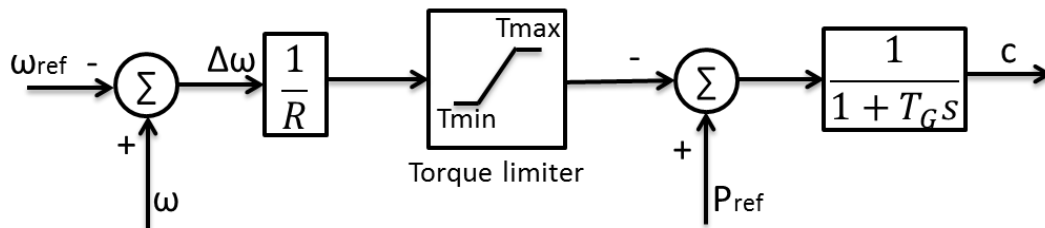


Figure 22: Simple turbine governor equivalent diagram

6.4 Excitation system

The excitation system modeled for the simulations in this report is an electronic digital voltage regulator for static excitation, called HPC 185. The model used here, is developed from the work done by Kjetil Uhlen, professor at NTNU, in [5]. The control functions of HPC185 and the Basler DECS 200 are very similar. Therefore the simulation model developed can be used to represent both systems.

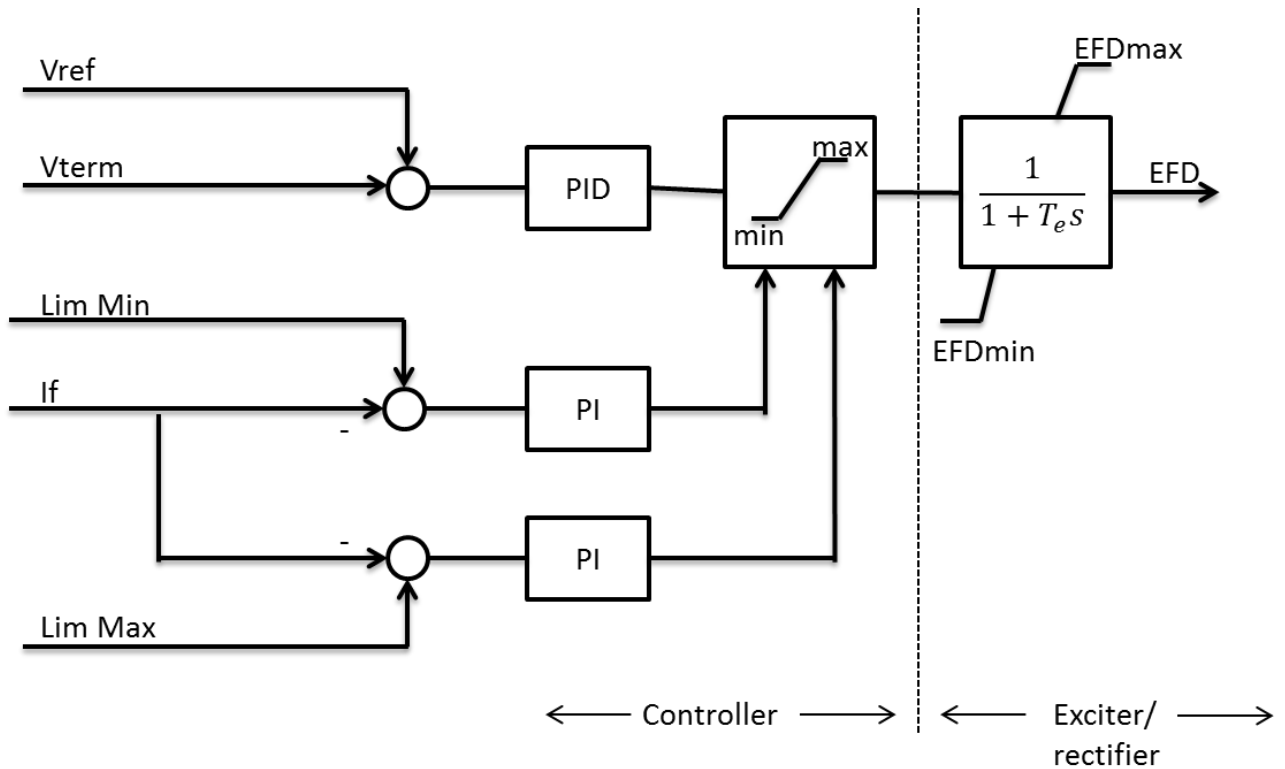


Figure 23: Simplified block diagram of excitation system HPC 185, based on figure from [5]. Vref: voltage reference value, Vterm: measured generator terminal voltage, If: field current, EFD: AVR output field voltage.

HPC 185 represents a complete excitation system, consisting of an exciter and an AVR. The exciter part is a three-phase thyristor controlled rectifier. The rectifier is assumed to be an approximately linear component with very fast dynamics.

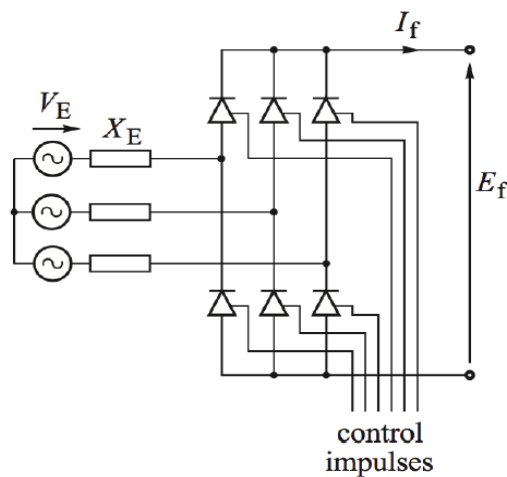


Figure 24: Three-phase thyristor converter for static excitation.

Under normal operational conditions, the voltage regulator is modeled as a limited PID-regulator. The regulator can operate either as a voltage regulator or a field current regulator. In this report the focus is on the voltage regulation mode. HPC 185 has the possibility for both active and reactive power versus voltage compensation and reactive droop.

HPC 185 includes several protection- and limitation functions. The field current limiters are dynamic, and operate through dynamic PI-regulators controlling the upper and lower limit of the regulator output. The field current is measured continuously, and if it exceeds a certain limit, the PI-regulator for the upper limit will subtract the actual value of the field current from the maximum limit. This will give a negative input to the PI-regulator, which will lower the maximum limit of the PID-voltage regulator. The lower limit operates the same way. When the field current is lower than the minimum limit, the input to the PI-regulator will become positive and the lower limit of the PID- voltage regulator will increase.

7 Model validation

The small hydro power plant model in the renewable energy laboratory at NTNU/SINTEF can be a useful model for future power system stability studies at NTNU. In the first part of this report, the laboratory model will be used for validation of a simple simulation model consisting of a synchronous generator connected to a stiff grid. An important part of the model is the excitation system including the AVR. The simulation model also includes a simplified model of the turbine governing system.

This part of the report concerns validation of the simulation model, as well as validation and verification of the laboratory model and its parameters and characteristics. The main focus will be on the small signal stability of the system.

7.1 Laboratory testing

In this part of the report the model considered is the small hydro power plant model in the renewable energy laboratory at NTNU.

A number of tests are done in the Renewable Energy Laboratory at NTNU to validate the simulation model, and to document different aspects regarding the “small hydro power plant model” in the laboratory. Voltage, current, rotor speed and field voltage are measured as different disturbances is applied to the system. The tests are done with different initial operational states, to see how this affects the response and the stability of the system.

7.1.1 Model setup and test scenarios

A simplified per phase equivalent of the laboratory test system is shown in Figure 25. The network impedance can be changed by connecting or disconnecting the parallel branch including Z_1 and Z_2 .

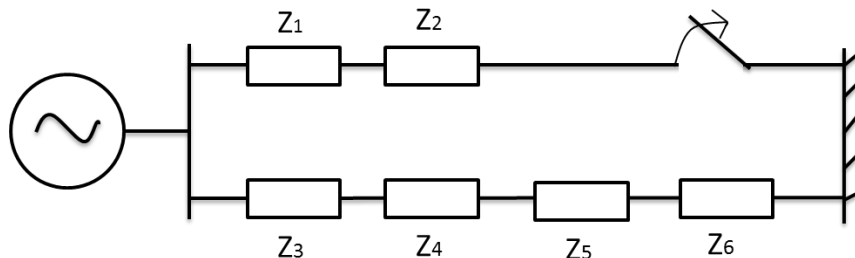


Figure 25: Per phase equivalent of laboratory system network

Mainly three different aspects of the stability of the laboratory model are studied through these tests;

- How torque limiting operation affect the system response and behavior.
- How the initial operational state of the generator affects the system stability (initial active and reactive power production/consumption).
- How the AVR gain affects the Stability.

These factors are studied by applying two different disturbances to the system;

- Increasing the system impedance, by disconnecting parallel branch, representing outage of this branch.
- Applying a 200ms short-circuit.

The settings for the excitation system are the same for every test, except for the AVR gain which is varied as shown in Table 3. These settings are shown in the following table:

Table 3: AVR parameters, laboratory model

Parameter	Value
Kp	Varying (std. 55)
Ki	120
Kd	0
Td	0

Table 4 shows the different test scenarios. All tests are done with the system operating at its torque limit if nothing else is commented. This is to prevent exaggerated damping of the oscillations:

Table 4: Test scenarios for model validation.

Test nr	Disturbance	P [kW]	Q [kVAr]	AVR gain Kp	V[V] Measured	Vf[V] Measured	Remarks
1	Low-high Impedance	5	5	55	429	15	Oscillations stabilizes
2	Low-high Impedance	5	-5	55	388	10	Less oscillations
3	Low-high impedance	5	5	110	430	16	Sustained oscillations,
4	Short-circuit	10	0	100	-	-	Not at torque limit.

For each case, the line to line voltage and the current is measured directly from the measuring cabinet in the laboratory, and scaled according to the information on the cabinet. A photo of the laboratory model including this cabinet is shown in appendix A4. The voltage and current phasors are calculated from the measured values using a MATLAB algorithm representing a PMU. These phasor values are used to calculate the output active and reactive power for the generator, by the following equations:

$$\begin{aligned}
 P &= 3I_{ph}U_{ph} \cos \varphi \\
 Q &= 3I_{ph}U_{ph} \sin \varphi \\
 U_{ph} &= \frac{1}{\sqrt{3}}U_{LL} \angle 30^\circ
 \end{aligned}
 \tag{7.1}$$

Where φ is the angle between the voltage and the current phasor. The MATLAB codes used can be found in appendix A6.

The field voltage is measured from within the excitation system cabinet, and the response is not processed to give an appropriate output signal. To obtain the appropriate output signal the measured values are scaled and run through a simple low pass MATLAB filter.

7.1.2 Laboratory test results

Only a selection of the tests done in the laboratory is presented in this report. The remaining test scenarios and the resulting Voltage, current, active- and reactive power response for all cases can be found as MATLAB plots in appendix A8.

The turbine governor model, represented by in induction motor with a frequency converter for torque control, clearly affects the response of the system. To demonstrate this, the system is set to operate at its torque limit, to give a more realistic representation of the relatively slow response of hydro turbine governors.

The active power response of the system in operation scenario 1, not operating at its torque limit, is shown in Figure 26 (a) and (b). In this case the turbine governing system clearly has a dampening effect on the response, which is very well damped. The response of the system operating at its torque limit is shown in Figure 26 (b). This response shows clearly that the system has a lower damping of the oscillations.

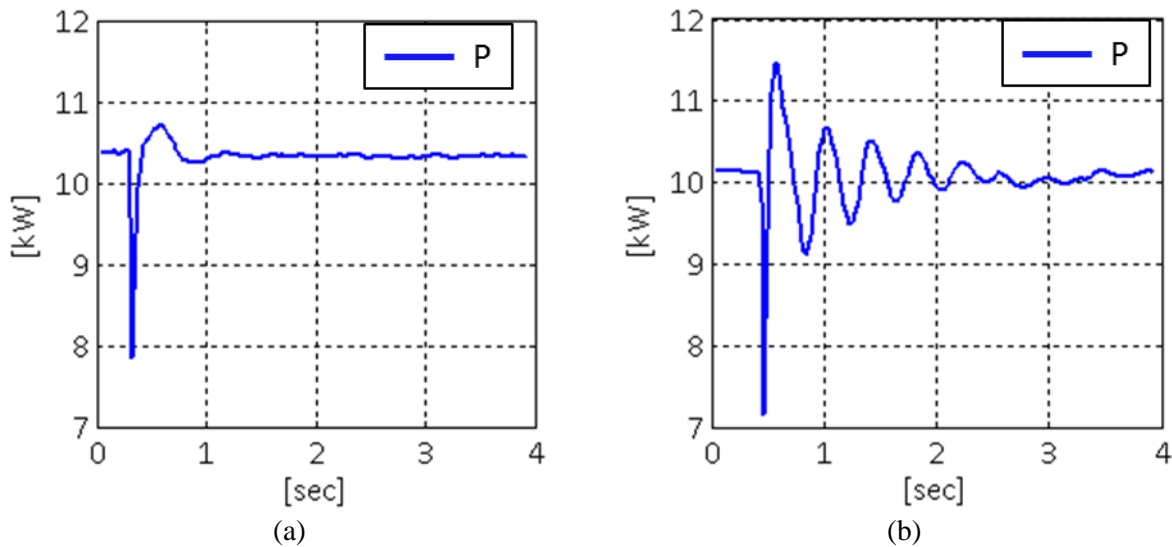


Figure 26: Active power output response of generator initially producing $P=10\text{kW}$, subjected to a small disturbance represented by increased system impedance. (a) Not at torque limit, (b) At torque limit

The effect of the system operating at its torque limit is similar for all measured responses in this system, but has the greatest impact on the active power and current response, as can be seen in appendix A8. To give a more realistic approximation of the relatively slow response of hydro turbine governors, the system is set to operate at torque limit in this part of the report.

Case 1

Table 5: Operation situation, laboratory model, case 1

Active power production	P	5100W
Reactive power production	Q	5750VAr
AVR proportional gain	P(PID)	55
AVR Integral gain	I(PID)	120
Initial voltage (Line to line)	V	430V
Initial Field voltage	Vf	12V
Disturbance	Sudden increase of network impedance	

In test scenario 1 and 2, the main aim is to study the difference in the response in two different operating situations as a sudden change in the network impedance is applied. The initial operating

conditions are different for the two cases. In case 1 the generator is producing reactive power, while in case 2 it is consuming. For both cases the disturbance applied is an increase in the network impedance.

In the first operating scenario, the generator is producing approximately 5kW (≈ 0.3 pu) active power and 5kVAr (≈ 0.3 pu) reactive power as described in Table 4 and 5. A small disturbance, represented by an increase in the network impedance, is applied to the system initially operating at steady state. The voltage and current response of the system is shown in Figure 27.

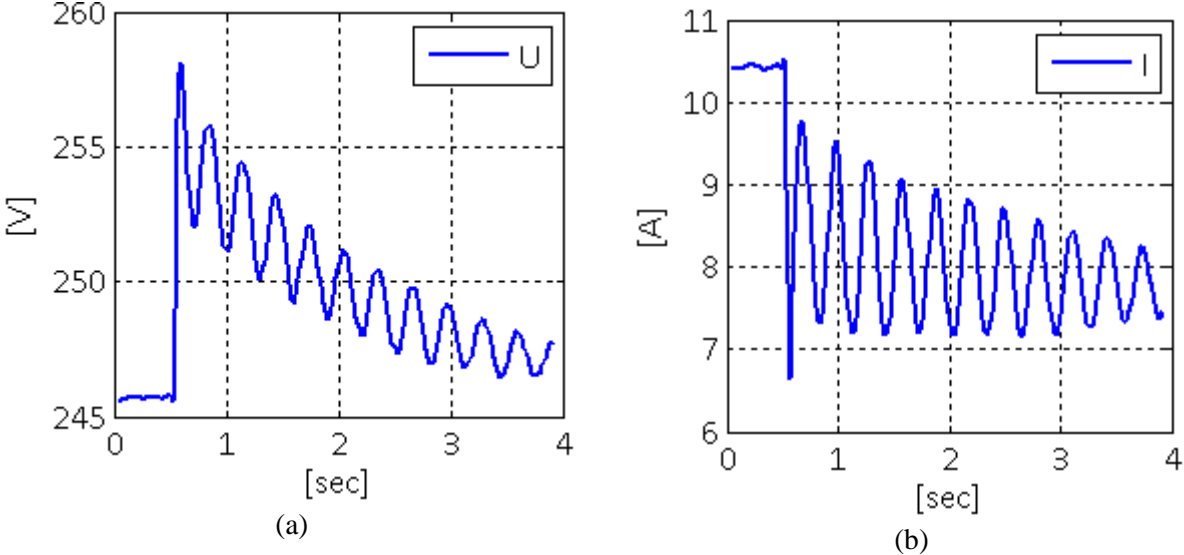


Figure 27: System response following a small disturbance, of the system initially operating at $P=5$ kW, $Q=5$ kVAr. (a) Generator output voltage (b) Generator output current

The voltage and current response shows a poorly damped system, with an oscillation frequency of approximately 3Hz. The voltage has an initial steady state value of 245V ($=1.065$ pu). As the disturbance occurs, the voltage increases, before it relatively slowly while oscillating returns to its initial value.

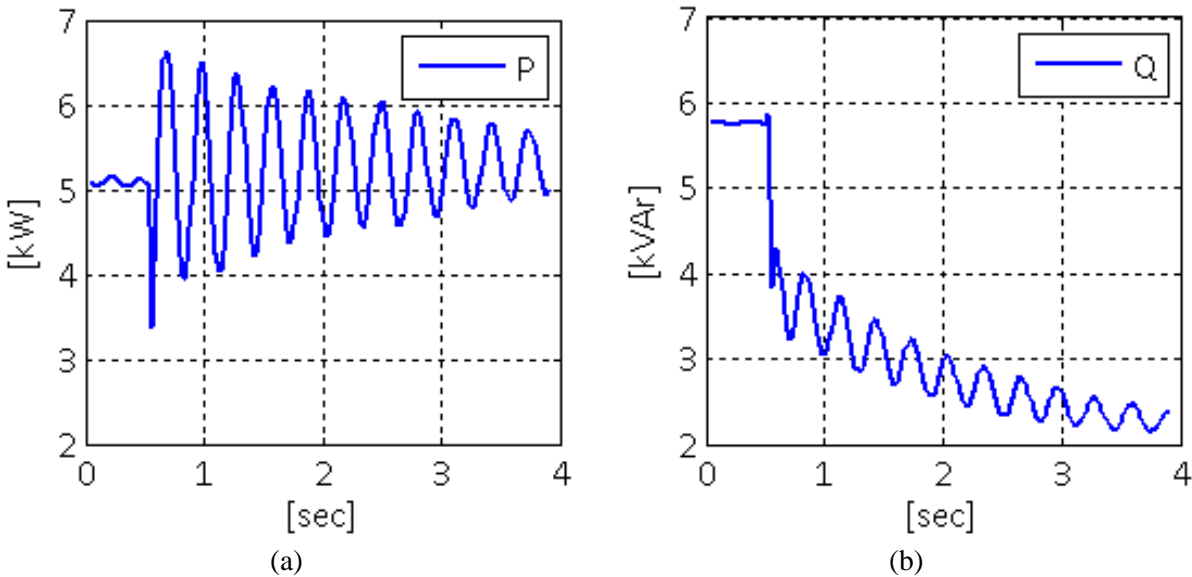


Figure 28: Output power response following a small disturbance, of the system initially operating at $P=5$ kW, $Q=5$ kVAr. (a) Active power, (b) Reactive power

Figure 29 shows the field voltage response of the system. This response particularly, gives an indication of the characteristics and the parameter settings of the AVR.

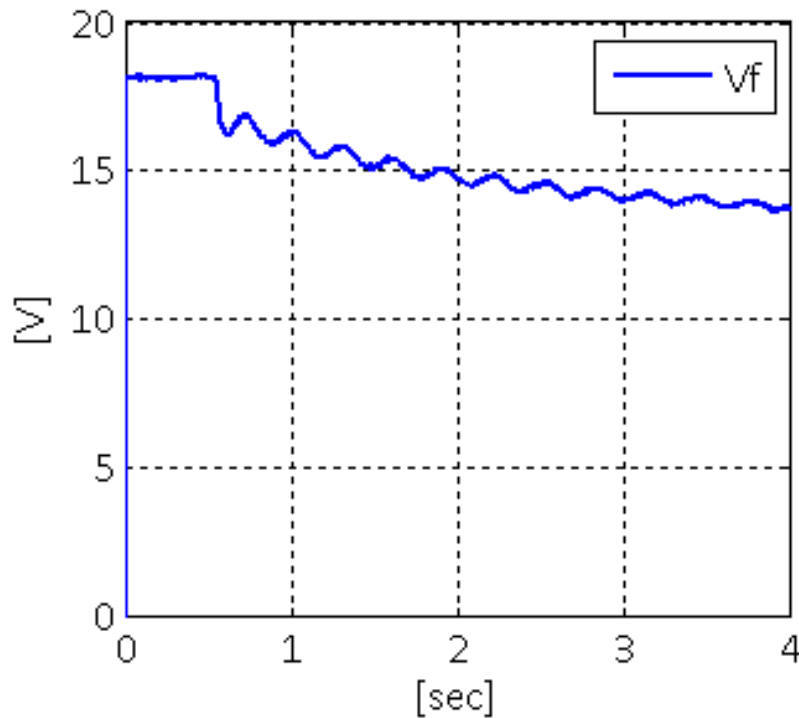


Figure 29: Field voltage response following a small disturbance, for the system initially operating at $P=5\text{kW}$, $Q=5\text{kVAr}$

The AVR field voltage response shown in Figure 29 shows an initial steady state value of 18V. Following the sudden increase of the system impedance, the field voltage drops rather slowly until it reaches a new steady state value at approximately 14V.

Case 2

In the second case considered in this report the generator is consuming reactive power as shown in Table 6.

Table 6: Operation situation, laboratory model, case 2

Active power production	P	5100W
Reactive power production	Q	-4900VAr
AVR proportional gain	P(PID)	55
AVR Integral gain	I(PID)	120
Initial voltage (Line to line)	V	430V
Initial Field voltage	Vf	12V
Disturbance	Sudden increase of network impedance	

The system response to the disturbance in this case is shown in the following figures. Output generator voltage and current are shown in Figure 30 and Figure 31, while the active and reactive power response is shown in Figure 32 and Figure 33. The initial operating situation in this case seems to give a better damped system response with a lower oscillation frequency. The oscillation frequency is now reduced to approximately 2Hz, and the response is significantly better damped.

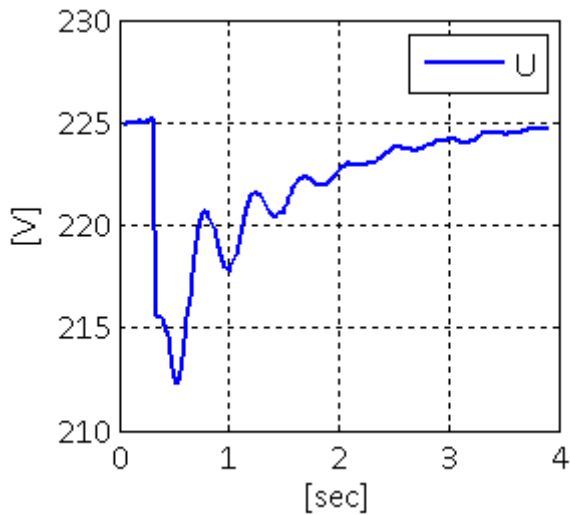


Figure 30: Generator output voltage response following a small disturbance, of the system initially operating at $P=5\text{kW}$, $Q=-5\text{kVAr}$.

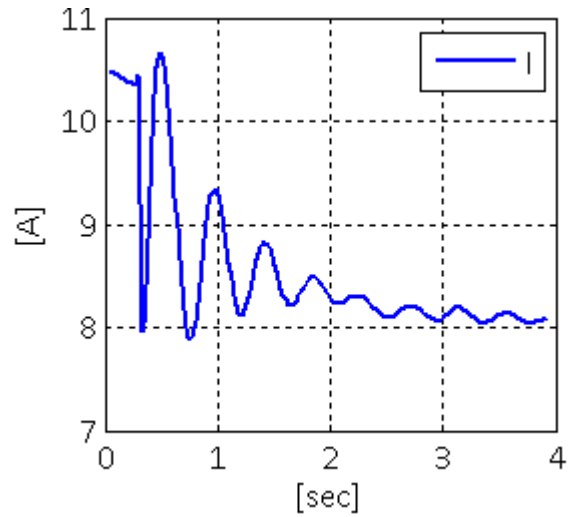


Figure 31: Generator output current response following a small disturbance, of the system initially operating at $P=5\text{kW}$, $Q=-5\text{kVAr}$.

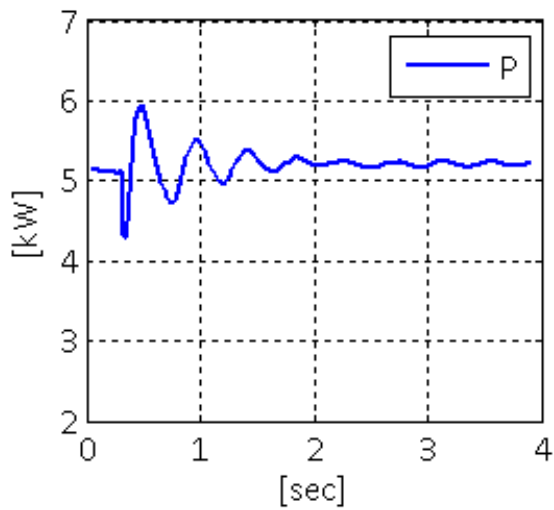


Figure 32: Active power response following a small disturbance, of the system initially operating at $P=5\text{kW}$, $Q=-5\text{kVAr}$.

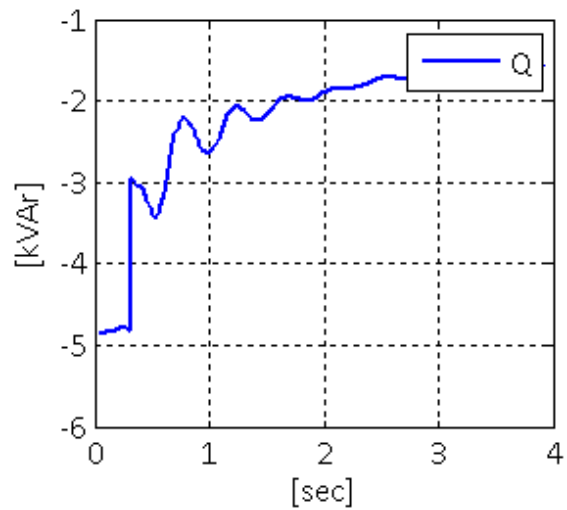


Figure 33: Reactive power response following a small disturbance, of the system initially operating at $P=5\text{kW}$, $Q=-5\text{kVAr}$.

The corresponding AVR output field voltage is shown in Figure 34. The field voltage increases to compensate for the generator voltage drop.

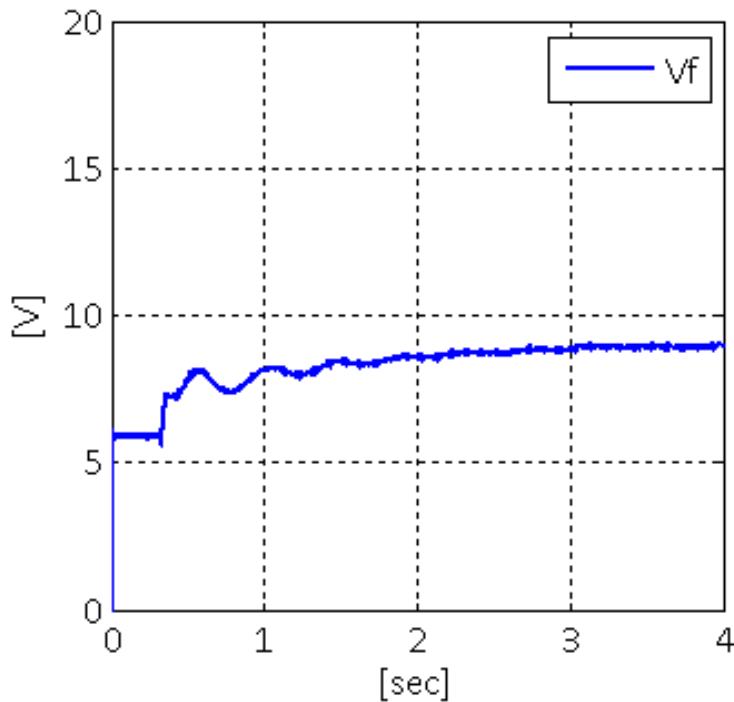


Figure 34: AVR output field voltage response following a small disturbance, of the system initially operating at $P=5\text{kW}$, $Q=-5\text{kVar}$.

Case 3

In case 3 the operating situation is approximately the same as for case 1, except from the AVR proportional gain which is doubled as shown in Table 7.

Table 7: Operation situation, laboratory model, case 3

Active power production	P	5100W
Reactive power production	Q	-4900Var
AVR proportional gain	P(PID)	110
AVR Integral gain	I(PID)	120
Initial voltage (Line to line)	V	430V
Initial Field voltage	V_f	12V
Disturbance	Sudden increase of network impedance	

The field voltage response to the disturbance in case 3 is shown in Figure 35. Output generator voltage and current are shown in Figure 36 and Figure 37, while the active and reactive power response is shown in Figure 38 and Figure 39. From these responses it is obvious that the AVR proportional gain affects the stability for this system. In this case it leads to an unstable system. The AVR can in some cases add a negative component to the system damping as explained in 5.2.2.

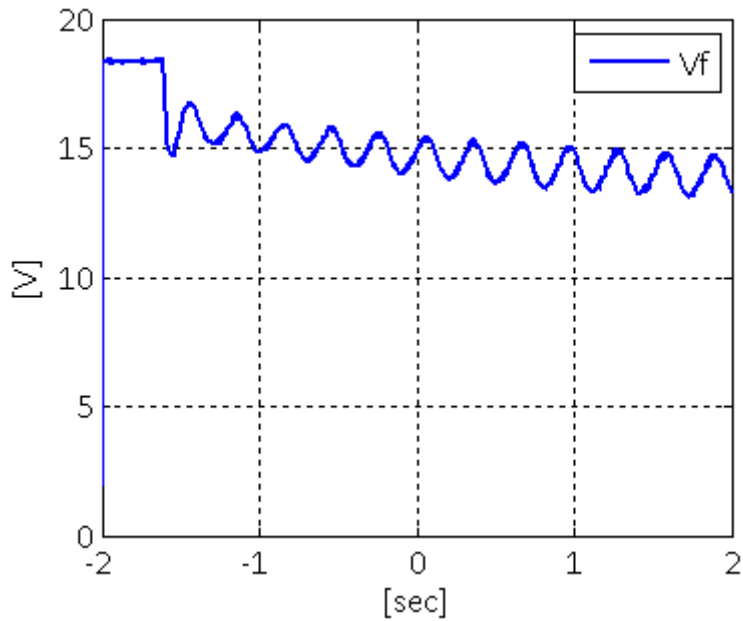


Figure 35: Field voltage response, Laboratory model case 3

The voltage, current, active and reactive power responses are all similar to the response of case 1, with the same initial operation and approximately the same oscillation frequency. The lack of damping torque cases instability for the system in this case, while for case 1 the oscillations decreases in amplitude, and stabilizes at a new steady state operation point.

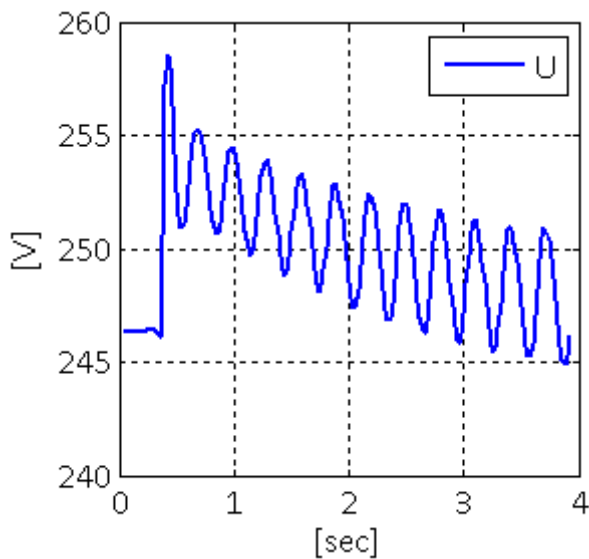


Figure 36: Generator output voltage response following a small disturbance, $K_{pr}(AVR)=110$

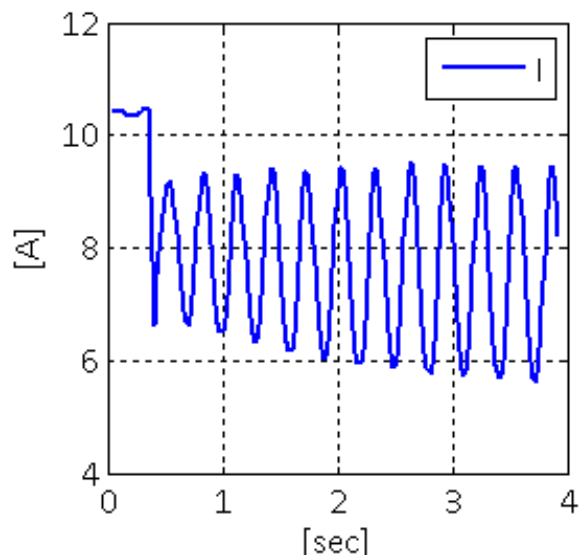


Figure 37: Generator output current response following a small disturbance, $K_{pr}(AVR)=110$

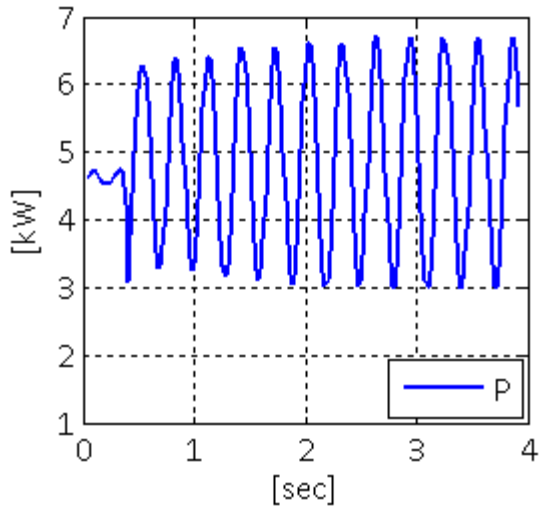


Figure 38: Active power response following a small disturbance, of the system

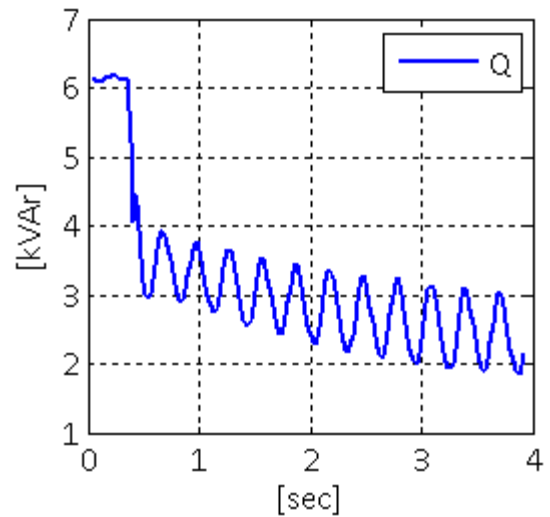


Figure 39: Reactive power response following a small disturbance, of the system

Case 4

In case 4 a 200ms short circuit is applied to the system. The generator is initially operating as shown in Table 8. With no reactive power production and the AVR proportional gain set to 100. In this case the system is not operating at its torque limit.

Table 8: Operation situation, laboratory model, case 4

Active power production	P	10 000W
Reactive power production	Q	0VAr
AVR proportional gain	P(PID)	100
AVR Integral gain	I(PID)	120
Initial voltage (Line to line)	V	415V
Initial Field voltage	Vf	16V
Disturbance		200ms short circuit

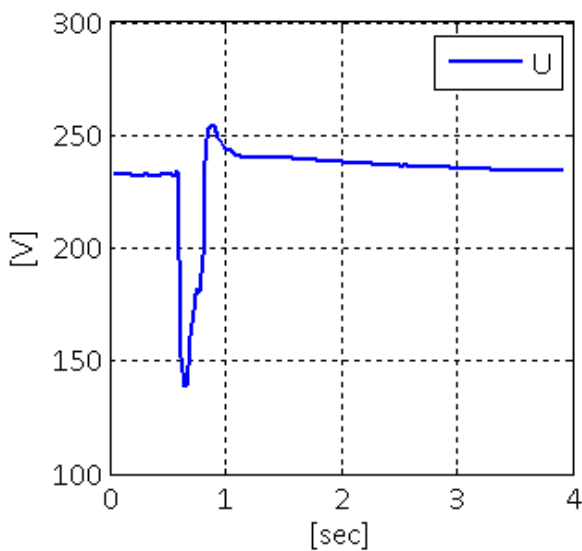


Figure 40: Case 4. Voltage response following a 200ms short circuit

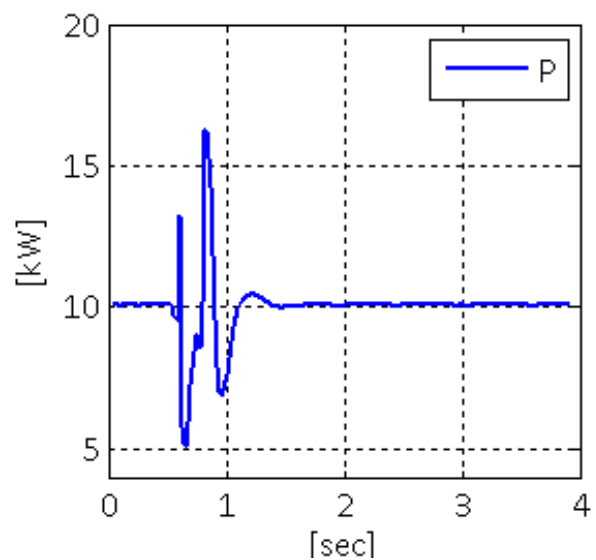


Figure 41: Case 4. Active power response, following a 200ms short circuit.

Following the short circuit, the voltage drops approximately 100V. When the fault is cleared, the voltage returns to its initial value. Because the system is not operating at its torque limit, the system is very well damped, and the voltage returns to its steady state value without oscillating about this value.

Figure 42 shows the field voltage response for case 4. As the voltage drops following the short circuit, the field voltage increases correspondingly, and more field current is supplied to the generator field windings to maintain a constant voltage at the generator output.

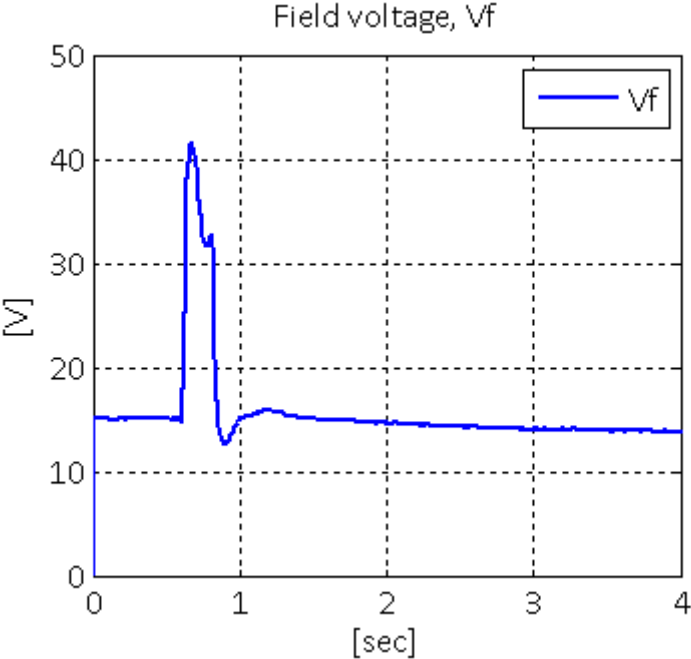


Figure 42: Case 4. AVR field voltage response following a 200ms short circuit

7.2 Simulations

7.2.1 Simulation model

The simulation test system is a simple model of a synchronous generator connected to a stiff grid, modeled as a three-phase programmable voltage source. The generator model contains the automatic voltage regulator AC8B from the IEEE standard 421.5 for excitation systems. This represents a complete excitation system consisting of a digital electronic AVR part, and a three-phase thyristor controlled rectifier for power supply.

The synchronous generator model used in Simulink is represented by a sixth-order state-space model, and includes the dynamics of the stator, field and damper windings. The model of the machine is represented in rotor reference frame, and is shown in Figure 43.

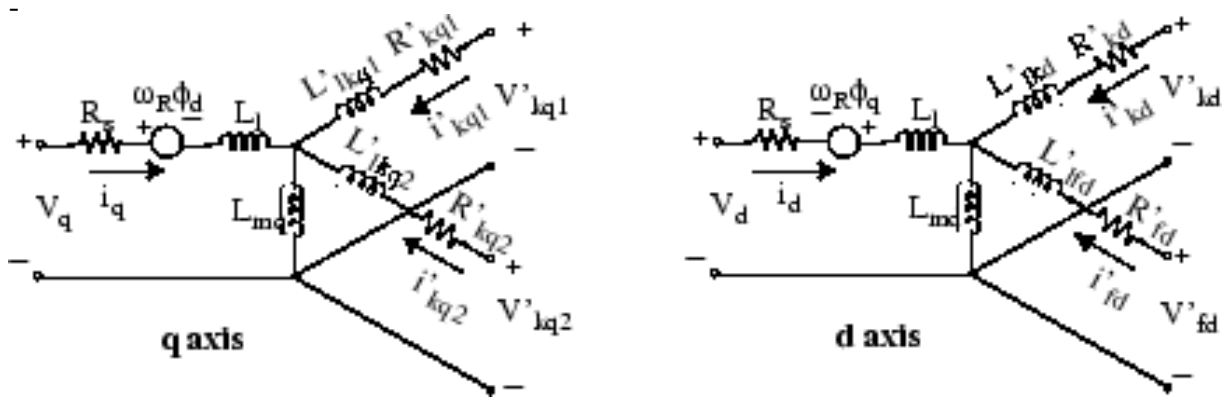


Figure 43: Electrical model of the synchronous generator. d,q, d and q axis quantity; R,s, rotor and stator quantity; l,m, leakage and magnetizing inductance; f,k, field and damper winding quantity. [22]

With the following related equations:

$$\begin{aligned}
 V_d &= R_s i_d + \frac{d}{dt} \varphi_d - \omega_R \varphi_q & \varphi_d &= L_d i_d + L_{md} (i'_{fd} + i'_{kd}) & (7.2) \\
 V_q &= R_s i_q + \frac{d}{dt} \varphi_q - \omega_R \varphi_d & \varphi_q &= L_q i_q + L_{mq} i'_{kq} \\
 V'_{fd} &= R'_{fd} i'_{fd} + \frac{d}{dt} \varphi'_{fd} & \varphi'_{fd} &= L'_{fd} i'_{fd} + L_{md} (i_d + i'_{kd}) \\
 V'_{kd} &= R'_{kd} i'_{kd} + \frac{d}{dt} \varphi'_{kd} & \varphi'_{kd} &= L'_{kd} i'_{kd} + L_{md} (i_d + i'_{fd}) \\
 V'_{kq1} &= R'_{kq1} i'_{kq1} + \frac{d}{dt} \varphi'_{kq1} & \varphi'_{kq1} &= L'_{kq1} i'_{kq1} + L_{mq} i_q \\
 V'_{kq2} &= R'_{kq2} i'_{kq2} + \frac{d}{dt} \varphi'_{kq2} & \varphi'_{kq2} &= L'_{kq2} i'_{kq2} + L_{mq} i_q
 \end{aligned}$$

The synchronous generator model used in these simulations is one of the standard Simulink models called *Synchronous Machine pu Standard*.

To recreate the tests done in the laboratory, a simulation model is made in MATLAB/Simulink, similar to the small hydro power plant model in the renewable energy laboratory at NTNU. Most of the system parameters are known from the laboratory model description [4]. The parts of the system which are not fully described in in that report are found by simulations and customized for the response to be as similar to the laboratory measurements as possible.

A simplified per phase diagram of the simulation model is shown in Figure 44. The generator model includes simplified AVR and governor models, adjusted to recreate the response found for the laboratory model. To simulate the small disturbance applied to the laboratory model, the generator is connected to the grid through two transmission lines, and one is disconnected to simulate an increase of the system impedance. The impedance values are adjusted through simulations, and are shown in Table 9.

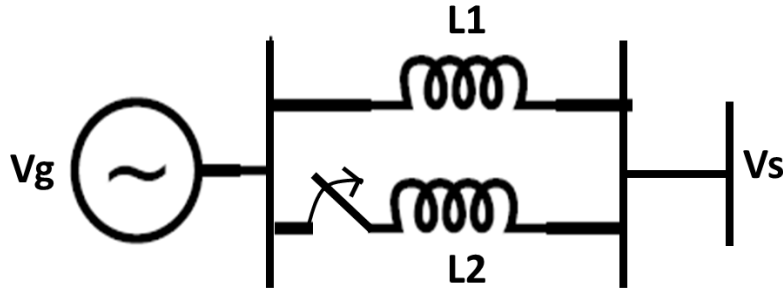


Figure 44: Per phase equivalent diagram for the simulation model.

Table 9: Network parameters

Description	Parameter	value
Grid voltage	Vs	1.028
Line 1 inductance	L1	7.958mH
Line 1 resistance	R1	0.25ohm
Line 2 inductance	L2	5.694mH
Line 2 resistance	R2	0.2ohm
Breaker resistance	Ron	0.00001ohm
Snubbers resistance	Rp	10 ⁶ ohm

Most of the generator parameters are given in the report describing the laboratory model. The parameters given in Table 10, are all given in this report, except for the inertia constant H, the quadrature axis short-circuit sub-transient time constant, and the leakage reactance. The leakage reactance is given the value of 0.104, while the quadrature axis short-circuit sub-transient time constant is set to be equal to the Direct axis short-circuit sub-transient time constant. This is decided through simulations.

Table 10: Generator parameters

Description	Parameter	value
Direct axis synchronous reactance	X _d	2.5 pu
Direct axis transient reactance	X _d '	0.245 pu
Direct axis sub-transient reactance	X _d ''	0.12 pu
Quadrature axis synchronous reactance	X _q	1.4 pu
Quadrature axis sub-transient reactance	X _q ''	0.132 pu
Armature reactance	R _a	0.005 pu
Leakage reactance	x _l	0.104
Direct axis open-circuit transient time constant	T _{d0} '	0.4 s
Direct axis short-circuit transient time constant	T _d '	0.035 s
Direct axis short-circuit sub-transient time constant	T _d ''	0.008 s
Quadrature axis short-circuit sub-transient time constant	T _q ''	0.008 s
Inertia constant	H	0.4
Pole pairs	p	2

The moment of inertia of the laboratory distribution generator model, is given as $J=0.109\text{kgm}^2$, corresponding to an inertia constant $H=0.079$. In addition the induction motor flywheel and the shaft add inertia to the system. The total inertia is set to be $H=0.4\text{s}$. This value is decided through evaluating the response of the simulation model at different values of H.

The turbine governing system is briefly described in the report [4]. It is represented by an induction motor with a frequency converter controlling the motor torque. This system is modeled as shown in Figure 45. This is a simple model representation of a turbine governing system consisting of a proportional gain, a time delay and torque limiters.

When operating at its torque limit, the response of the laboratory model is poorly damped. This is attempted to recreate by operating the simulation governing model at torque limit. To obtain the desired responses the governing model parameters are adjusted by simulations and the final values are shown in Table 11. The system response and the stability limit are quite sensitive for changes in these parameters. A brief sensitivity analysis of the most uncertain parameters will be presented in part 7.3.

Table 11: Governor settings

Description	Parameter	Value
Speed reference value	wref	1
Active power reference value	Pref	0.301
Governor gain	Kgov	14
Governor time constant	Tgov	0.022
Maximum power limit	Max_lim	0.3
Minimum power limit	Min_lim	-0.3

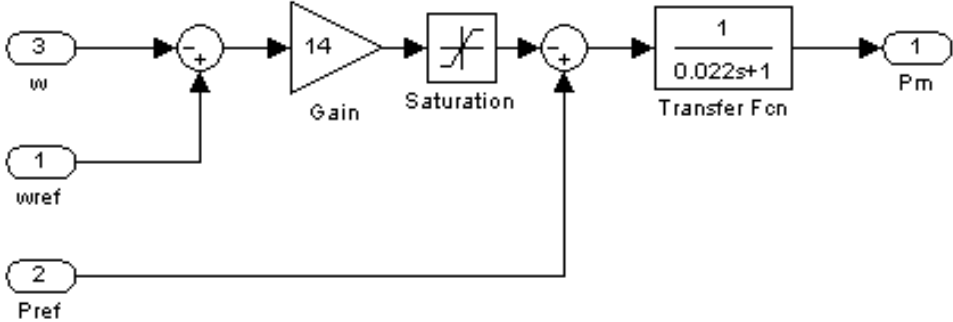


Figure 45: Simulink model of the simplified turbine governing system

The excitation system model, including the AVR, represents the voltage regulator HPC 185. Under normal operation conditions the AVR is modeled as a limited PID-regulator. The Simulink block diagram of the excitation system is shown in Figure 46.

The excitation system includes dynamic excitation limiters for over- and under- excitation operation, as shown in the figure. These both consist of PI-regulators, to reduce the field current if it crosses a certain limit. The excitation limiters will be further described in part 8 of the report, and are only briefly mentioned here.

HPC 185 has the possibility for both active and reactive compensation and reactive statics. From the model in Figure 46, a positive value of D_r or D_a gives compensation. A negative value of D_r gives static function. These compensation functions are not considered in the simulations in this part.

Table 12: AVR settings

Description	Parameter	Value
PID regulator proportional gain	P(PID)	(55)
PID regulator integral gain	I(PID)	(120)
PID regulator derivative gain	D(PID)	0
PI regulator proportional gain	P(PI)	10
PI regulator integral gain	I(PI)	2
Regulator time constant	Tr	0.03s
Voltage reference value	Vref	1.065 pu
Maximum voltage limit	Max_Lim	5 pu
Minimum voltage limit	Min_Lim	-5 pu
Reactive compensation factor	Dr	0
Active compensation factor	Da	0

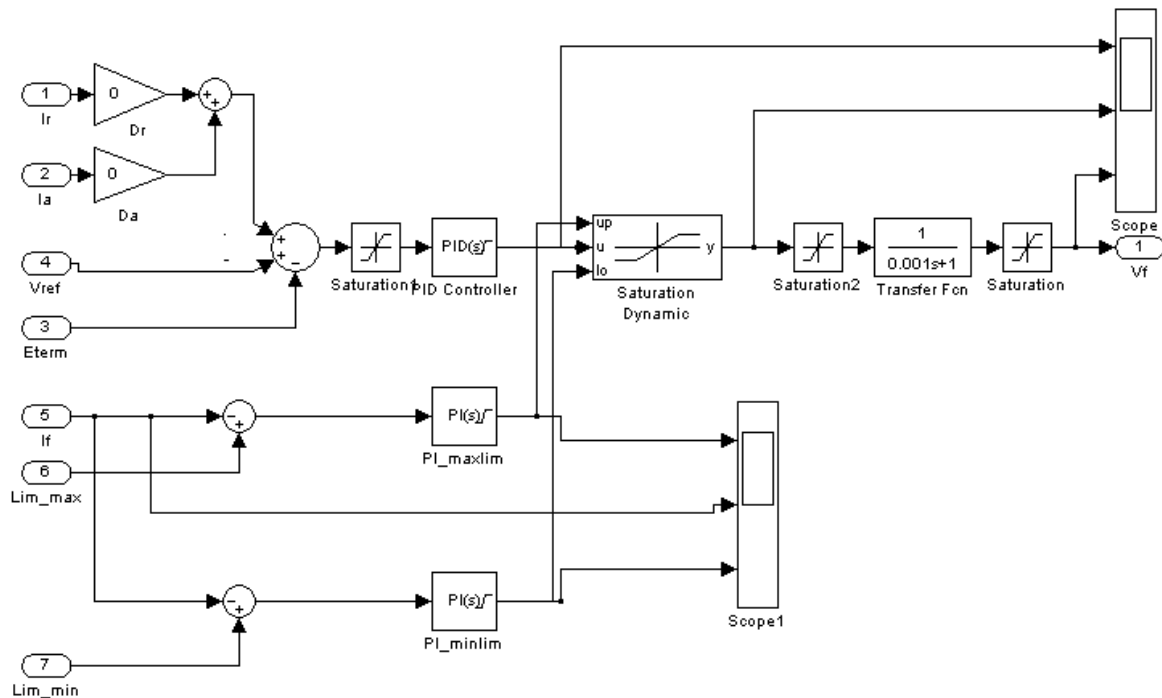


Figure 46: AVR/excitation system simulation model

7.2.2 Simulation results

The simulations in this part of the report are done to recreate the responses from the laboratory tests, for model validation. The simulations are done of the system operating at torque limit, to avoid the exaggerated damping of the induction motor and the torque controlling frequency converter in the laboratory tests.

Details of operation scenario 1 from the laboratory testing are given in the following table. To simulate this situation, the simulation generator model is set to produce the same amount of power as in the laboratory, and the voltage reference value is adjusted to give the appropriate initial condition. As the system has reached a steady state operation, the network impedance is increased by disconnecting branch L2.

Disturbance	Before	After
System impedance is increased	L=0.00332	L=0.00569

Case 1

Table 13: Generator operating situation, simulation case 1

Active power production	P	5100W
Reactive power production	Q	5750VAr
Grid voltage	V_s	1.028pu
Simulink model reference value for AVR field voltage	V_{ref}	1.068pu
AVR proportional gain	P(PID)	55*
AVR Integral gain	I(PID)	120*

*The AVR proportional gain and integral gain are changed later for this case.

For this first case the AVR parameters are set equal to the AVR settings in the laboratory, P=55 and I=120 (D=Td=0). Figure 47 shows the field voltage response for this case.

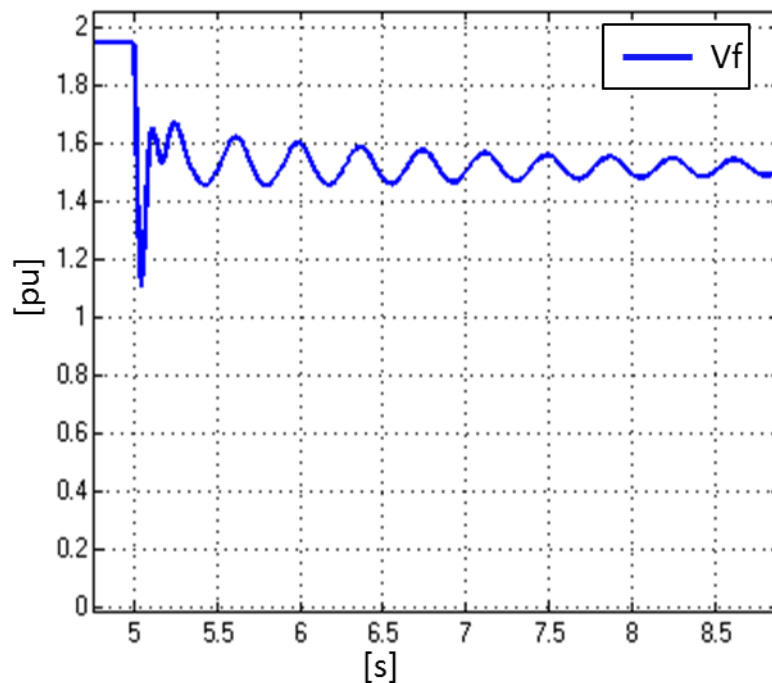


Figure 47: Simulated field voltage response following a small disturbance, for the system initially operating at P=5kW, Q=5kVAr. AVR P=55, I=120.

This figure shows the field voltage dropping from approximately 2pu to 1.55pu, which is a voltage drop of approximately 22%. This is very close to the percentage field voltage drop for the laboratory model shown in Figure 29. As mentioned, the field voltage response in particular gives a good indication of the characteristics and the parameter settings of the AVR. For the simulated case the response indicates a high value of the AVR proportional gain and the AVR integral gain. The drastic voltage drop immediately after the disturbance indicates a large proportional gain. A large proportional gain gives a great amplification of the deviation between the reference value and the actual voltage signal, and gives an output signal proportional to this deviation. A large proportional gain gives a large change in the output signal for a given deviation from the reference value. The integral gain affects the time the output signal takes to reach its steady state value. In the simulated response shown in Figure 47, the field voltage reaches its new steady state value immediately

following the disturbance, and continues to oscillate around this value. This indicates a higher value of the integral gain than the laboratory model response which takes significantly longer to reach its steady state value.

Although the DECS-200 AVR model for the synchronous generator in the NTNU laboratory is set to have the same values for the proportional- and the integral gain as the simulation model, the details of the structure of this model brings some uncertainty. Because of the lack of knowledge about the details of the structure of this model, and the indications from the simulations, it is chosen to reduce the two mentioned parameters. The values shown in Table 14 are used for further simulations.

Table 14: Generator operating situation, simulation case 1, adjusted AVR parameters

Active power production	P	5100W
Reactive power production	Q	5750VAr
Grid voltage	V_s	1.028pu
Simulink model reference value for AVR field voltage	V_{ref}	1.068pu
AVR proportional gain	P(PID)	5
AVR Integral gain	I(PID)	16

Figure 48 shows the field voltage response when the AVR settings are adjusted as shown in Table 14. The first voltage drop following the disturbance is now reduced, caused by the reduced proportional gain. A higher integral gain means a smaller integral time constant and slower integral action. The field voltage of the adjusted AVR model with a lower integral gain takes longer to reach its steady state value compared to the case with a higher gain. This model also seems to be better damped as the amplitude of the oscillations reduces significantly during the first few seconds.

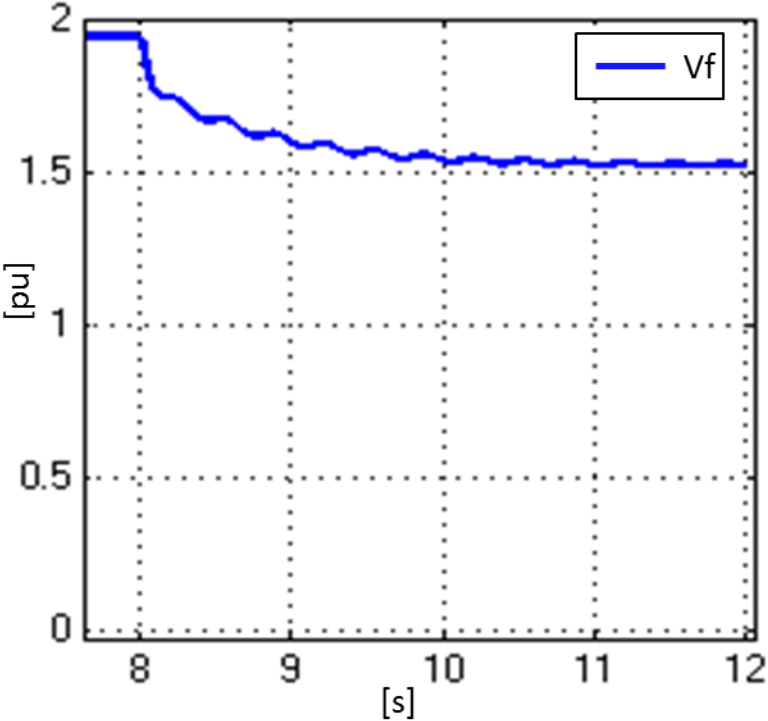


Figure 48: Simulated field voltage response following a small disturbance, for the system initially operating at P=5kW, Q=5kVAr. AVR P=20, I=43.

Figure 49 (a) and (b) shows the generator output voltage and current response following the disturbance. The figures shows zoomed in graphs to get a clear view of the oscillations. The output

voltage is initially in steady state at a value of 245V equal to 1.065pu, phase to ground rms. Following the disturbance the voltage oscillates for the next 5-6 seconds before it stabilizes at its initial steady state value of 245V. The generator current has an initial steady state value of approximately 10.3A. Following the disturbance the response shows poorly damped oscillations until it stabilizes at about 7.5A. The output current is now lower due to the increase of the system external impedance. The responses show a natural oscillation frequency of approximately 3Hz.

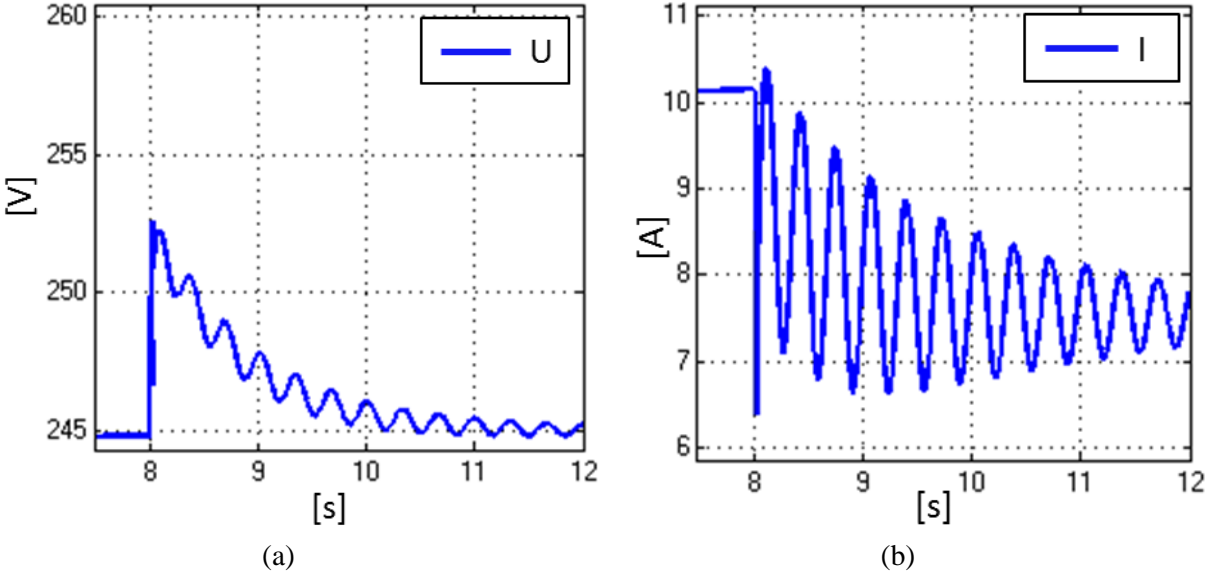


Figure 49: Case 1. Generator output rms (a) phase to ground voltage and (b) current, zoomed in to show the oscillations following a small disturbance represented by a sudden increase in the external system impedance.

The Generator output active and reactive power is shown in Figure 50 (a) and (b). The generator is initially set to produce 5000W active power and 5500VAr reactive power to be comparable to the laboratory results. Following the disturbance the active power behaves similar to the current, while the reactive power oscillations are similar to the voltage response. The active power stabilizes at its initial value after a few seconds, while the reactive power production is reduced to approximately 2200VAr due to the increased system external impedance.

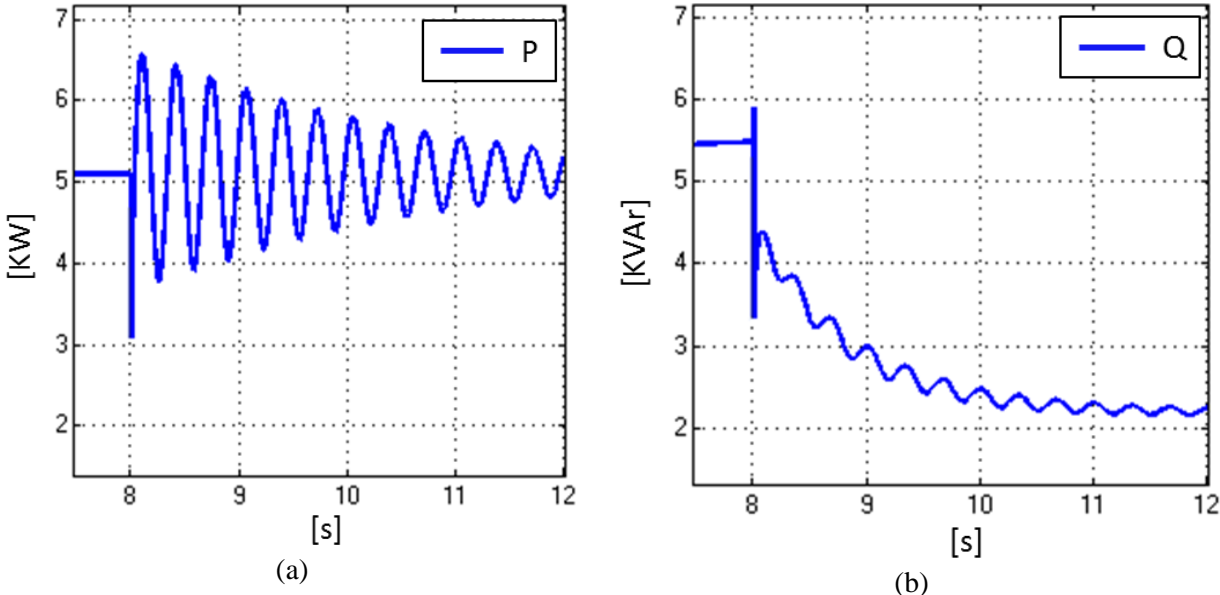


Figure 50: Case 1. Generator output (a) active and (b) reactive power, zoomed in to show the oscillations following a small disturbance represented by a sudden increase in the external system impedance.

Case 2

Table 15: Generator operating situation, simulation case 2

Active power production	P	5100W
Reactive power production	Q	-5000VAr
Grid voltage	V_s	1.028pu
Simulink model reference value for AVR field voltage	V_{ref}	0.98pu
AVR proportional gain	P(PID)	5
AVR integral gain	I(PID)	16

For the second case the generator is consuming reactive power. Apart from this the generator, excitation system and governor settings are identical to case 1. In this case the generator is initially set to produce 5kW (≈ 0.3 pu) active power, and to consume 5kVAr (≈ 0.3 pu) reactive power. Figure 51 (a) and (b) show the generator output voltage and current following a small disturbance represented by an increase of the system external impedance, identical to the disturbance applied in case 1.

Initially the generator operates at steady state with an output voltage of approximately 225V ($=0.98$ pu) and an output current of 10.5A ($=0.41$ pu). The disturbance leads to an instant voltage drop followed by a period of oscillations, before the voltage gradually seems to stabilize at its initial value. The current drops due to higher network impedance to a value of approximately 8A ($=0.33$ pu).

The oscillation frequency is clearly reduced compared to case 1 where the generator was producing reactive power. A similar reduction of the oscillation frequency was seen for this specific case in the laboratory. The amplitude of the oscillations is also smaller for this case, and the damping factor is significantly higher.

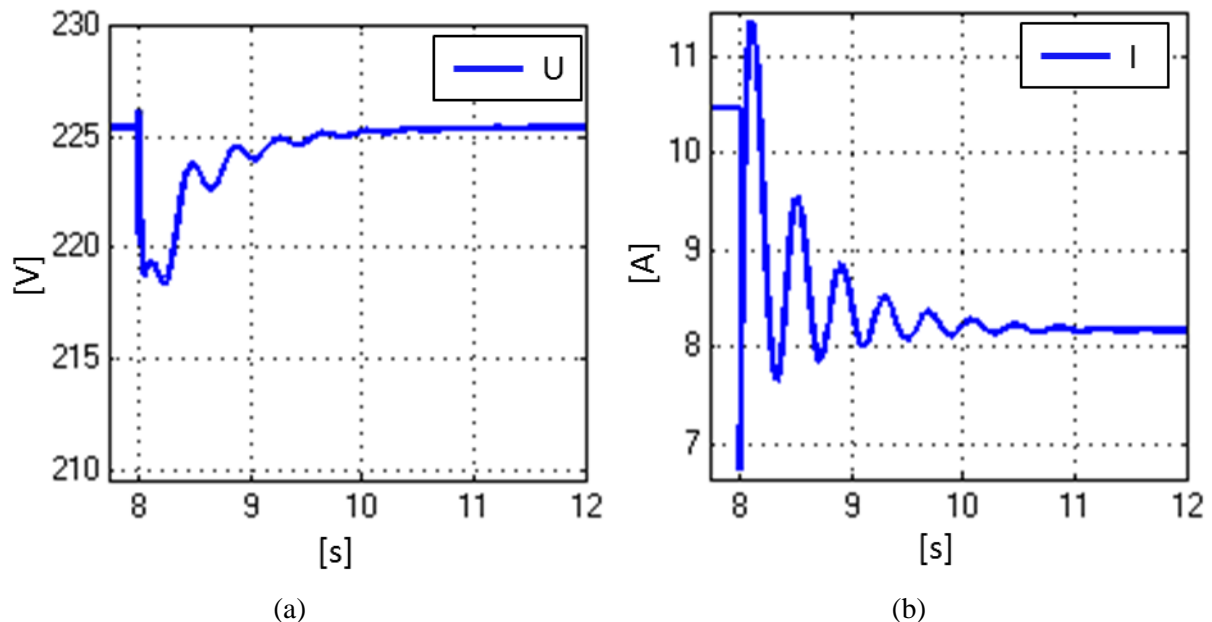


Figure 51: Case 2. Generator output rms (a) phase to ground voltage and (b) current, zoomed in to show the oscillations following a small disturbance represented by a sudden increase in the external system impedance.

Figure 52 (a) and (b) show the generator output active and reactive power. The active power response is very similar to the current response, and the oscillations are equally good damped. While the active power returns to its initial value following the disturbance, the reactive power consumption decreases due to increased network impedance. As the network impedance is almost exclusively inductive it makes sense that the disturbance mainly affects the steady state value of the reactive power.

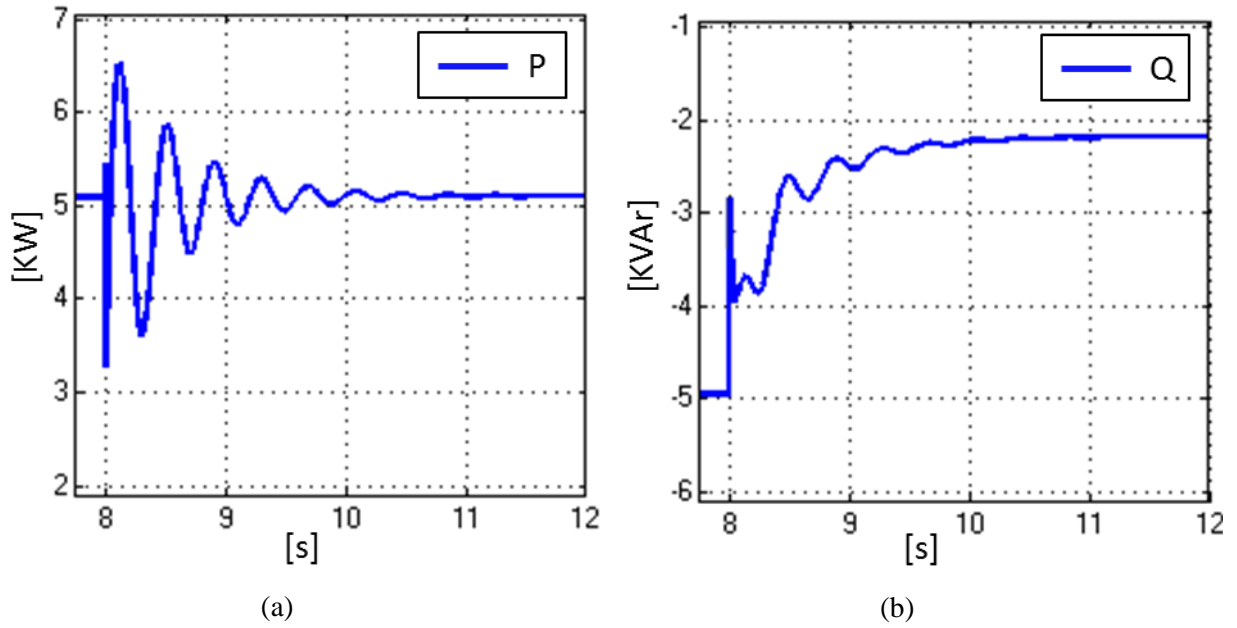


Figure 52: Case 2. Generator output (a) active and (b) reactive power, zoomed in to show the oscillations following a small disturbance represented by a sudden increase in the external system impedance.

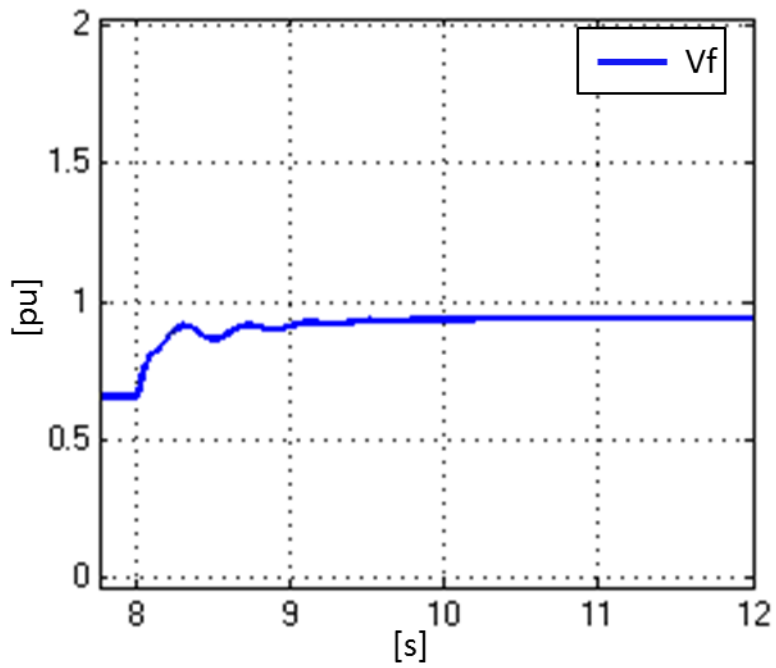


Figure 53: Field voltage case 2

Case 3

Table 16: Generator operating situation, simulation case 3

Active power production	P	4700W
Reactive power production	Q	6000VAr
Grid voltage	V_s	1.028pu
Simulink model reference value for AVR field voltage	V_{ref}	0.98pu
AVR proportional gain	P(PID)	10
AVR integral gain	I(PID)	16

For case 3 the operational situation is basically the same as for case 1. The main difference is that the proportional gain of the AVR PID controller is increased as shown in Table 16. The disturbance applied in this case is the same increase of the system impedance as for case 1 and 2. Figure 54(a) and (b) show the voltage and current response following the disturbance. The generator output active and reactive power is shown in Figure 55 (a) and (b) respectively.

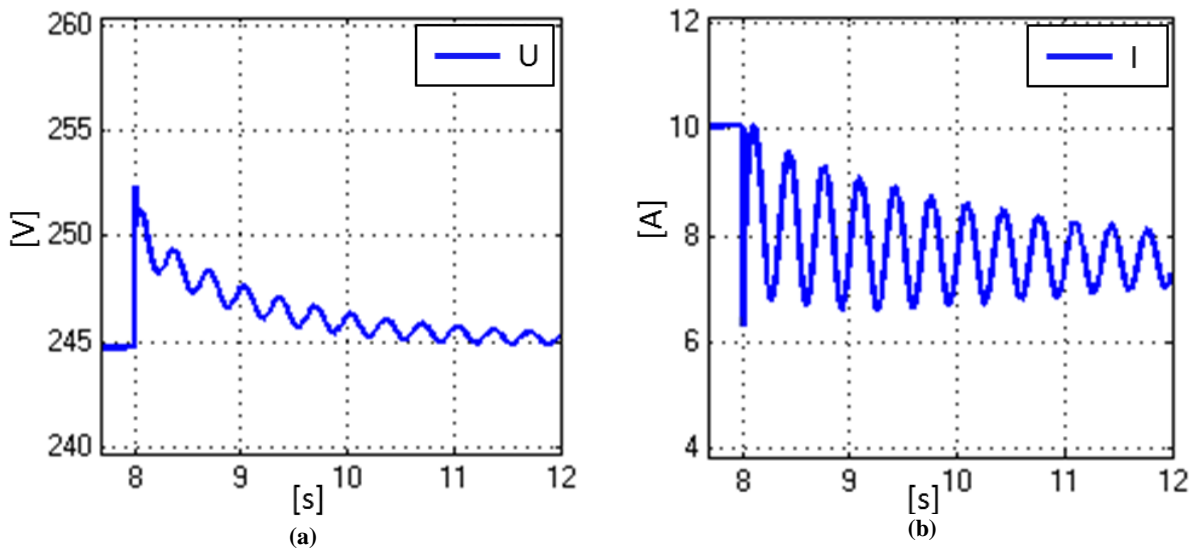


Figure 54: Case 3. Generator output rms (a) phase to ground voltage and (b) current, zoomed in to show the oscillations following a small disturbance represented by a sudden increase in the external system impedance.

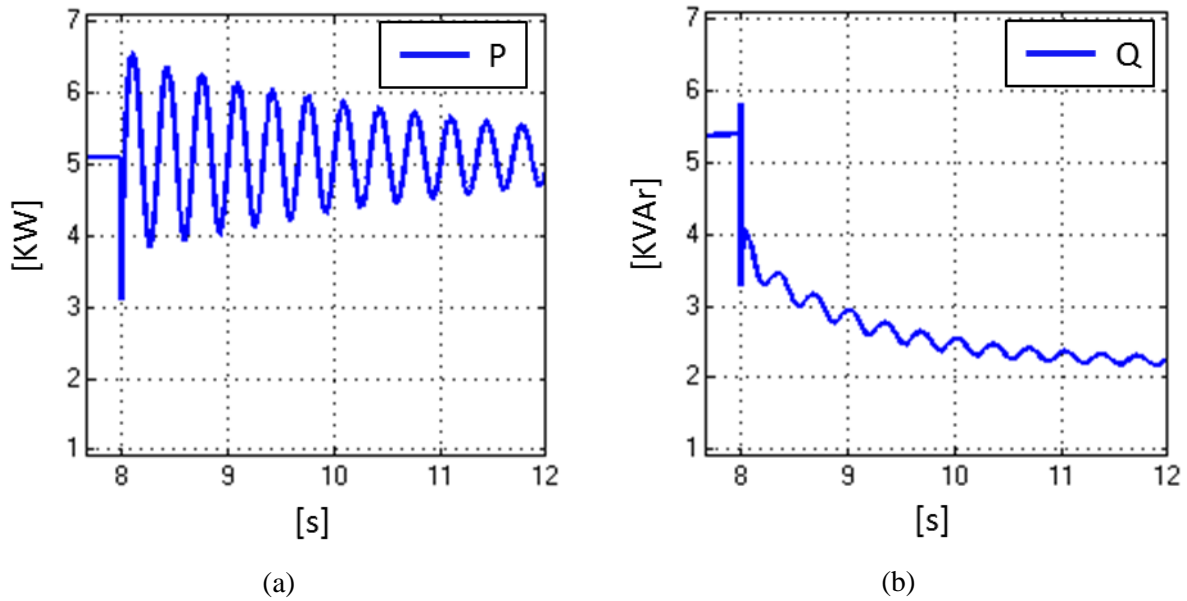


Figure 55: Case 3. Generator output (a) active and (b) reactive power, zoomed in to show the oscillations following a small disturbance represented by a sudden increase in the external system impedance.

The system response following the disturbance in case 3 is very similar to case 1. The main difference is the damping of the oscillations. Comparing the current or active power response for the two cases it can be seen that the system in case 3, with a higher gain for the AVR PID controller, has a weaker damping of the oscillations and hence a lower stability margin than the system in case 1.

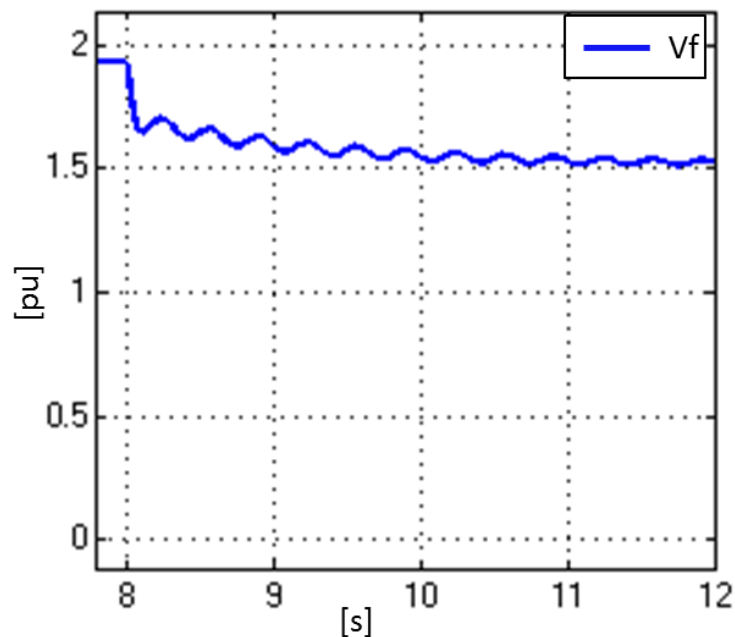


Figure 56: AVR field voltage

The measurements done in the laboratory shows an unstable response for the system in case 3. The simulations done of this case, where the AVR gain is twice the value of the one in case 1, show a response less stable than case 1 but yet not unstable. A further increase of the AVR gain shows that the system eventually gets unstable. Figure 57 shows the field voltage for an AVR gain 4 times the value in case 1. This confirms that a high AVR gain can cause stability problems as explained in part 5.2.2.

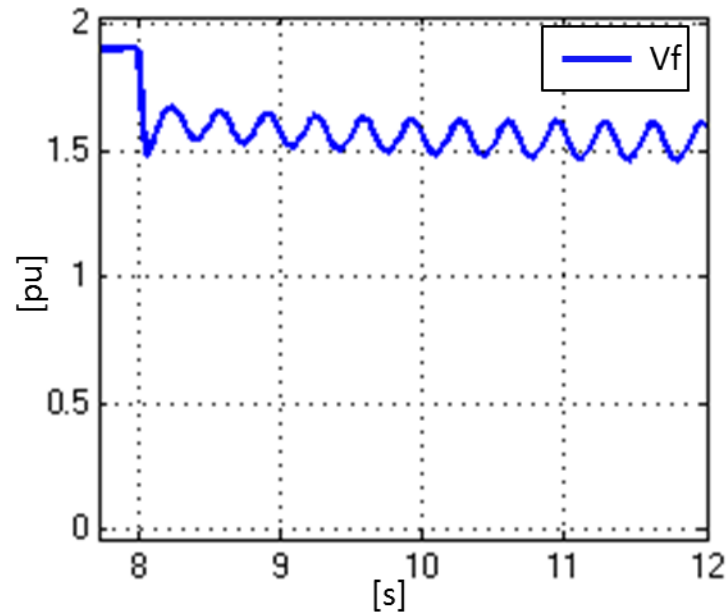


Figure 57: AVR field voltage, high AVR gain → unstable response

7.3 Sensitivity analysis

The simulation results show that the generator parameters and the excitation system settings have a great influence on the system response and stability limit. In the simulation model described in part 7.2.1 several parameters have a significant uncertainty and a deviation in these values will affect the resulting response of the system. The parameters considered in this brief sensitivity analysis are the inertia constant H , the quadrature axis short circuit subtransient time-constant T_q'' and the exciter time constant T_e .

The inertia for the generator is given in [4] to be $J=0.109\text{kgm}^2$, corresponding to an inertia constant $H=0.079\text{s}$. This is a very low value for this constant, which is natural as the generator is small and light. In addition the induction motor flywheel and the shaft add inertia to the system. The total inertia is set to be $H=0.4\text{s}$. This value is decided through evaluating the response of the simulation model at different values of H . Simulations show that the inertia constant clearly affects the system oscillation frequency. A lower value of H gives a higher oscillation frequency and weakens the system stability, while a higher value has shown to decrease the frequency and improve the damping of the system in the simulated cases.

The quadrature axis short circuit subtransient time-constant T_q'' , is initially set to be equal to $T_d''=0.008$. Increasing this time constant seems to increase the system stability margin, while decreasing the value below the value of T_d'' gives less damping and a lower stability margin for this model.

Simulations with different values of the excitation system time constant T_e , shows that the value of this parameter has a significant influence on the shape of the system response following the disturbance. A high value of this time constant makes e.g. the voltage return to its steady state value faster and oscillate around this value with higher oscillation amplitude. While a low time constant gives oscillations with lower amplitude which gradually approaches the steady state value. To recreate the laboratory model response, a time constant $T_e=0.03$ is chosen for the previous simulations.

The governor model brings a significant uncertainty to these simulations. The turbine governing system is modelled as a simplified controller consisting of a proportional gain, a time delay and static limiters, as described in 3. Both the value of the proportional gain and the time constant can have an influence on the system response. These parameters are adjusted through simulations to obtain an acceptable system response. The turbine governing model adds damping to the system. Too high values of the governor proportional gain seem to decrease the damping and increase the oscillation frequency, and hence decrease the stability.

In addition to the turbine governing system proportional gain and the time constant, the output limiters has an influence on the system damping as explained earlier.

7.4 Comparison

For Case 1, described in part 7.1, the simulation results are very close to what was measured in the laboratory. The current and voltage response shows that the initial steady state values of the voltage and current is approximately the same for the laboratory model and for the corresponding simulations. Following the disturbance, the current responses are very similar. The oscillations seem to have approximately the same damping and an oscillation frequency of about 3Hz. For the voltage response the simulation shows smaller amplitude for the oscillations, and it returns to a value very close to its steady state value faster than the response for the laboratory model. A comparison of the measured and the simulated voltage is shown in Figure 58. The oscillation frequency is approximately the same, and the resulting steady state value is approximately 245V for the results of the simulation and the laboratory test. For the active and reactive power the pattern is the same as for the voltage and current. The steady state values before and after the disturbance, is approximately the same for the laboratory- and the simulation model. The active power response of the simulated model follows the measured response closely following the disturbance while the reactive power oscillations have deviations similar to the voltage response.

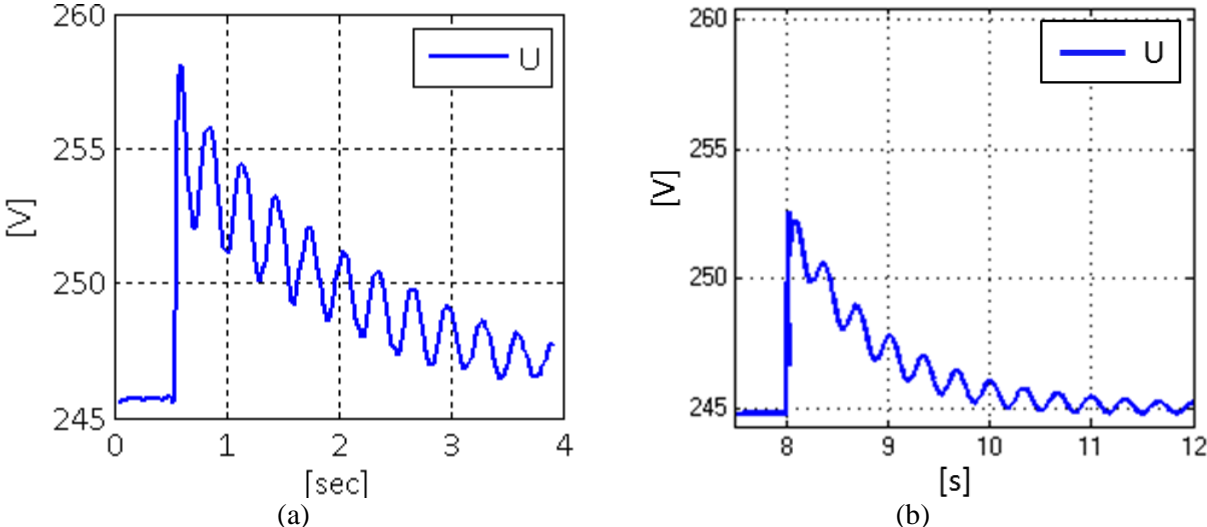


Figure 58: Case 1. Generator output voltage Case 1 (a) laboratory model (b) Simulation model

For case 2, when the generator is consuming reactive power, the oscillation frequency decreases and the damping of the laboratory model is better than when producing reactive power. This is confirmed by simulations. Figure 59 shows a comparison of the measured and the simulated voltage response for the operating situation in case 2.

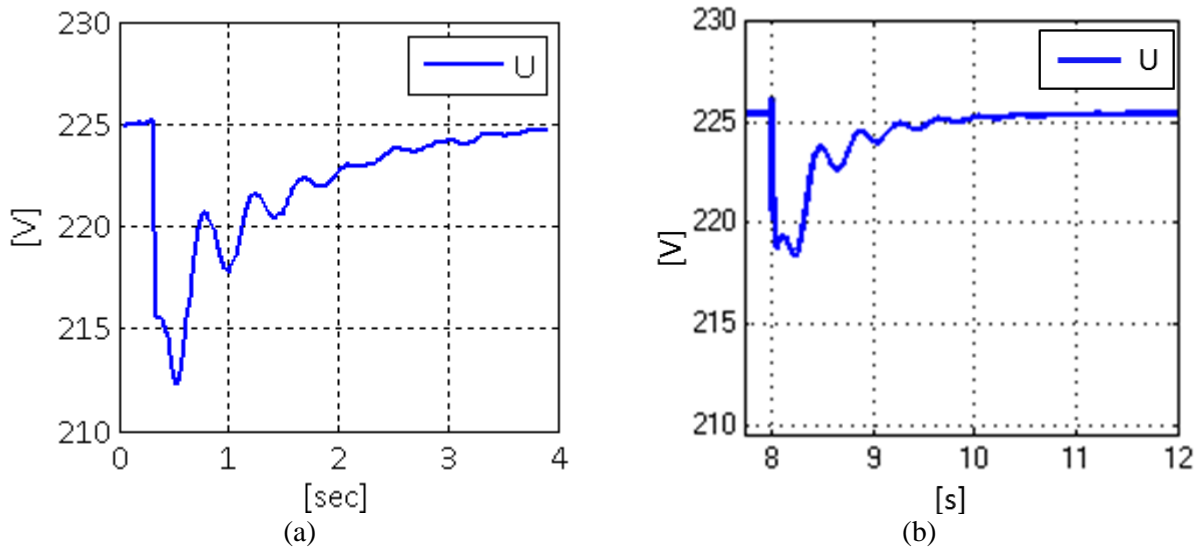


Figure 59: Case 2. Generator output voltage (a) laboratory model (b) Simulation model

In case 3 the AVR gain is increased from 5 to 10 compared to case 1. Disregarding this, the operation situations are the same for the two systems. The response for case 1 is better damped and this system seems to have a higher stability margin than case 3 which is close to its stability limit. For the laboratory model the operation scenario in case 3 gives an unstable response as shown in Figure 60 a. This shows a deviation between the two models. The tendency is still the same, as both models indicate a less stable system for an increased value of the AVR gain. As the details of the excitation system structure in the laboratory are poorly documented, the details of the simulation model may be different at some points which may lead to some deviations in the response. Further increase of the AVR gain eventually gives an unstable system as described in part 5.2.2. This may indicate that the AVR proportional gain for the simulation model should have been higher to give a closer representation of the laboratory model.

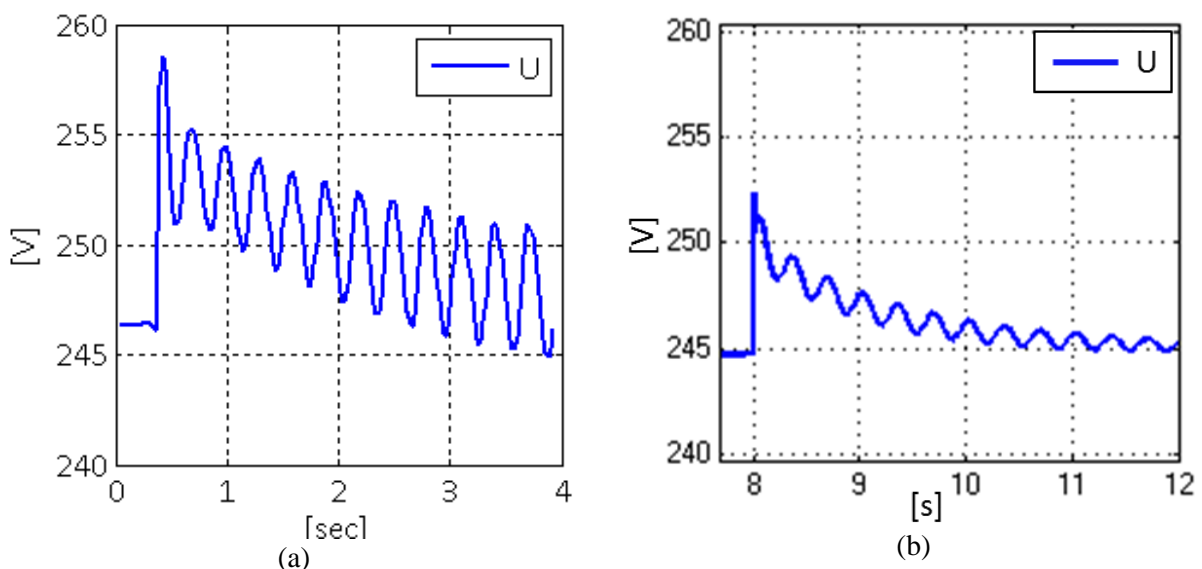


Figure 60: Case 3. Generator output voltage (a) laboratory model (b) Simulation model

8 Excitation limiters studies

This part of the report concerns the excitation limiters and their effect on the system response. As described in part 4.3, the excitation limiters are included in the excitation system to keep the excitation level within given limits. These limiters affect the response of the power system by limiting the maximum field current which naturally limits the field voltage and hence the generator output voltage and reactive power. This effect is demonstrated in the laboratory by lowering the overexcitation limit, and operating the generator at an excitation level exceeding this limit. The effect of the excitation limiters settings is further studied by simulations.

8.1 Laboratory testing

8.1.1 Setup/case description

As earlier mentioned, the exact structure of the excitation system in the laboratory is not known. This brings some uncertainty to the implementation of this part of the simulation model. The excitation limiters implemented in the laboratory model seems to be controlled by PI controllers, as the digital settings of the limiters includes the parameters P and I and a time t, assumed to represent the amount of time the field current is allowed to exceed its upper limit.

The settings used in the laboratory are shown in Table 17 below. The parameters for the simulation model are adjusted by studying the response of the simulations.

Table 17: Laboratory model, excitation system parameters

Parameter	Value	Description
P(PID)	55	AVR PID controller proportional gain
I(PID)	120	AVR PID controller integral gain
D(PID)	0	AVR PID controller derivative gain
P(PI)	1	OEL PI controller proportional gain
I(PI)	10	OEL PI controller integral gain
t(lim)	5s	Time the field current is allowed to exceed its upper limit

8.1.2 Laboratory test results

To demonstrate the field current limiting operation, the overexcitation limiter is set to limit the field current at 1.5A, and to allow the field current to exceed this value for maximum 5 seconds. The generator is initially set to operate at an excitation level below the limit, and the field current is increased to exceed the limit by decreasing the system impedance.

Figure 61 shows the AVR output field voltage as the field current is limited at 1.5A. The stapled red line represents the field voltage limit corresponding to $I_f=1.5A$. The generator is initially operating at steady state with field voltage at approximately 12V. At time $t\approx 0.2s$, the parallel branch is suddenly re-connected so that the network impedance decreases. This causes a voltage drop at the generator output, and the field current supplied to the generator is increased by the AVR to maintain the voltage level. At $t\approx 3s$ the field current exceeds its upper limit of 1.5A corresponding to a field voltage $V_f\approx 16.5V$. The field current is allowed to exceed its limit for a few seconds due to the time delay for the limiters. At $t\approx 8s$, the field current, and hence the field voltage, is regulated back to its limited value, and is kept at this limit. Figure 62 and Figure 63 show the generator output voltage and reactive power, corresponding to the field voltage presented in Figure 61.

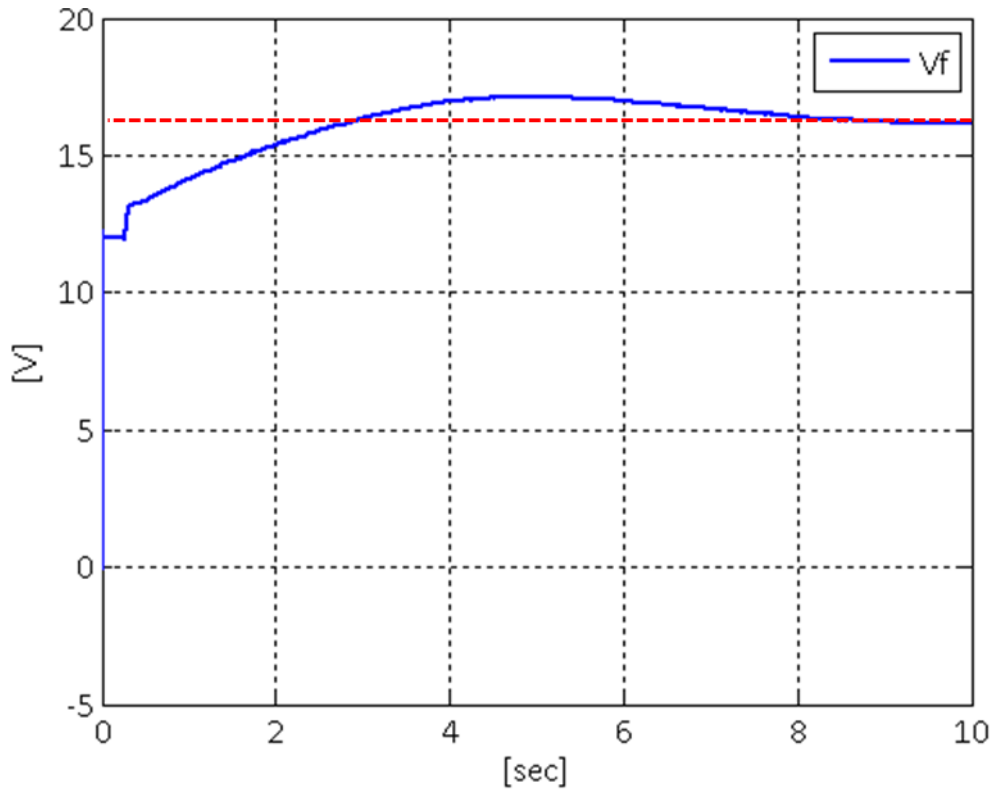


Figure 61: AVR output field voltage, at field current limiting operation

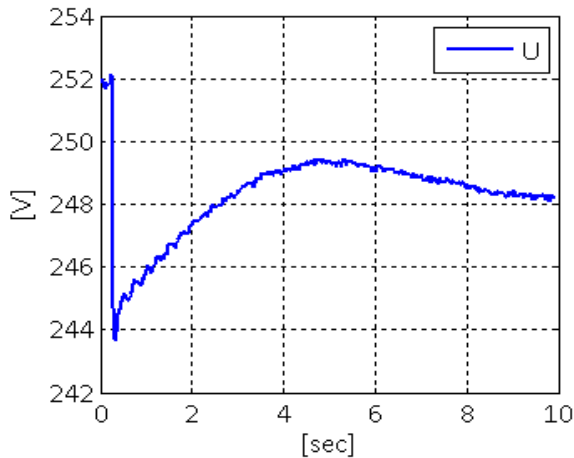


Figure 62: Generator output voltage, during FCL operation

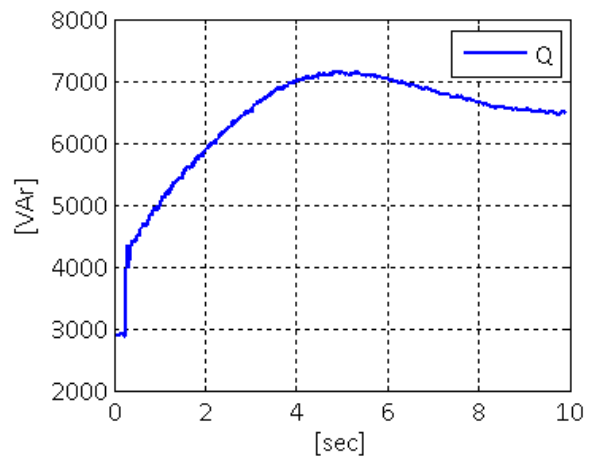


Figure 63: Generator output reactive power FCL operation.

For the following case, the parallel branch is disconnected hence the network impedance increases. In this case the field current and field voltage decreases and returns to a value below the overexcitation limit and back to regular AVR action. Figure 64 shows the field voltage for this case. The corresponding generator output voltage and reactive power is shown in Figure 65 and Figure 66.

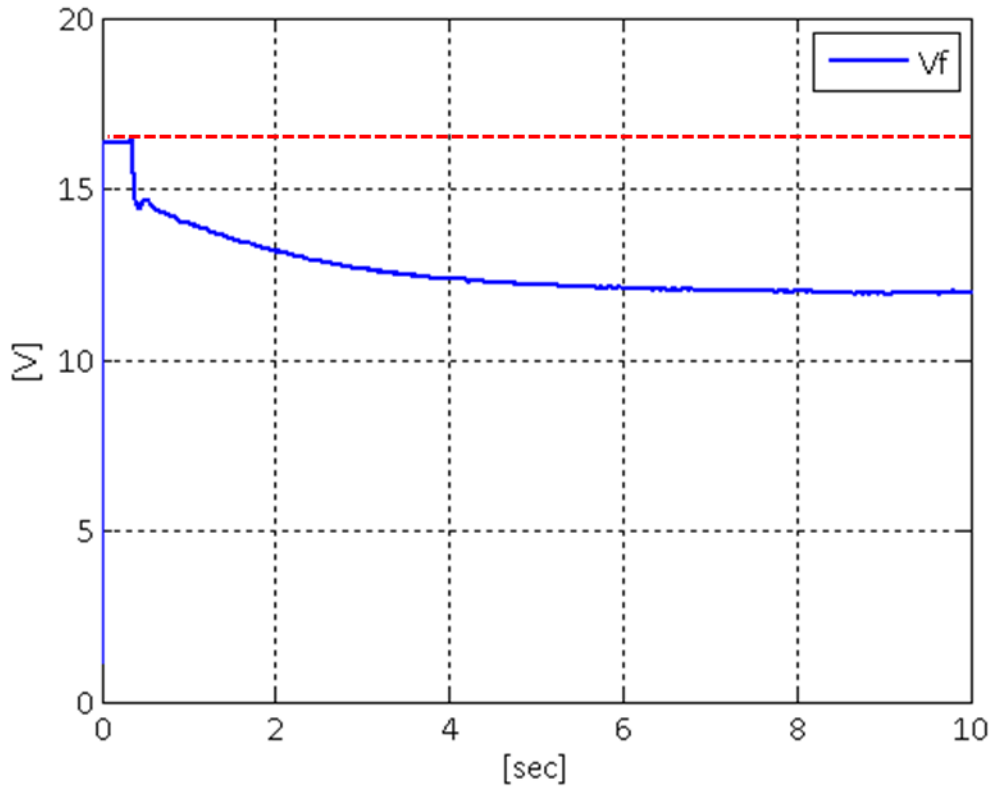


Figure 64: AVR output field voltage, returning from field current limiting operation of regular AVR action

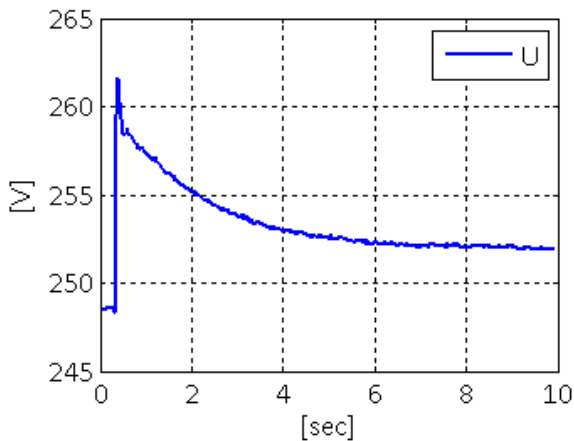


Figure 65: Generator output voltage, returning from FCL operation to regular AVR operation.

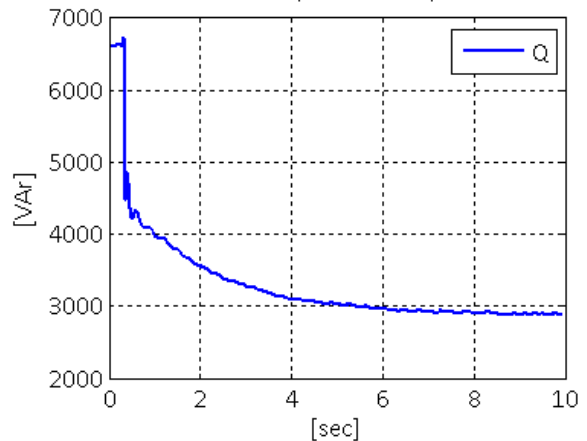


Figure 66: Generator output reactive power, returning from FCL operation to regular AVR operation.

8.2 Simulations

The validated simulation model is now used to study the effect of the excitation limiters. As earlier mentioned the structure of the laboratory model excitation system is not known in details. This is also the case for the excitation limiters. The limiters implemented in the simulation model are dynamic field current limiters controlled by PI controllers. This system is described in [5]. This simulation model is further used to study the effect of the parameters of the PI regulator in the field current limiters, when the system goes into FCL mode, and as it returns to AVR mode.

8.2.1 Simulation model and setup

The field current limiters are modeled as PI controllers, controlling the field current if it exceeds the given limit. The excitation system including the field current limiters is shown in Figure 67. Excitation current and voltage in the regulator model, and the output current, voltage, speed and power from the generator are measured in different operational scenarios. In addition, the output from the different regulators and saturation blocks in the excitation system is measured to see the effect of the different components. The excitation system with the measuring points is shown in Figure 67.

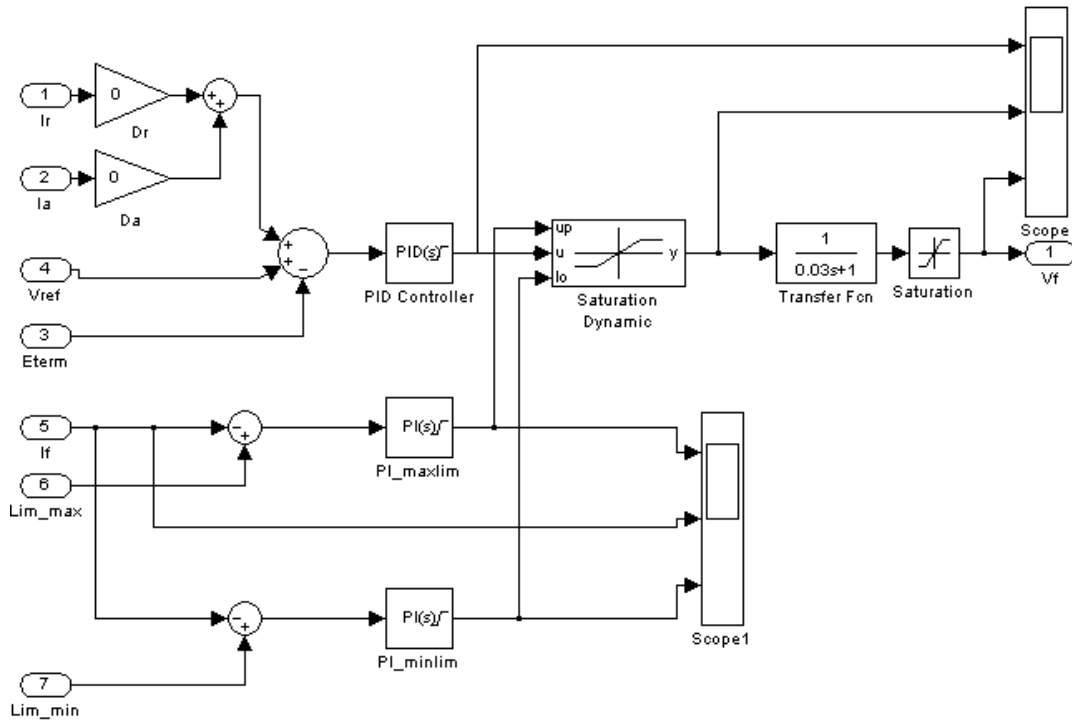


Figure 67: Simulink model of the excitation system

8.2.2 Simulation results

To see how the voltage regulator acts when the field current exceeds the upper limit, the network impedance is reduced the same way as in the laboratory. The line inductance is found through simulations and shown in Table 18. The line resistance is neglected in these simulations.

Table 18: Line inductance, simulation model

Disturbance	Line 2 is disconnected
Line 1 inductance	$L=0.0032\text{H}$
Line 2 inductance	$L=0.00234\text{H}$

The upper field current limit is set to 1.8pu. At this point the produced reactive power is equal to approximately 6500VAr, which is where the limit was set in the laboratory. Following the impedance change, the field current will increase until it exceeds its limits of 1.8pu. The field current is allowed to exceed this limit for a few seconds. As the field current limiter is activated, the field current is gradually regulated back to the value set as its upper limit. The response to the field current regulation is decided by the PI regulator proportional gain and integral gain. The PI regulator proportional and integral gain is initially set as proposed in the description of this AVR model in [5] and given in

Table 19: Field current limiter PI controller parameters as given in [5].

Parameter	Value
P(PI)	10
I(PI)	2

The field current response and the output of the over excitation field current limiter (OEL) PI controller is shown in Figure 68 and Figure 69. The figures are zoomed in at the time where the OEL is activated to get a better view of the regulation process. The OEL is activated at the time shown as 15s. At this time the field current reaches its upper limit of 1.8pu as shown in Figure 68. The OEL is from this point gradually regulated towards its limiting value of 1.8pu. As the PI controller decreases the field current limit, the field current is reduced as shown in Figure 69. The red stapled lines show the values corresponding to the upper field current limit.

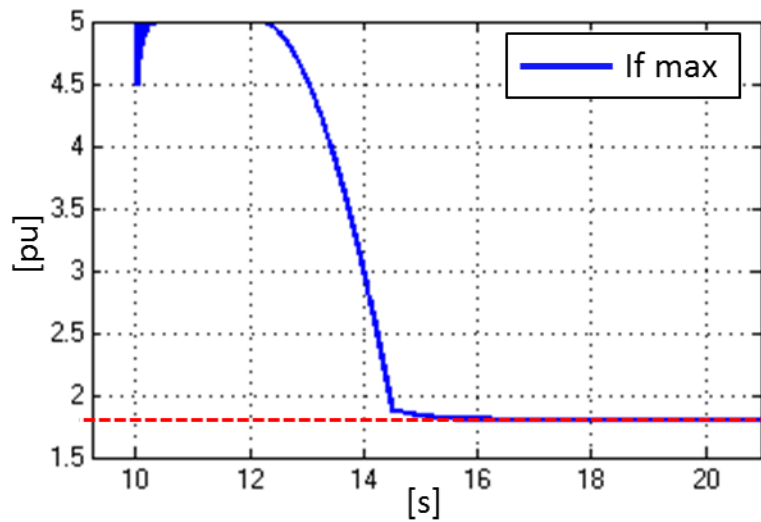


Figure 68: Upper field current limit, output from OEL PI controller

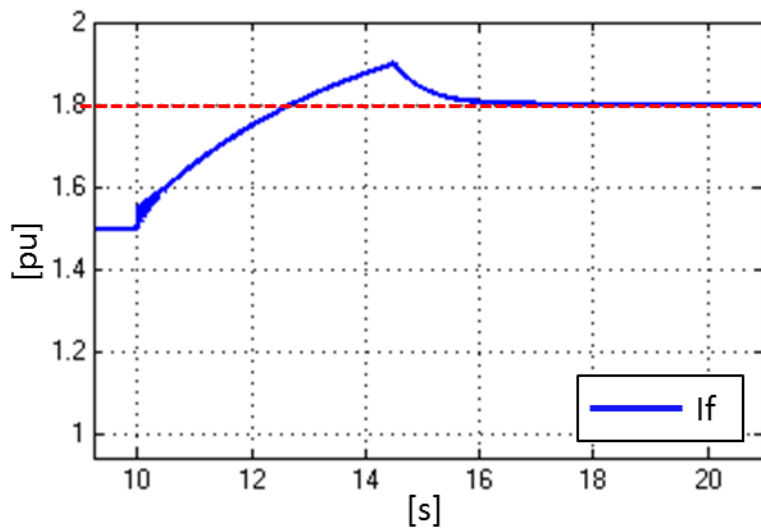


Figure 69: Field current, limited by the OEL

Figure 70 and Figure 71 shows the effect of the excitation limiters on the AVR field voltage. Figure 70 shows the output of the AVR PID controller as it would be disregarding the dynamic excitation limiters. Figure 71 shows the output from the dynamic saturation block after the signal is limited by the field current limiters.

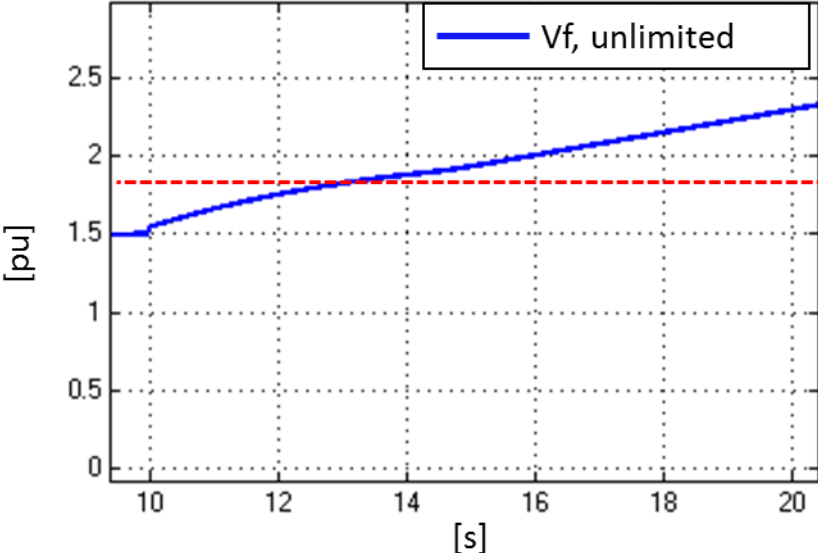


Figure 70: Field voltage without limiter action

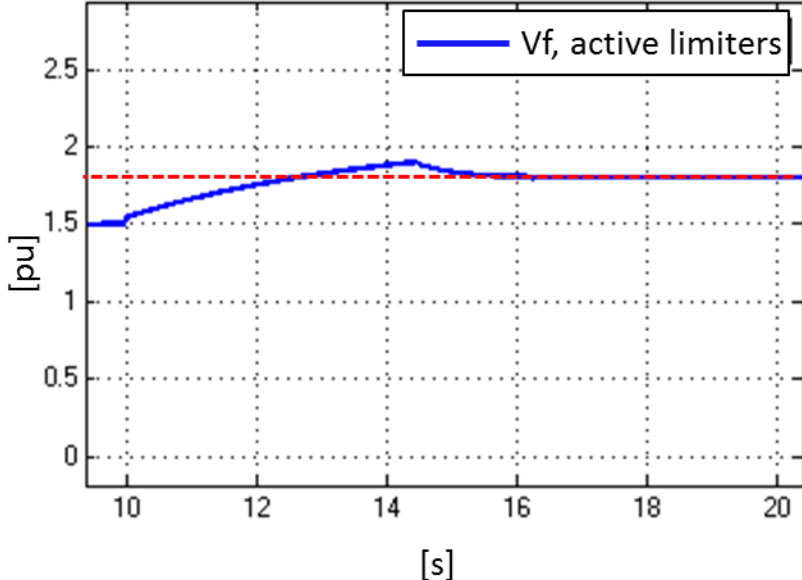


Figure 71: Field voltage with active limiters

The response of the simulation model indicates a high integral gain compared to the laboratory model, as the field current response shows a low integral time and returns to its steady state value in less than a second. To adjust the OEL settings to simulate the laboratory model response, the integral gain should be lower than first assumed. The parameters are adjusted as shown in Table 20.

Table 20: Adjusted field current limiter PI controller parameters

Parameter	Value
P(PI)	10
I(PI)	0.5

Figure 72 and Figure 73 shows field current and the upper field current limit of the system with adjusted parameters. This response has a longer integral time, due to a lower integral gain, and is more similar to the response from the laboratory model.

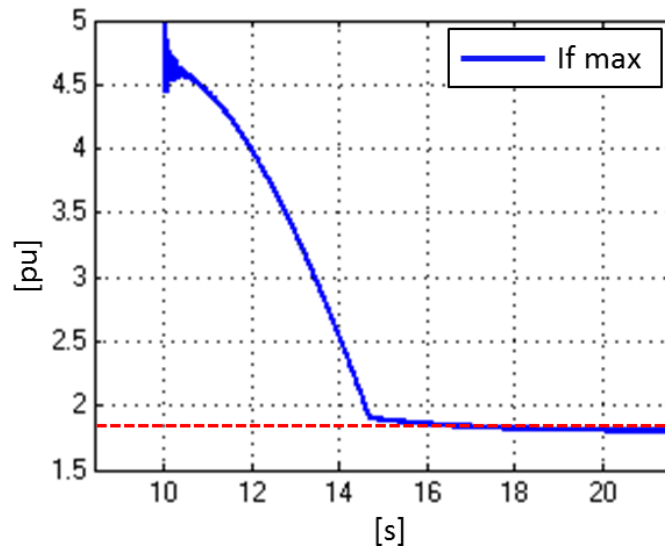


Figure 72: Upper field current limit, output from OEL PI controller, adjusted parameters

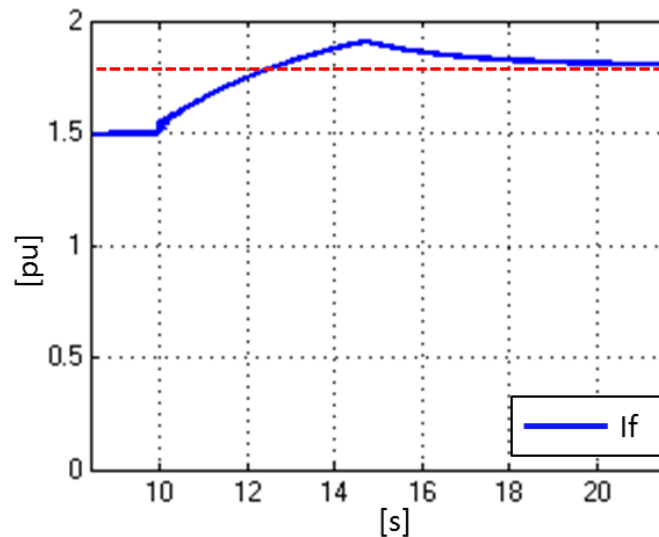


Figure 73: Field current, limited by the OEL, adjusted parameters

Figure 74 and Figure 75 shows the corresponding field voltage and output reactive power. The field voltage is proportional to the field current and is similar to the response of the laboratory model. The reactive power is limited at approximately 5kVAr (≈ 0.3 pu). The high frequent oscillations shown in Figure 75, are assumed to be switching transients, and are not further considered in this report.

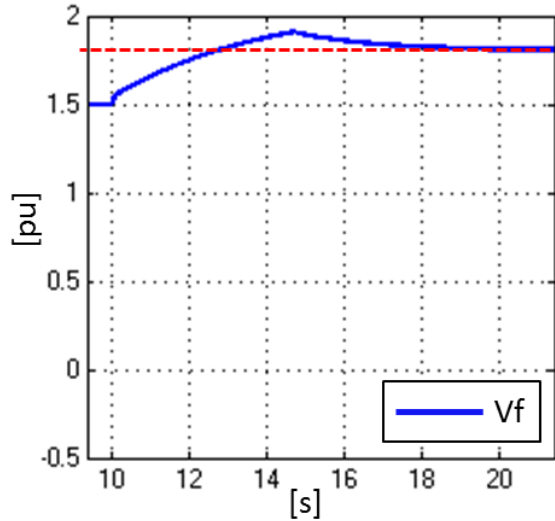


Figure 74: Field voltage, FCL operation, adjusted PI controller parameters

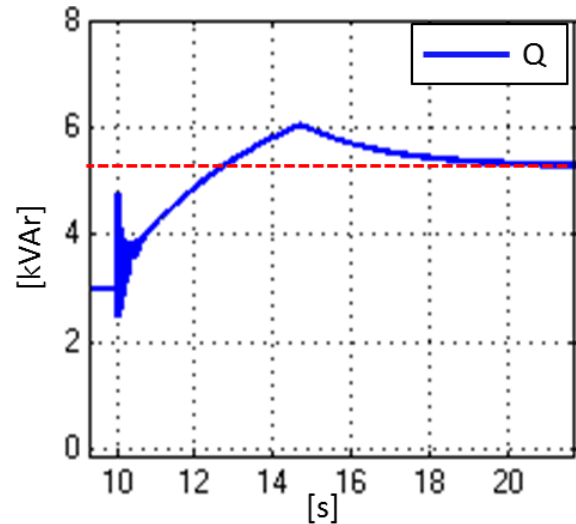


Figure 75: Reactive power, FCL operation, adjusted PI controller parameters

To study how the system reacts to a small disturbance while operating in FCL mode, the impedance is increased so that the excitation system goes out of field current regulation mode, and back into regular AVR mode. As shown in the following figures, the FCLs are deactivated and the system returns to AVR mode as soon as the value of the field current is lower than the given limit.

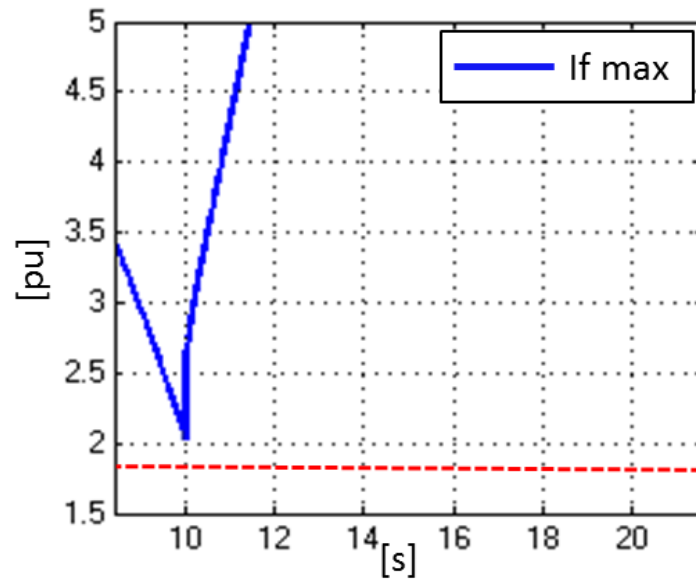


Figure 76: Upper field current limit, output from OEL PI controller, out of FCL mode by increasing system impedance

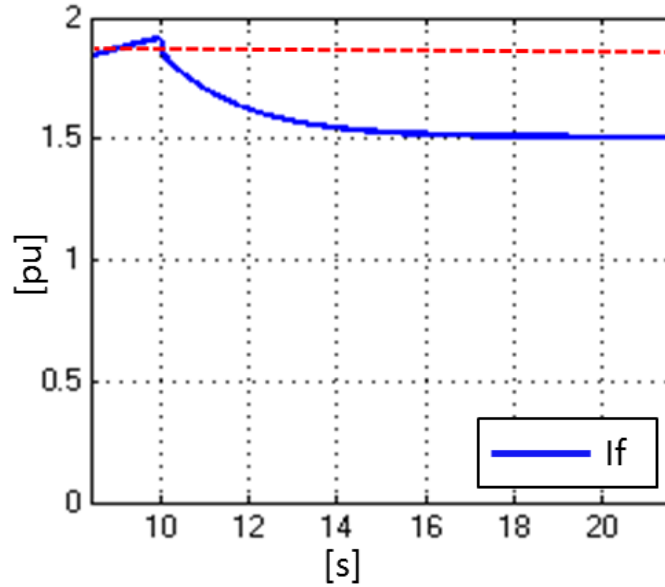


Figure 77: Field current, out of FCL mode by increasing system impedance

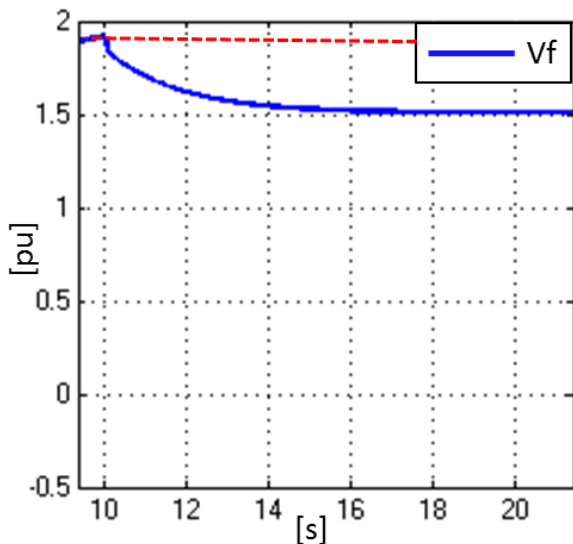


Figure 78: AVR field voltage, out of FCL mode by increasing system impedance

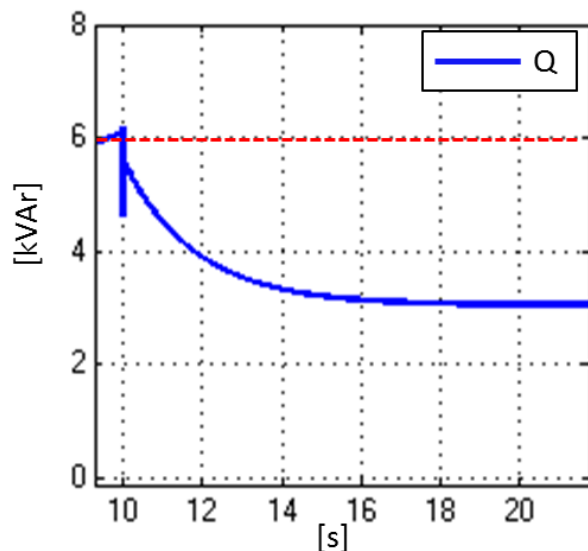


Figure 79: Reactive power, out of FCL mode by increasing system impedance

Simulations are done to study the system response for different parameters for the PI controllers. These simulations confirm that a high proportional gain gives a faster system and that a high integral gain gives the integrating function greater effect on the regulation process as shown in Figure 68 and Figure 69. For all the tested cases the system seems to be stable. Simulations are done with the PI controller proportional gain as high as 200 and the system still seems to be stable for this operating situation.

9 Discussion

9.1 Model validation

In the first part of this report, the small hydro power plant laboratory model was modelled in MATLAB/Simulink by using the power system module. The final simulation model has a response similar to the laboratory model, and the model is found to be valid for this kind of studies. Even though the simulation model is found to be valid in this master thesis, there are still some deviations in the simulated response compared to the laboratory model.

9.1.1 Generator model

The generator model used for the simulations is relatively detailed as described in part 6, and most of the parameters are given in the report describing the laboratory model [4]. The parameters which are not given in this report are found through adjustments while comparing the response of the simulation model to the actual response measured in the laboratory. Two important parameters are found this way for the generator model, the generator inertia constant H , and the quadrature axis subtransient time constant Tq'' . Both these parameters affect the system response. The inertia constant H , has a significant effect on the oscillation frequency and the damping, and also Tq'' affects the damping of the oscillations and hence the system stability.

In the specialization project [1] a sensitivity analysis was done to see the effect of increasing the inertia constant H , for Kuråsfossen power plant. Figure 80 shows how the inertia constant H can affect the eigenvalues and the system stability. A sensitivity analysis is done where H is increased from 0.5-5, using MATLAB. The MATLAB code and description of the evaluated system is given in [1]. The value of the inertia constant, H , in the original system was 3.2s. Figure 80 shows how the eigenvalues changes when H is increasing from 0.5-5.0 in the direction of the arrow.

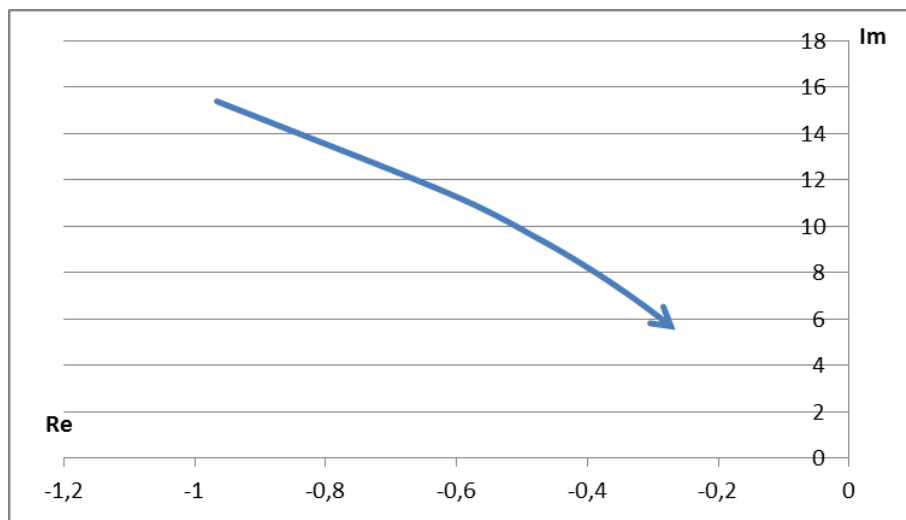


Figure 80: Sensitivity analysis, increasing Inertia constant 0.5-5. [1]

As for the regulator gain, the stability margin is decreasing for an increasing value of the inertia constant. As shown in Figure 80, the inertia constant also affects the oscillation frequency. The real part of the eigenvalue increases while the imaginary part decreases. For this case both the damping and

the oscillation frequency decreases. This shows that exact knowledge about the system inertia is important for accurate simulation results.

The moment of inertia of the laboratory distribution generator model, is given as $J=0.109\text{kgm}^2$, corresponding to an inertia constant $H=0.079$. In addition the induction motor shaft and the flywheel add inertia to the system. The total inertia constant is found to be $H=0.4\text{s}$, which is a low value for this constant. This is chosen based on the response of the laboratory model, which has shown to be fast during normal operation (not at torque limit). As the machine is relatively small and light, the inertia constant is expected to be small, and this result is considered to be realistic

9.1.2 Excitation system

An important part of this master thesis is to study the excitation system of the laboratory model, and how it affects the system stability. As explained in part 5.2.2, the AVR structure and parameters can affect the stability significantly. The details of the structure of the laboratory model excitation system are not described in the report [4] and finding the exact parameters for the simulation model is therefore challenging. These are adjusted by simulations, and might cause certain deviations in the system responses.

In part 7.1.2 and 7.2.2 it is shown that increasing the AVR gain above a certain value decreases the system stability margin. Figure 18 shows a sensitivity analysis from the specialization project [1], showing how the eigenvalues changes as the AVR proportional gain is increased from 0-100. This graph is based on Kuråsossen power plant and is described in the specialization project report. The pattern of how the eigenvalues moves corresponding to the AVR gain is expected to be valid for the case evaluated in this report too, but the values shown in the graph in Figure 18 would be different as they depend on the system parameters and characteristics.

Below a certain value of the AVR gain, the AVR contributes with a positive damping component to the power system. For the Kuråsossen case it was shown that it was only for high values of the regulator gain that the voltage was oscillating in counter phase to the rotor angle, and hence contributing with a negative damping component. This is demonstrated in Figure 81. This explains why the damping and the stability margin increases for low values of the regulator gain, and decreases for higher values. This explanation is expected to be valid for the case studied in this master thesis as well.

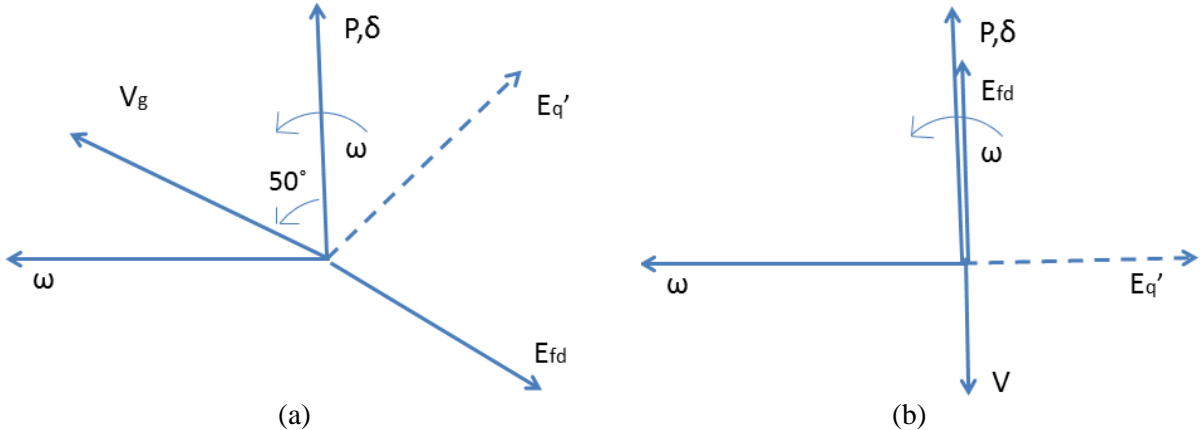


Figure 81: Examples of phasor diagrams of a system with (a) Low AVR gain (b) High AVR gain

9.1.3 Turbine governing system

The turbine governing system for the small hydro power plant laboratory model is represented by an induction motor with a frequency converter for torque control. The simulations in the first part of this thesis show that the modeling of the turbine governing system clearly affects the system response. Measurements in the laboratory show a stable well damped response when the system is subjected to a small disturbance represented by a sudden change of the network impedance. This response implies that the governing system acts fast and efficient to stabilize the system, by adding the necessary input to the turbine to compensate for the speed drop. A regular hydraulic turbine governing system acts relatively slowly caused by the high water pressure and friction, as explained in part 3.

To give a more realistic representation of the relatively slow response of hydro turbine governors, the system is set to operate at its torque limit. This gives a very different response to the same disturbance. As the governing system in this case cannot increase the torque the same way as in the previous case, the response of the governing system is slower and the dampening effect is reduced. The motor drive operating as a turbine governing system for the laboratory model does not seem to give a realistic representation of a hydraulic turbine governing system. For further use of the laboratory model for small hydro power plant studies it would be interesting to update the motor drive to respond more slowly, to better reflect the characteristics of a hydro power plant. In the description of the renewable energy laboratory [4], it says that there are two different flywheels which can be included to add inertia to the system. This would result in a slower response, and could be a possible way to represent a more realistic model.

When the system is operating at its torque limit (the torque limit is adjusted to be at the operating point) the system stability margin is significantly reduced. When the laboratory generator model does not operate at the torque limit, the torque is adjusted to dampen the oscillations following a disturbance.

9.1.4 Underexcited operation

For the cases evaluated in this report, the laboratory model seems to have better small signal stability characteristics when it is operated underexcited. When the generator is consuming reactive power of approximately 0.3pu, a small disturbance represented by increased impedance gives less and better damped oscillations than in the case where it is producing the same amount of reactive power. The active power production is the same for the two cases. The responses for both of these cases are very similar for the simulation model as for the laboratory model. Underexcited operation was earlier expected to give a lower stability margin, but studies, including the specialization project [1], have indicated that this is not necessarily the case. These studies have shown, through measurements and simulations, that some generators are better damped and have a higher stability margin when operating underexcited. These results are only valid for this exact generator and for the tested operating situations.

9.1.5 Laboratory measurements – excitation system studies

Measurements in the laboratory have been an important part of this master thesis. The laboratory model is of great interest for model validation and for stability studies concerning the excitation system. As the excitation system included in the laboratory model is digital and it is simple to change the parameters, this is a great way to get an insight to the effect of the different parameters and operating situations on the system response. To study the effect of the excitation system, including the excitation limiters, the field current and field voltage are of great interest. The field voltage is possible to measure by opening the measurement cabinet and attach the measuring instrument to the output

terminals. It is assumed that the output from the exciter is a pulse-width-modulated voltage. This gives a signal which has to be scaled and run through a low pass filter to get an appropriate display of the field voltage response. All this signal processing leads to a higher uncertainty. For future studies it would be of great interest to be able to log the field voltage response directly from outside the cabinet, the same way as for the generator voltage and current.

9.1.6 Simulink power system module as simulation program

MATLAB/Simulink power system module has been used for the simulations in this master thesis. This simulation program is relatively intuitive, and has detailed standard models for most of the regular power system components. For this kind of studies, the models are almost too detailed. For some of the simulations the program requires a sampling time of 10^{-6} s and one simulation can last for more than one hour.

9.2 Excitation limiters stability studies

In the second part of this master thesis, the validated simulation model is used to study the effect of the excitation limiters. The structure of the laboratory model excitation system and the excitation limiters are not known in detail, and the limiters implemented in the simulation model might therefore be different. The limiters implemented in the simulation model are dynamic field current limiters controlled by PI controllers. This system is described in [5].

The excitation limiters implemented in the laboratory model seems to be controlled by PI controllers, as the digital settings of the limiters includes the parameters P and I and a time t (assumed to represent the amount of time the field current is allowed to exceed its upper limit). The response of the laboratory model is similar to the response of the simulation model, which confirms this assumption.

The small hydro power plant model in the laboratory includes numerous limiting and protection functions. This makes the studies of the field current limiters in the laboratory a challenging task, as other limiters, relays and protective functions are easily activated as the generator gets close to its operating limits. The maximum voltage limits was particularly sensitive in this case. To succeed with the studies, and make the system operate in field current limiting mode, the upper field current limit was set at a relatively low value. To create a more realistic operating situation the relays and protection functions should be set to be less sensitive and allow a higher voltage.

10 Conclusions and Recommendations for Further Work

10.1 Main conclusions

10.1.1 Model validation

In this master thesis the small hydro power plant model in the NTNU renewable energy laboratory, is modeled in Simulink and validated by laboratory testing. The final simulation model of the laboratory system has a response very similar to the actual model. The simulation model is however somewhat inconvenient for this kind of studies because it includes very detailed models for the system components, and requires a very low sampling time which makes the simulations very time consuming. The response of the simulation model has some deviations from the laboratory model, but these are considered small and it is concluded that the model is valid for further studies of excitation limiters for these master thesis.

The motor drive representing the turbine governing system for the laboratory model does not seem to give a realistic representation of a hydraulic turbine governing system. The motor drive responds fast and efficient to disturbances, and contributes greatly to a well damped system with a high stability margin. The motor drive should respond more slowly to give a more realistic representation of the relatively slow response of hydro turbine governors.

The excitation system parameters have great influence on the behavior of the synchronous generator in the laboratory model. The details concerning the excitation system structure are partly unknown, which makes it challenging to decide the exact AVR parameters for the Simulink model. The parameters found through studying the simulated response seems to be satisfying, as the voltage response of the simulation model is regulated similarly as for the laboratory model.

For the cases evaluated in this report, the laboratory model seems to have better small signal stability characteristics when operating underexcited. Whether the stability margin is higher for under- or overexcited operating situations seems to depend on the characteristics of the generator.

10.1.2 Excitation limiter studies

The dynamic field current limiters implemented in the simulation model are found to be a close representation of the excitation limiters in the laboratory model. The limiters, controlled by PI controllers are activated as the field current has exceeded a given limit for a certain amount of time. The field current response in field current limiting operation mode depends on the proportional- and integral gain of the PI controller. Changes of these parameters affect the response significantly. The results found from this master thesis do not give any indication of stability problems caused by adverse interaction with excitation limiters. Further studies are needed to draw any conclusions if, and for which cases, this can provoke instability when the field current limiters are activated.

10.2 Recommendations for further work

Measurements in the laboratory have been an important part of this master thesis. The laboratory model is of great interest for model validation and for stability studies concerning the excitation system. As the excitation system included in the laboratory model is digital and it is simple to change the parameters, this is a great way to get an insight in the effect of the different parameters and operating situations on the system response.

For further use of the laboratory model for small hydro power plant studies it would be interesting to update the motor drive to respond more slowly, to better reflect the characteristics of a hydro power plant. In the description of the renewable energy laboratory [4], it says that there are two different flywheels which can be included to add inertia to the system. This would result in a slower response, and could be a possible way to represent a more realistic model.

To study the effect of the excitation system, including the excitation limiters, the field current and field voltage are of great interest. The field voltage is possible to measure by opening the measurement cabinet and attach the measuring instrument to the output terminals. This gives a signal which has to be scaled and run through a filter to get the appropriate field voltage response. All this signal processing leads to a higher uncertainty. For further studies it would be of great interest to be able to log the field voltage response directly from outside the cabinet, the same way as for the generator voltage and current.

The simulation model does also have potential for improvements. More detailed information about the excitation system and the turbine governing system representation should be found to improve the model. Maybe it should be implemented in another simulation program to reduce the simulation time.

Further studies of the effect of the field current limiters are required to draw any conclusions regarding their effect on the system stability. Simulations with different parameters for the PI controllers, trying to provoke instability should be done. It would also be interesting to perform a linear analysis to study how the eigenvalues moves for different operation situations and different controller parameters, and how they change when the system goes from voltage regulation mode to field current limiting mode.

Bibliography

- [1] I. L. Loen, "Stability problems at Kuråsfossen power plant," NTNU, Trondheim, 2013.
- [2] O. M. Thu, "Stabilitetsproblemere i regionalnettet i Sør-Rogaland," NTNU, Trondheim, 2013.
- [3] O. M. Thu, "Analysis of stability problems at Kuråsfossen Power Plant," NTNU, Trondheim, 2013.
- [4] A. Petterteig, "Distribution Network Laboratory Model," SINTEF Energy Research, Trondheim, 2011.
- [5] K. Uhlen, "PSS/E-modell for spenningsregulator "NOREX2"," SINTEF Energiforskning AS, Trondheim, 2013.
- [6] J. Machowski, J. W. Bialek and J. R. Bumby, Power System Dynamics Stability and Control 2nd edition, Trondheim: John Wiley & Sons Ltd, 2008.
- [7] A. E. Fitzgerald, C. Kingsley Jr. and S. D. Umans, Electric Machinery sixth edition, Trondheim: McGraw-Hill Education (Asia), 2003.
- [8] S. J. Chapman, Electrical Machinery Fundamentals, New York: McGraw-Hill, 2012.
- [9] P. Kundur, Power System Stability and Control, McGraw-Hill Inc, 1994.
- [10] K. Uhlen, Writer, *5- Synchronous generators, dynamic models, Lecture from the course TET4180 Electrical power system stability*. [Performance]. 2013.
- [11] "IEEE Recommended Practice for Excitation system Models for power System Stability Studies," IEEE, New York, 2006.
- [12] T. A. a. B. A. F. J. G. Balchen, Regulerings-teknikk, Trondheim: Institutt for teknisk kybernetikk, NTNU, 2003.
- [13] V. Storvann, "Excitation limiters and their influence on Voltage Stability and Control," NTNU, Trondheim, 2011.
- [14] S. Patterson, "Overexcitation Limiter Modeling for Power System Dynamics," IEEE, Denver, 2005.
- [15] J. D. Hurley, "Underexcitation Limiter Models for Power System Stability Studies," IEEE, Orlando, 2005.
- [16] I. T. F. o. E. Limiters, "Recommended model for overexcitation limiter devices," IEEE, 1995.
- [17] P. Kundur, J. Paserba, V. Ajjarapu, G. Andersson, A. Bose, C. Canizares, N. Hatziargyriou, D. Hill, A. Stankovic, C. Taylor, T. Van Cutsem and V. Vittal, "Definition and Classification of

- Power System Stability," IEEE/IGRE Joint Task Force on Stability Terms and Definitions, 2004.
- [18] K. Uhlen, Writer, *Introduction lecture from course; TET4189 Power System Stability and control*. [Performance]. 2012.
- [19] M. Basler and R. Schaefer, "Understanding Power System Stability," IEEE, 2005.
- [20] K. Uhlen, Writer, *Electromechanical dynamics-small disturbances, Lecture from TET4180 Electric Power Stability*. [Performance]. February 8. 2013.
- [21] K. Uhlen and O. B. Fosso, Writers, *Electromechanical dynamics small disturbances, regulated system. Lecture from course Power System Stability and Control, NTNU..* [Performance]. Dept. of Electrical Power Engineering NTNU, 2012.
- [22] "MathWorks," MathWorks, 1994-2013. [Online]. Available: <http://www.mathworks.se/help/physmod/sps/powersys/ref/synchronousmachine.html>. [Accessed 04 11 2013].
- [23] "Mathworks," [Online]. Available: <https://www.mathworks.com/products/datasheets/pdf/simpowersystems.pdf>. [Accessed 17 09 2013].
- [24] K. Uhlen, Writer, *Power System Components- Part 1, Lecture from course "Power System Stability and Control" at NTNU*. [Performance]. 2012.

Appendix

A1 Linearization constants.....	1
A2 State-space model for the linearized system.....	2
A3 Synchronous generator model, simulation parameters.....	3
A4 Small hydro generation unit, laboratory model.....	4
A5 Distribution network laboratory model ratings.....	5
A6 MATLAB function using voltage and current phasors to calculate active and reactive power.....	6
A7 Function MaxFlatDiffFourCycle, Representing a PMU, calculating phasors.....	8
A8 Voltage, current, active- and reactive power response, laboratory tests 1-16.....	10

A1 Linearization constants

The linearization constants can be derived from the block diagram in Figure 15, and are expressed as follows where V_g and V_s are the generator and infinite grid voltages respectively, X is the external system reactance, and f is the system frequency. Note that the coefficient K_5 is defined as the positive derivative of the generator voltage V_g .

$$K_1 = \frac{\partial P_{E'}}{\partial \delta} = \frac{E_q' V_s}{X_d'} \cos \delta - V_s^2 \frac{X_q - X_d'}{X_q X_d'} \cos 2\delta$$

$$K_2 = \frac{\partial P_{E'}}{\partial E_q'} = \frac{V_s}{X_d'} \sin(\delta)$$

$$K_3 = \frac{X_d'}{X_d}$$

$$K_4 = \frac{V_s * (X_d - X_d')}{X_d'} \sin \delta$$

$$K_5 = \frac{\partial V_g}{\partial \delta'} = -|V_s| * \frac{X_d' * V_q * \sin(\delta)}{(X_d' + X) * |V_g|} + \frac{X_q * V_d * \cos(\delta)}{(X_q + X) * |V_g|}$$

$$K_6 = \frac{\partial V_g}{\partial E_q'} = \frac{X}{(X + X_d')^2} * (E_q' + |V_s| \cos(\delta) * \frac{X_d'}{X} * \frac{1}{|V_g|})$$

$$D = V_s^2 * \left[\frac{(X_d' - X_d'') * X_d' * T_d'' * \sin(\delta)^2}{(X + X_d')^2 * X_d''} + \frac{(X_q' - X_q'') * X_q' * T_q'' * \cos(\delta)^2}{(X + X_q')^2 * X_q''} \right] * 2\pi f$$

The expressions for some of the linearization constants are derived from a simplified generator model. This may lead to small deviations for the model.

The MATLAB model is used to study how these linearization constants relate to the system stability in different operating situations, by studying the corresponding eigenvalues of the state-space model.

A2 State-space model for the linearized system

To calculate the eigenvalues for the system, the state-space model for the general linearized model is found from the following state equations derived from the linearized model. This model was also used for the eigenvalue sensitivity analysis in the specialization project [1].

$$\dot{\delta} = 2\pi f * \Delta\omega$$

$$\Delta\dot{\omega} = \frac{T_m}{2H} - \frac{K_1 * \delta}{2H} - \frac{K_2 * \Delta\psi_{fd}}{2H} - \frac{D * \Delta\omega}{2H}$$

$$\Delta\dot{E}_q = \frac{K_3 * \Delta E_f}{T_3} - \frac{\Delta E_q}{T_3} - \frac{K_3 * K_4 * \delta}{T_3}$$

$$\Delta\dot{E}_f = \frac{K_e * V_{ref}}{T_e} - \frac{\Delta E_f}{T_e} - \frac{\Delta v_1 * K_e}{T_e}$$

$$\Delta\dot{v}_1 = \frac{\Delta E_f * K_6}{T_R} - \frac{\Delta v_1}{T_R} + \frac{\delta * K_5}{T_R}$$

Matrix form:

$$\Delta\dot{\mathbf{x}} = \mathbf{A}\Delta\mathbf{x} + \mathbf{B}\Delta\mathbf{u}$$

$$\begin{bmatrix} \Delta\dot{\delta} \\ \Delta\dot{\omega} \\ \Delta\dot{E}_q \\ \Delta\dot{E}_f \\ \Delta\dot{v}_1 \end{bmatrix} = \begin{bmatrix} 0 & \omega_0 & 0 & 0 & 0 \\ \frac{-K_1}{2H} & \frac{-D}{2H} & \frac{-K_2}{2H} & 0 & 0 \\ \frac{-K_3 * K_4}{T_3} & 0 & \frac{-1}{T_3} & \frac{K_3}{T_3} & 0 \\ 0 & 0 & 0 & \frac{-1}{T_e} & \frac{-K_e}{T_e} \\ \frac{K_5}{T_R} & 0 & \frac{K_6}{T_R} & 0 & \frac{-1}{T_R} \end{bmatrix} * \begin{bmatrix} \Delta\delta \\ \Delta\omega \\ \Delta E_q \\ \Delta E_f \\ \Delta v_1 \end{bmatrix} + \begin{bmatrix} 0 & 0 \\ \frac{1}{2H} & 0 \\ 0 & 0 \\ 0 & \frac{K_e}{T_e} \\ 0 & 0 \end{bmatrix} * \begin{bmatrix} P_m \\ V_{ref} \end{bmatrix}$$

The system eigenvalues are given by the eigenvalues of the A-matrix, and are the values of λ fulfilling the equation

$$\det(A - I\lambda) = 0$$

A3 Synchronous generator model, simulation parameters

Block Parameters: Synchronous Machine pu Standard

Synchronous Machine (mask) (link)

Implements a 3-phase synchronous machine modelled in the dq rotor reference frame.

Stator windings are connected in wye to an internal neutral point.

Configuration Parameters Advanced Load Flow

Nominal power, line-to-line voltage, frequency [Pn(VA) Vn(Vrms) fn(Hz)]:
[10E6 10E3 50]

Reactances [Xd Xd' Xd'' Xq Xq'' Xl] (pu):
[1.04, 0.23, 0.15, 0.57, 0.44, 0.104]

d axis time constants: Short-circuit

q axis time constants: Short-circuit

Time constants [Td' Td'' Tq''] (s):
[1.22 0.055 0.05]

Stator resistance Rs (pu):
0.0021

Inertia coefficient, friction factor, pole pairs [H(s) F(pu) p()]:
[3.2 0 20]

Initial conditions [dw(%) th(deg) ia,ib,ic(pu) pha,phb,phc(deg) Vf(pu)]:
[0 -70.0385 0.550782 0.550782 0.550782 -3.57559 -123.576 116.424 1.25325]

Simulate saturation

OK Cancel Help Apply

Load flow:

Block Parameters: Synchronous Machine pu Standard

Synchronous Machine (mask) (link)

Implements a 3-phase synchronous machine modelled in the dq rotor reference frame.

Stator windings are connected in wye to an internal neutral point.

Configuration Parameters Advanced Load Flow

Generator type PQ

Active power generation P (W)
5.8E6

Reactive power generation Q (var)
0.8E6

A4 Small hydro generation unit, laboratory model

Photo showing the complete small hydro generation unit



A5 Distribution network laboratory model ratings

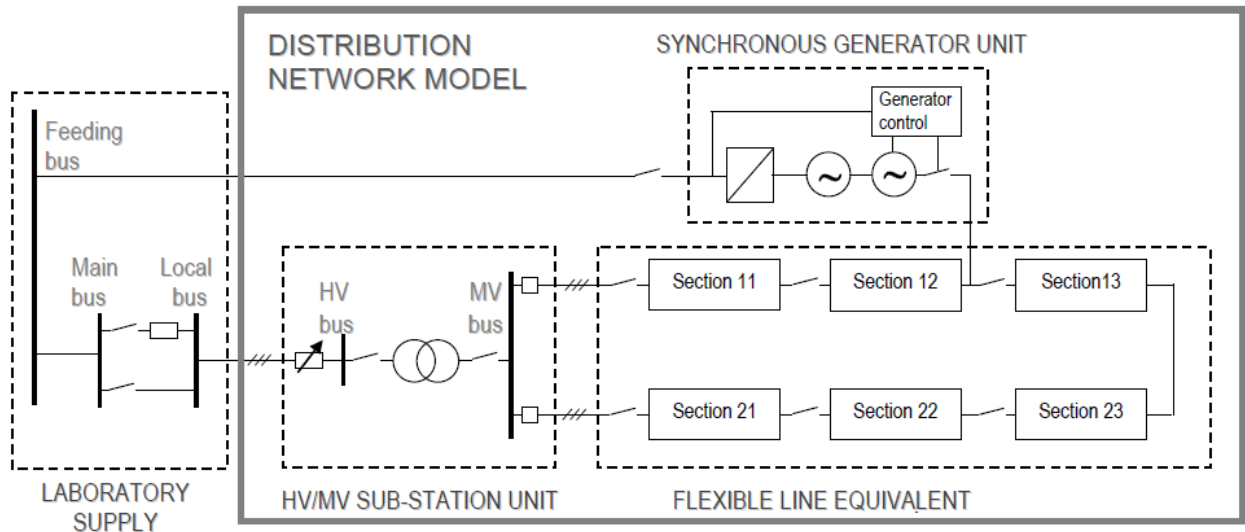


Figure 82: Single line diagram of the distribution network laboratory model and its connections.

Ratings of the laboratory model [9]

Unit:	Laboratory rating:		
	Voltage[V]	Current[A]	Power[kVA]
Laboratory supply (HV)	400 V	225/240 A	165/165 kVA
Laboratory (HV) Short circuit capability		4 kA	3.8 kVA
HV line feeding the HV/MV substation	400 V	63 A	44 kVA
HV/MV transformer (Oversized!)	400/400 V	72 A	50 kVA
Auto transformer in tap changing circuit	230 V	6.2 A (230 V) 42A (32.2 V)	4.2 kVA
Current transformer in tap changing circuit	32.2/230 V	6 A	4.2 kVA
MV line equivalent – Normal load	400 V	32 A	22 kVA
MV line equivalent – Maximum load	400 V	44 A	30 kVA
Short circuit at HV bus w/ X_{HV} 0.4-1.6mH		400 – 1200 A	
Short circuit at MV bus w/ X_{HV} 0.4-1.6mH		300 – 600 A	
Synchronous generator (DG) rating	400 V	25 A	17 kVA
Induction motor (DG turbine)	400 V	27 A	18.5 kVA
Frequency converter	400 V	32 A	22 kVA
Large load transformer (Oversized!)	400/230 V	125 A (230 V)	50 kVA
Small load transformer	400/230 V	6.3 A (230 V)	2.5 kVA

A6 MATLAB function using voltage and current phasors to calculate and plot active and reactive power.

```
function [P, Q]=effekt(maaling)

% Change default axes fonts.
set(0,'DefaultAxesFontName', 'Calibri')
set(0,'DefaultAxesFontSize', 12)

% Change default text fonts.
set(0,'DefaultTextFontname', 'Calibri')
set(0,'DefaultTextFontSize', 12)
u1=maaling(:,2);
i1=maaling(:,3);

fs=25000;

hold
[uph,tn,f]=MaxFlatDiffFourCycle(u1,25000);
hold
[iph,tn,f]=MaxFlatDiffFourCycle(i1,25000);

figure(9)
plot(tn, abs(uph), tn, abs(iph),'LineWidth',2);
legend('U','I')
xlabel('[sec]')
ylabel('[V], [A]')
title('Generator output voltage and current')
grid ON
figure(10)
plot(tn, angle(uph)*180/pi, tn, angle(iph)*180/pi,'LineWidth',2);
legend('U angle','I angle')
xlabel('[sec]')
ylabel('[degrees]')
title('Generator output voltage and current phasor angle')
grid ON

uphase=(1/(sqrt(3)*sqrt(2)))*uph.*exp(-j*(-150*pi/180));
iphase=iph/sqrt(2);
grid ON
figure(7)
plot(tn,angle(uphase)*180/pi,tn,angle(iphase)*180/pi,'LineWidth',2)
legend('U','I')
grid ON
figure(8)
```

```

plot(tn,abs(uptime),tn,abs(iphase),'LineWidth',2)
legend('U','I')
xlabel('[sec]')
ylabel('[V], [A]')
title('Generator output voltage and current')
grid ON

```

```

figure(11)
plot(tn,abs(uptime),'LineWidth',2)
xlabel('[sec]')
ylabel('[V]')
title('Voltage magnitude, U')
legend('U')
grid ON

```

```

figure(12)
plot(tn,abs(iphase),'LineWidth',2)
xlabel('[sec]')
ylabel('[A]')
title('Current magnitude, I')
legend('I')
grid ON

```

```

P=zeros(length(uptime),1);
Q=zeros(length(uptime),1);
for i=1:length(uptime);
    P(i)=3*abs(uptime(i))*abs(iphase(i))*cos(-angle(iphase(i))+angle(uptime(i)));
    Q(i)=3*abs(uptime(i))*abs(iphase(i))*sin(-angle(iphase(i))+angle(uptime(i)));
end

```

```

grid ON
figure(3)
plot(tn,P,'LineWidth',2)
xlabel('[sec]')
ylabel('[W]')
title('Generator output active power, P')
grid ON
legend('P')

```

```

figure(4)
plot(tn,Q,'LineWidth',2)
xlabel('[sec]')
ylabel('[VAR]')
title('Generator output reactive power, Q')
grid ON
legend('Q')
end

```

A7 Function MaxFlatDiffFourCycle, Representing a PMU, calculating phasors

Made by Dinh Thuc Duong

```

function [ph,tn,f]=MaxFlatDiffFourCycle(x,fs);
% Input x time series at sample frequency fs Hz
% Output phasor ph on time Tn
%SET PARAMETERS-----
%fs = 2400;           % sampling frequency
Ts = 1/fs;           % sampling cycle
f1 = 50;             % fundamental frequency
T1 = 1/f1;
N1 = fs/f1;         % data window = 1 cycle
N = 4*N1+1;
Nh = (N-1)/2;
w1 = 2*pi/N1;
kappa = 3;         % set Taylor order
Tend=length(abs(x))*Ts;
%-----

%MAIN PROGRAM BODY-----
b=[];
temp=[];
p=[];
deltaf=[];

%-----left matrix
for k=0:kappa
    for l=1:(Nh+1)
        temp(l) = ((-(Nh+1-l))^(kappa-k))*exp((Nh+1-l)*w1*1i);
        if l~=(N-Nh)
            temp(2*Nh+2-l) = (((Nh+1-l))^(kappa-k))*exp(-(Nh+1-l)*w1*1i);
        end
    end
    b=[b,temp.'];    % forming one column, from the left to the right
    temp=[];
end

%-----right matrix
for k=0:kappa
    for l=1:(Nh+1)
        temp(l) = ((-(Nh+1-l))^k)*exp(-(Nh+1-l)*w1*1i);
        if l~=(N-Nh)
            temp(2*Nh+2-l) = (((Nh+1-l))^k)*exp((Nh+1-l)*w1*1i);
        end
    end
end

```

```

b=[b,temp.'];
temp=[];

end

W = diag(kaiser(N,8));           % Kaiser window for weighting
B = ((b')*(W')*W*b)/((b')*(W')*W);

%-----phasor estimation-----

m=1;
for k=2*N1+1:N1:length(x)-3*N1

    p = 2*B*(x(k-Nh:k+Nh)');     % implementation of equation 10
    p = p(kappa+2:length(p));   % filter conjugated elements

    p(2) = p(2)*N1*f1;          % calculate phasor's derivatives
    p(3) = p(3)*2*(N1*f1)^2;

    fdelta = imag(p(2)/p(1))/2/pi; % freq deviation
    fdev = imag(p(3)/p(1) - (p(2)/p(1))^2)/2/pi; % freq's derivative

    phasor(m) = p(1);           % storing estimated phasor
    fest(m) = f1 + fdelta;      % freq estimation
    t(m) = (m+1)*T1;
    m = m+1;                    % just an index
end

% END OF MAIN PROGRAM BODY-----

ph=phasor;
tn=t;
f=fest;
disp(errmax);
grid ON
figure(1);
plot(tn,angle(phasor)*180/pi);
grid ON
figure(2);
plot(tn,abs(phasor));

```

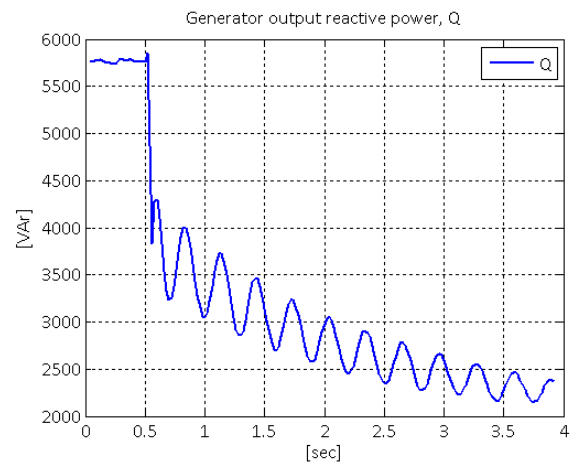
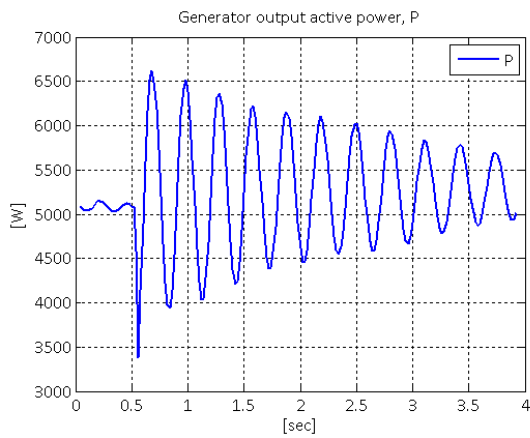
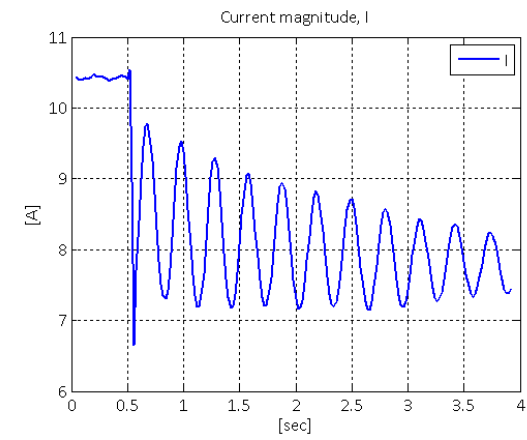
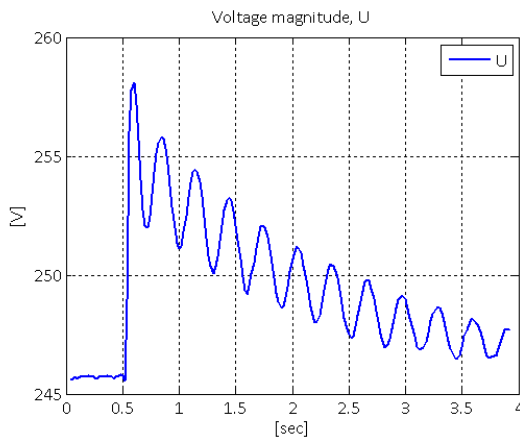
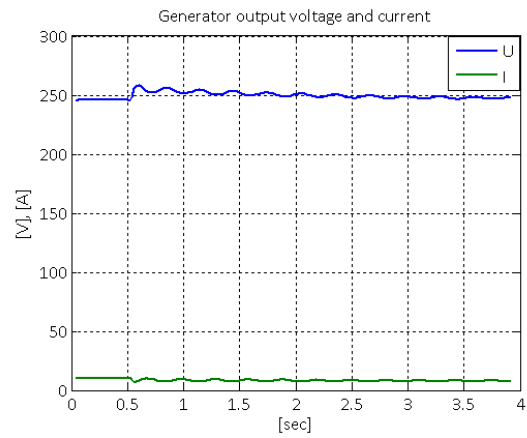
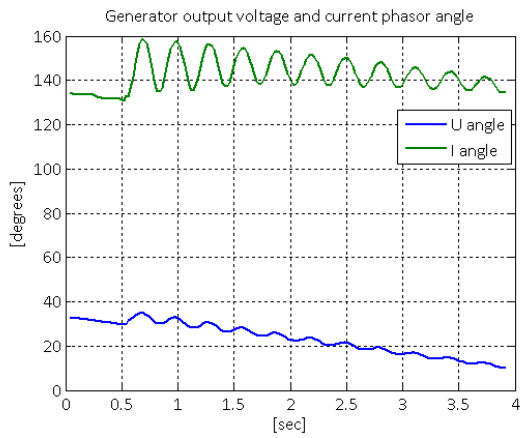
A8 Voltage, current, active- and reactive power response, laboratory tests 1-16.

Only a few of the measurements done in the laboratory are studied in this report. Table A8.1 shows a complete list of the different test scenarios. All tests are done with the generator operating at the torque limit if nothing else is commented. This is to prevent exaggerated damping of the oscillations:

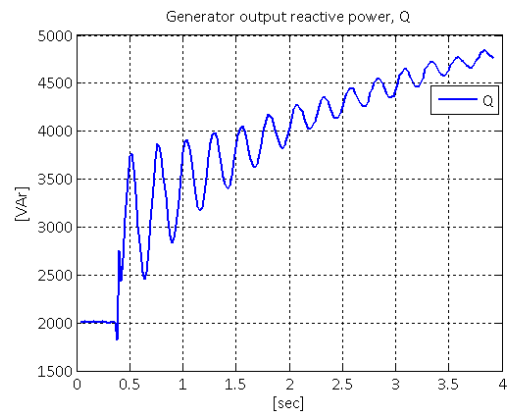
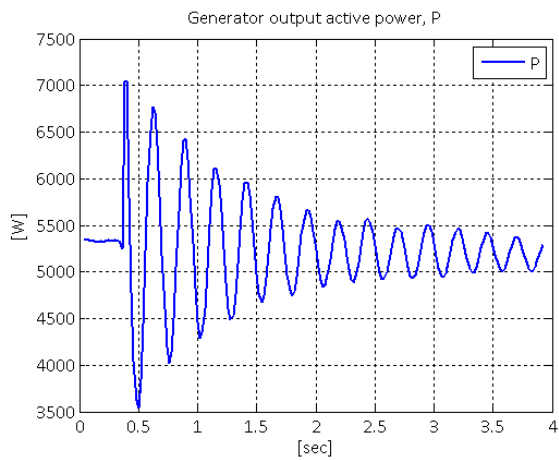
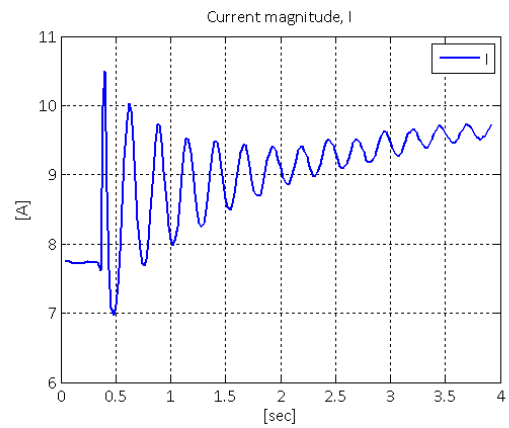
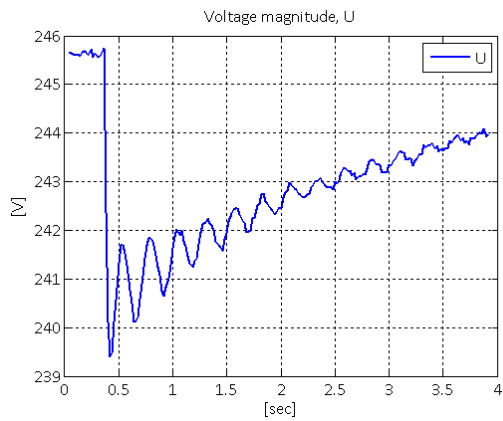
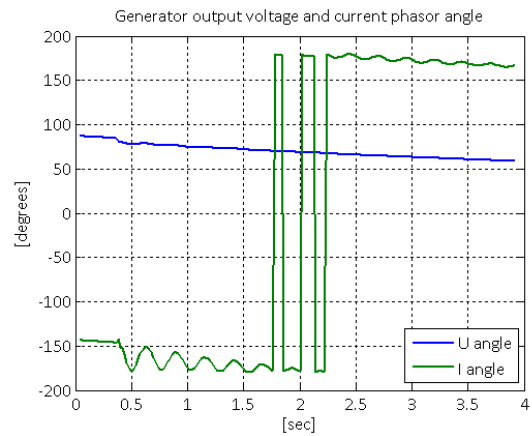
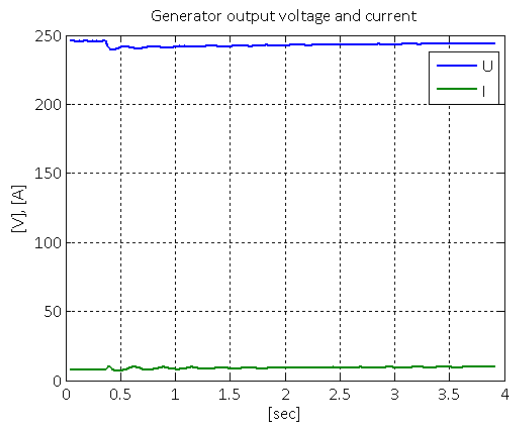
Table A8.1: Laboratory test scenarios

Test nr	Disturbance	P [kW]	Q [kVAr]	AVR gain Kp	V[V] Measured	Vf[V] Measured	Remarks
1	Low-high Impedance	5	5	55	429	15	
2	High-low Impedance	5	2	55	430	12	
3	Low-high Impedance	5	-5	55	388	10	
4	High-low Impedance	5	-2	55	388	7	
5	Low-high impedance	0	0	55	408	7	
6	Low-high impedance	5	0	55	412	10	
7	Low-high impedance	10	0	55	413	13	
8	Low-high impedance	5	5	110	430	16	Standing oscillations, Clearly less stable
9	Low-high impedance	5	-5	110	389	4	More stable than 8
10	Low-high impedance	0	0	110	406	6	
11	Low-high impedance	5	0	110	409	10	Long lasting oscillations
12	Low-high impedance	10	0	110	412	14	Oscillates clearly. Current amplitude is determining.
13	Short-circuit	5	0	110	412	10	System Shut-down
14	Short-circuit	10	0	100	415	14	Not at torque limit. Low system impedance → System shut-down
15	Short-circuit	10	0	100	-	-	Not at torque limit. High system Impedance → Ok
16	Short-circuit	10	0	100	-	-	At torque limit. High impedance → Oscillations, frequency oscillated clearly, loosing synchronism.

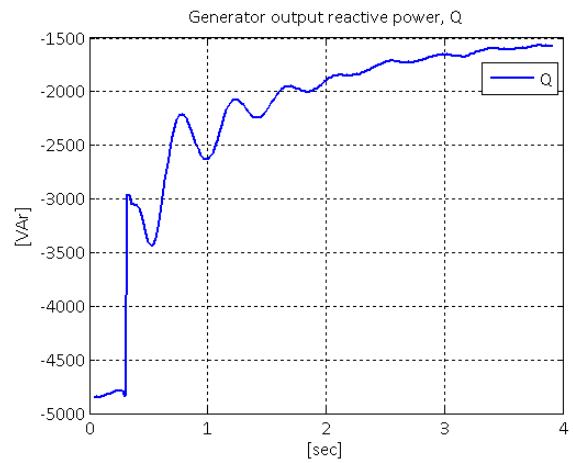
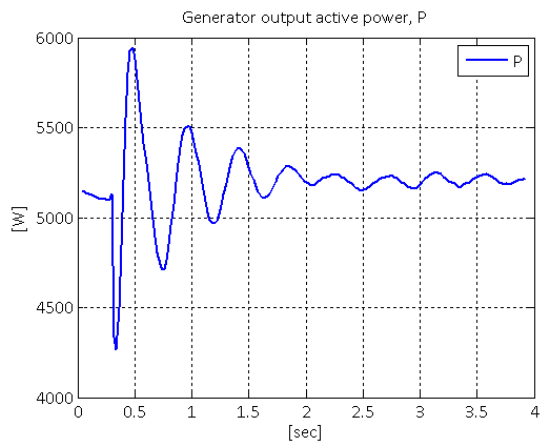
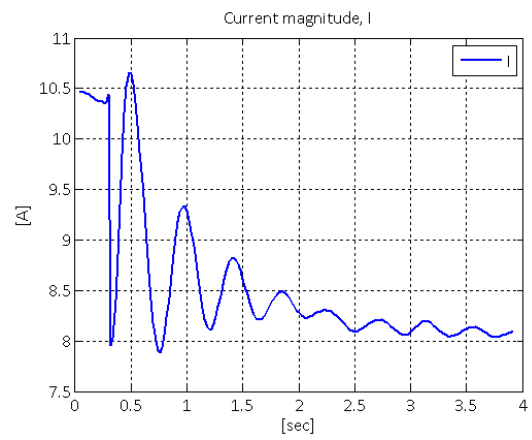
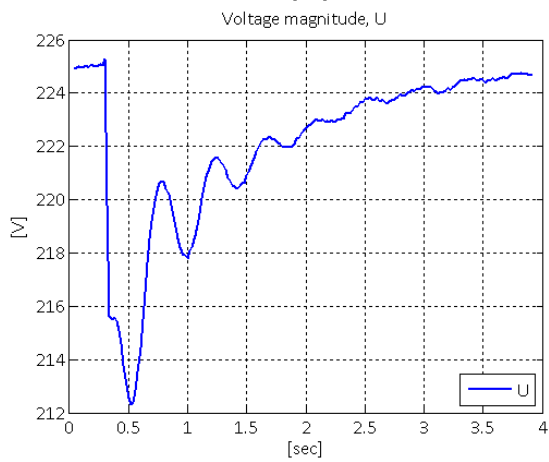
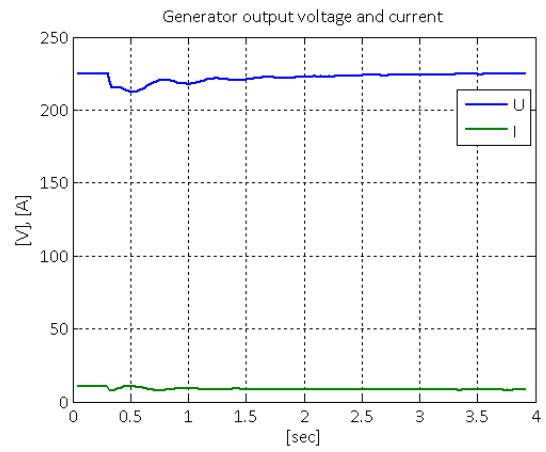
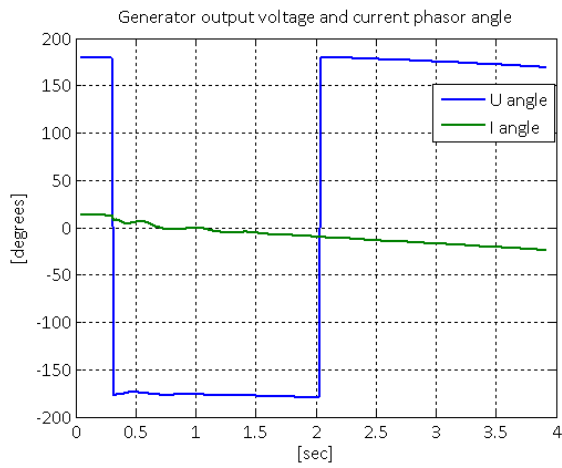
A8.1 Test scenario 1



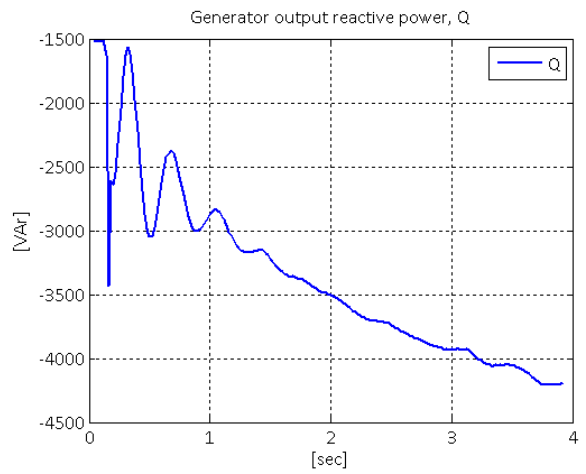
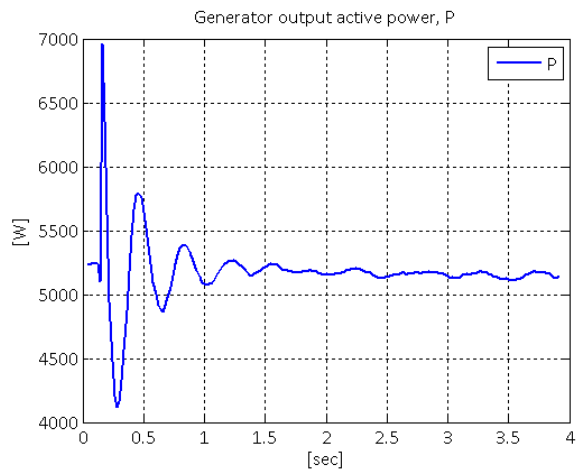
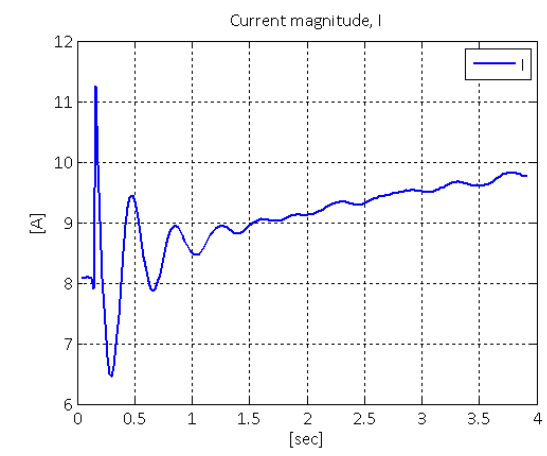
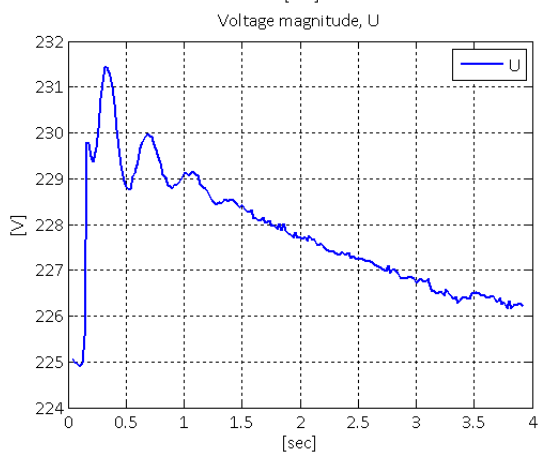
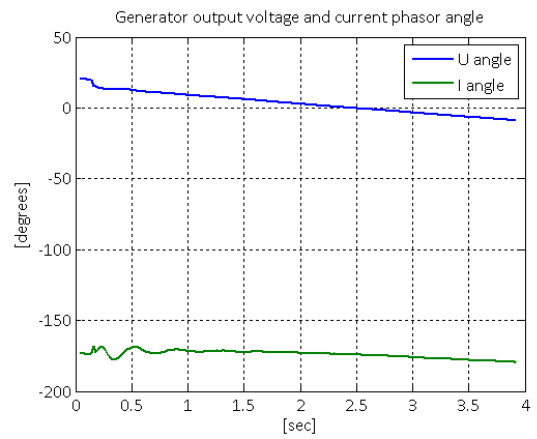
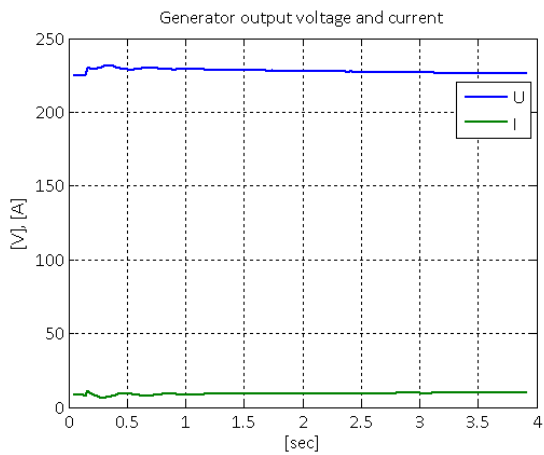
A8.2 Test scenario 2



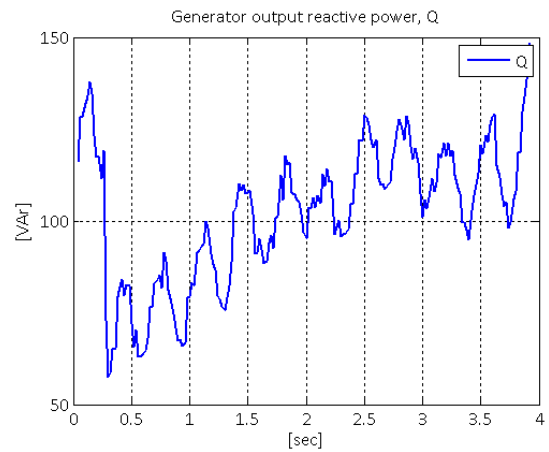
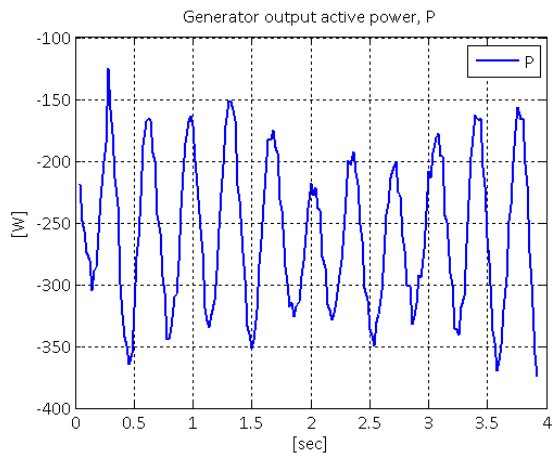
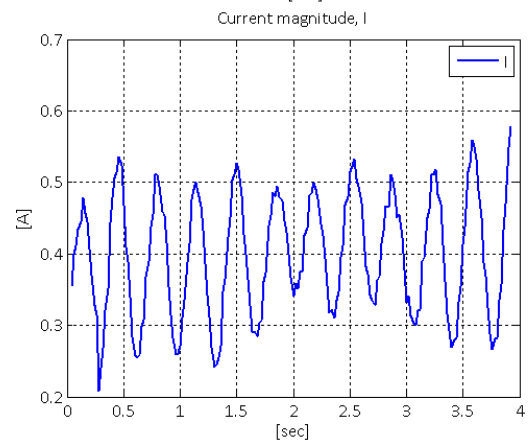
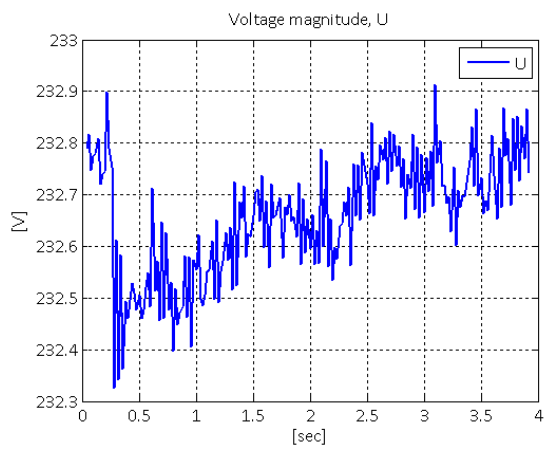
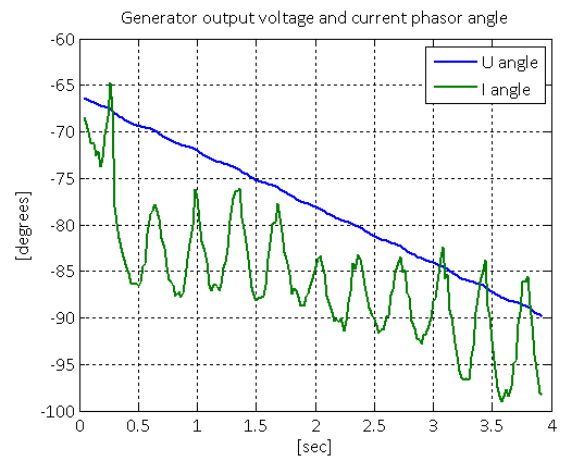
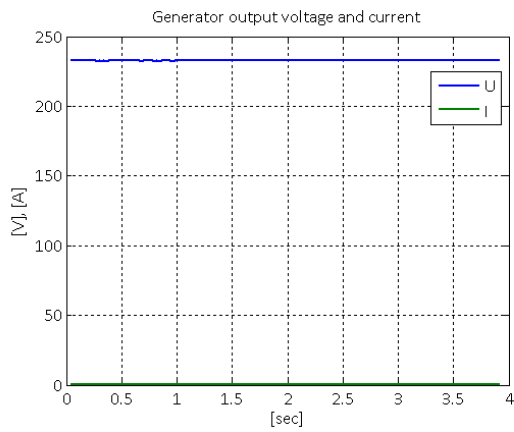
A8.3 Test scenario 3



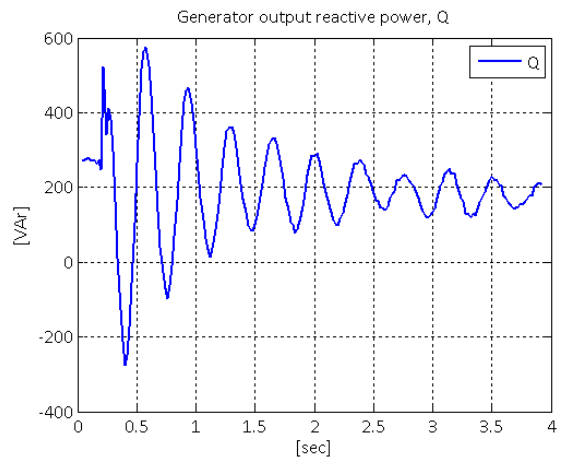
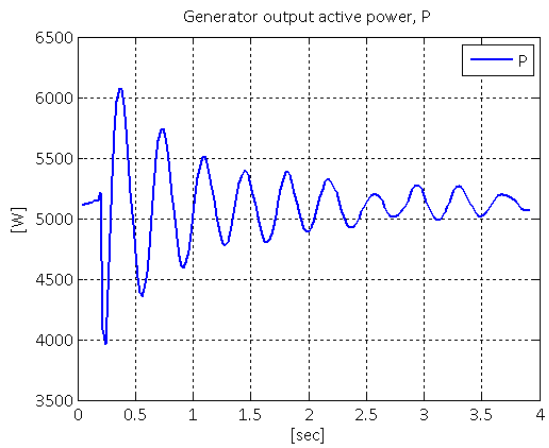
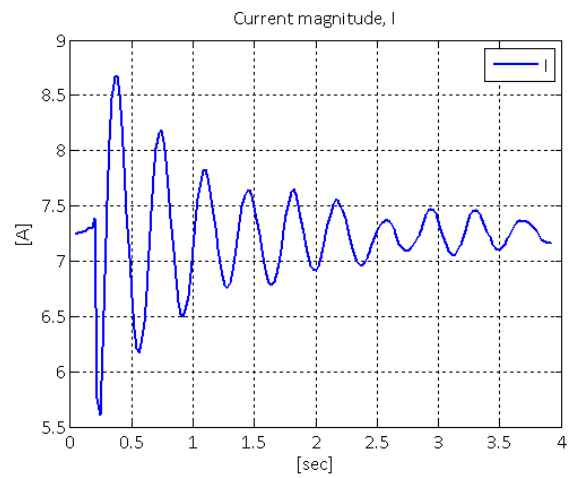
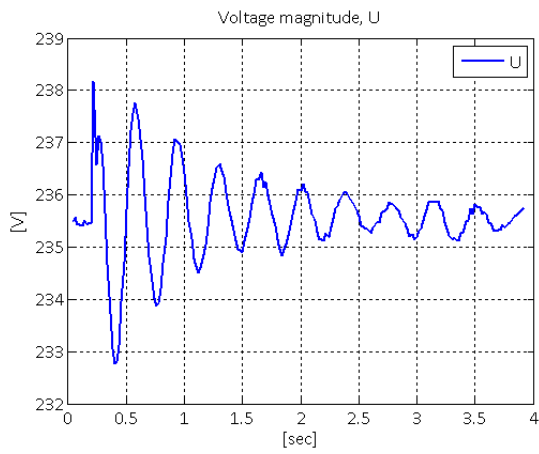
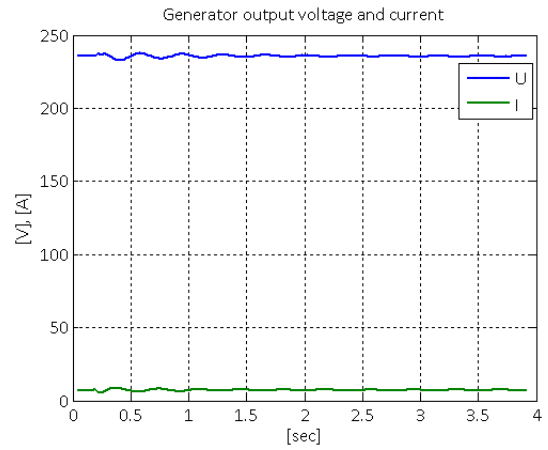
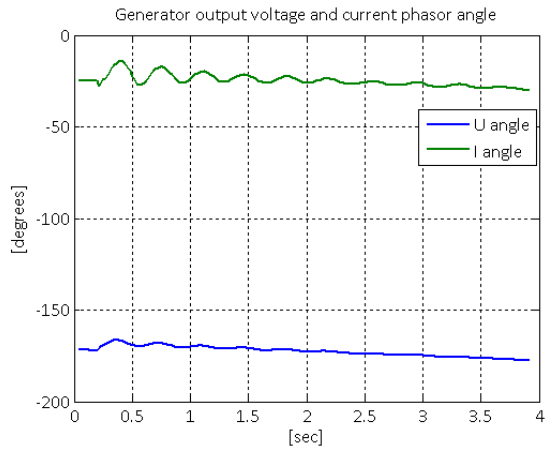
A8.4 Test Scenario 4



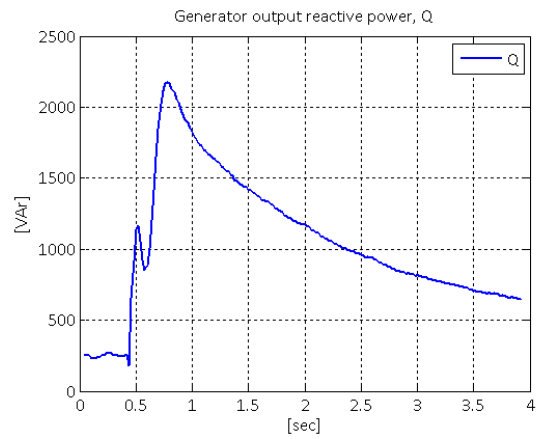
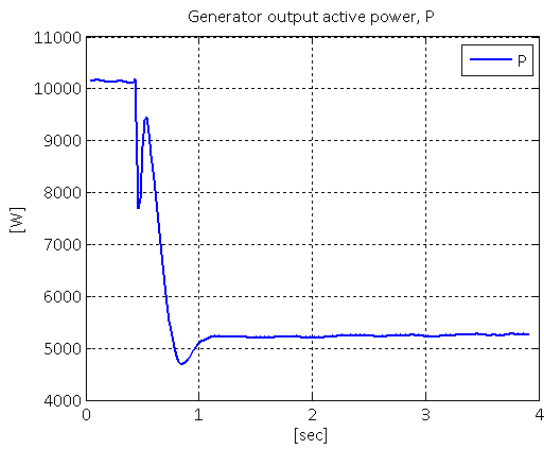
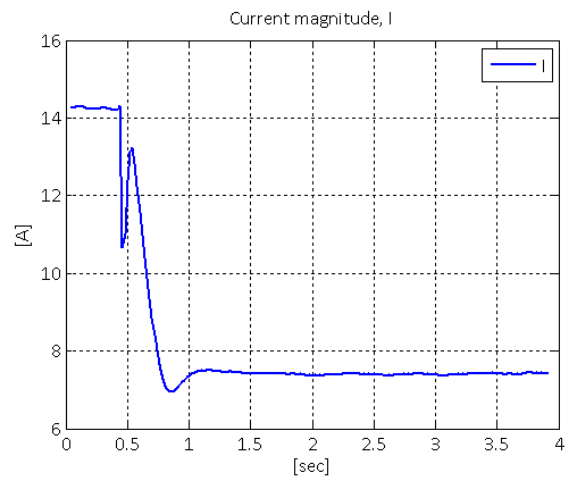
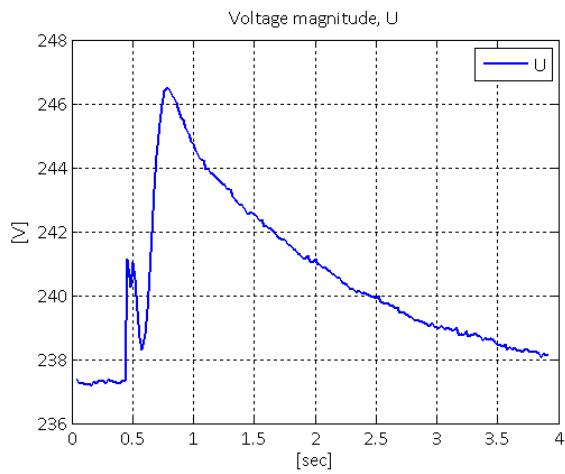
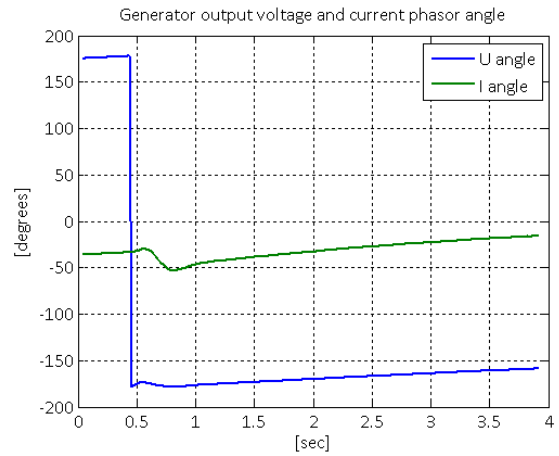
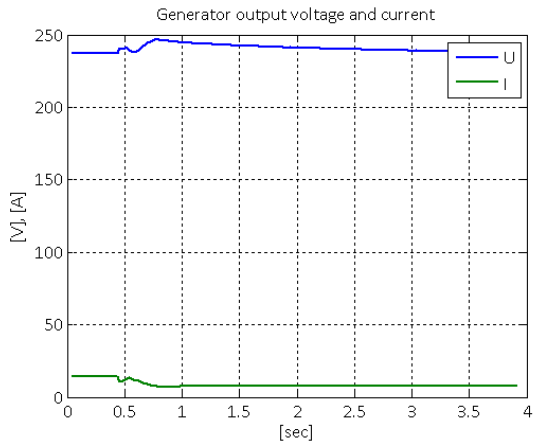
A8.5 Test scenario 5



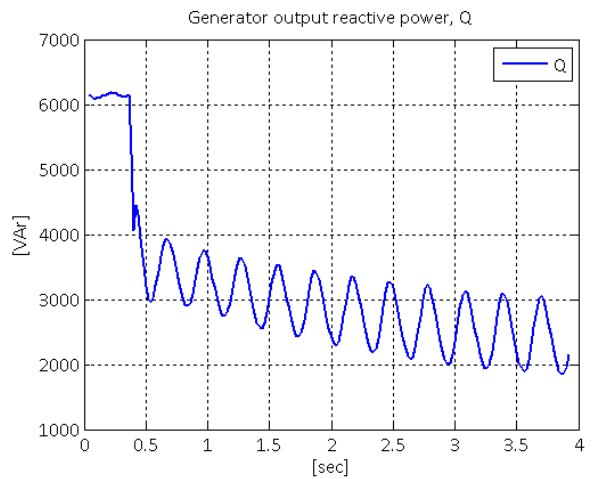
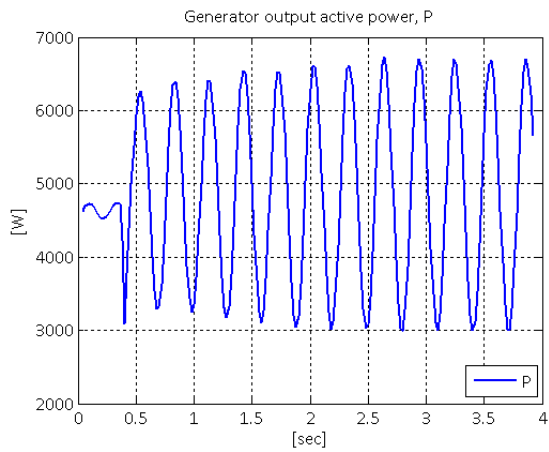
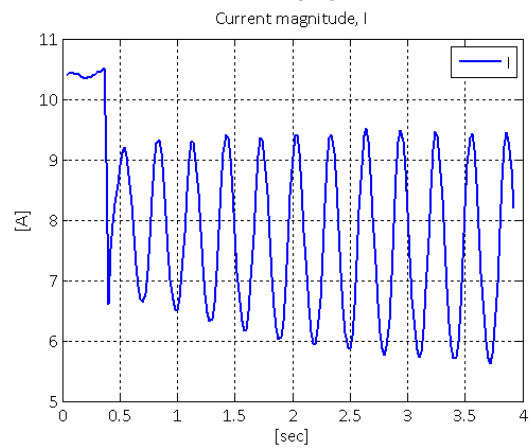
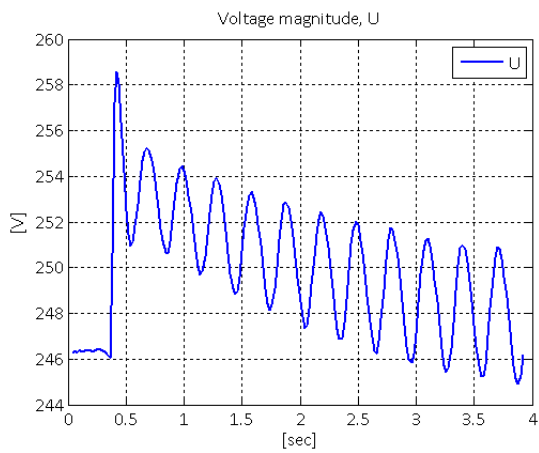
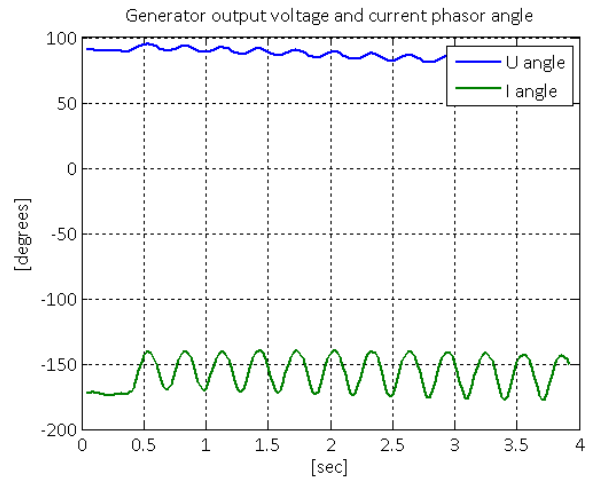
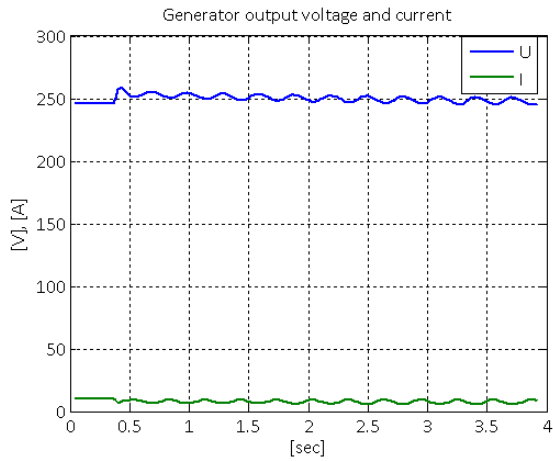
A8.6 Test scenario 6



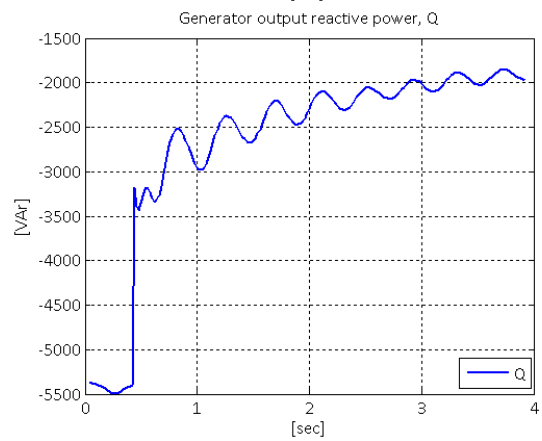
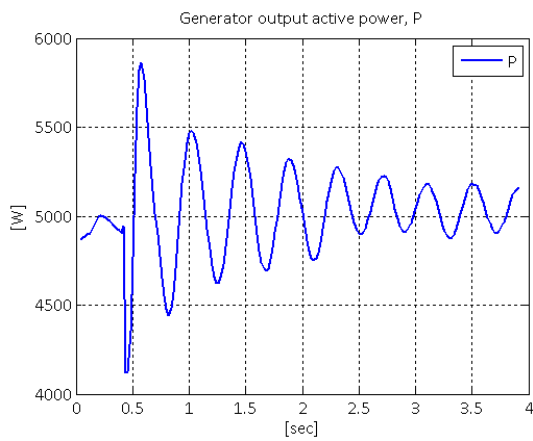
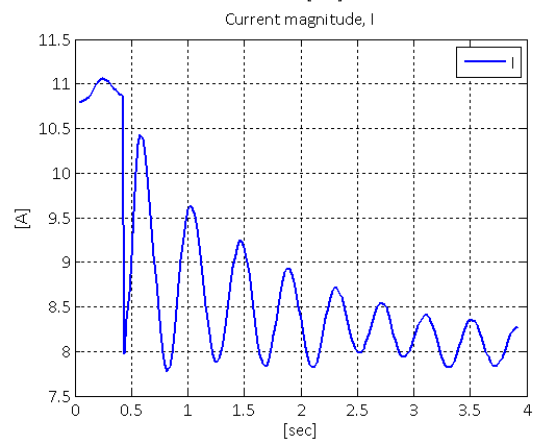
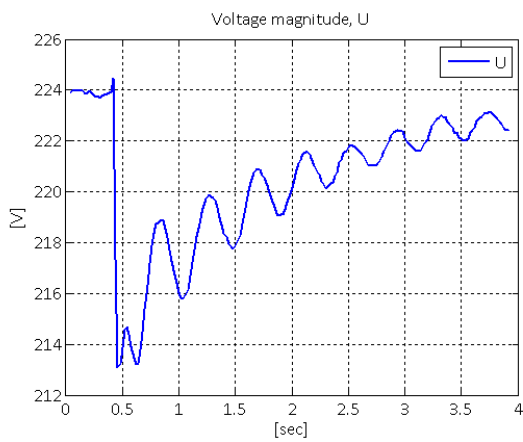
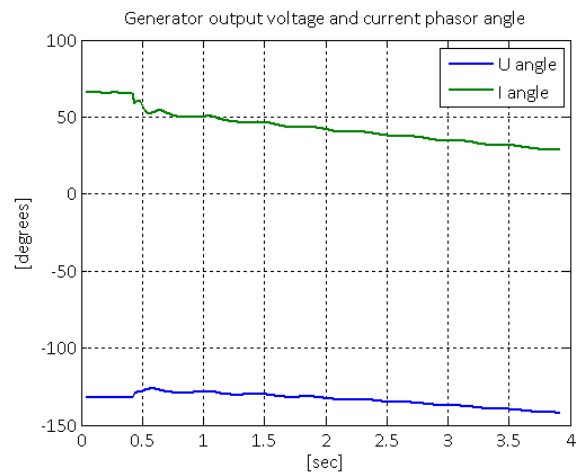
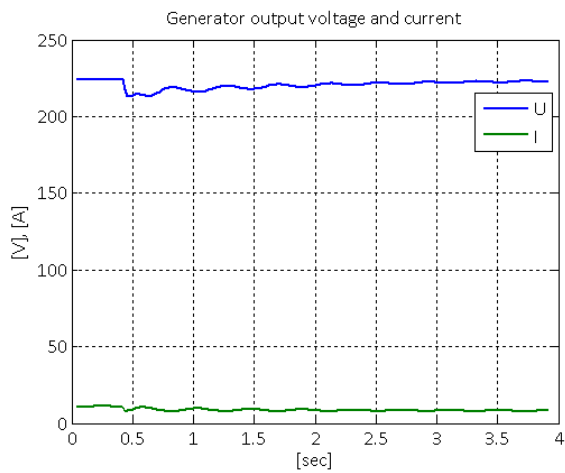
A8.7 Test scenario 7



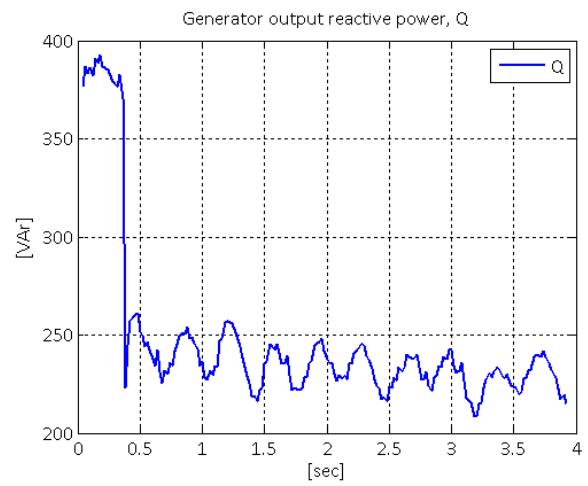
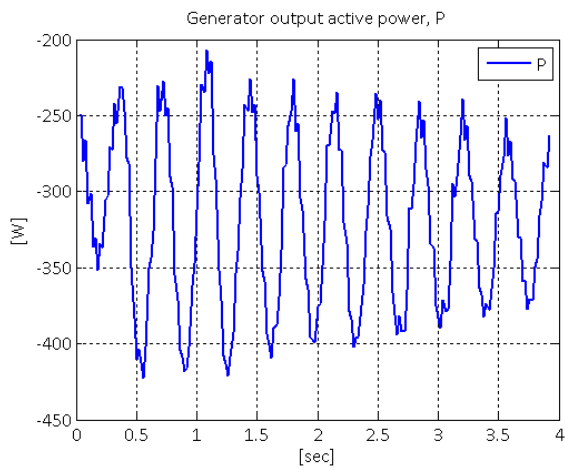
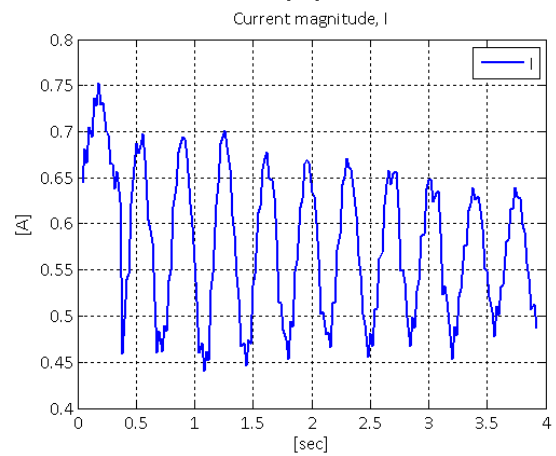
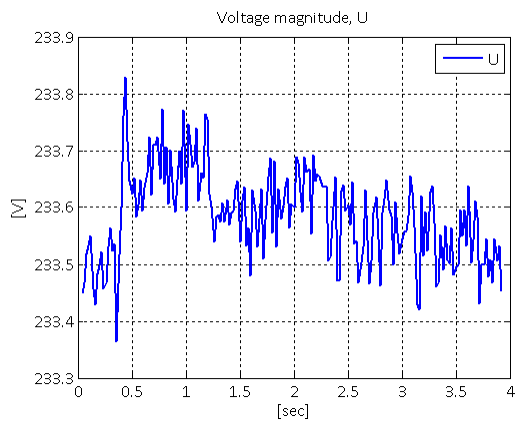
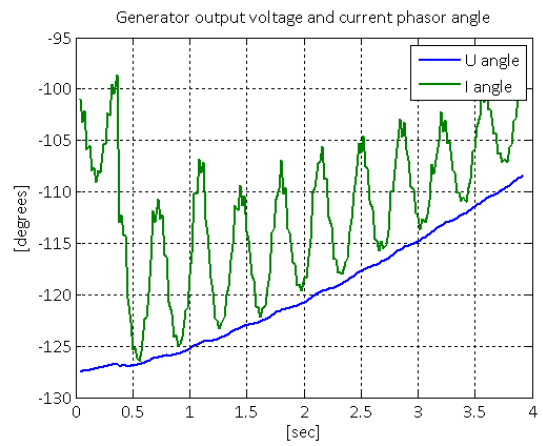
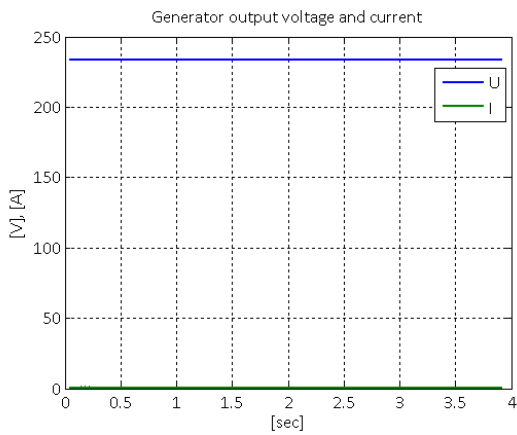
A.8.8 Test scenario 8



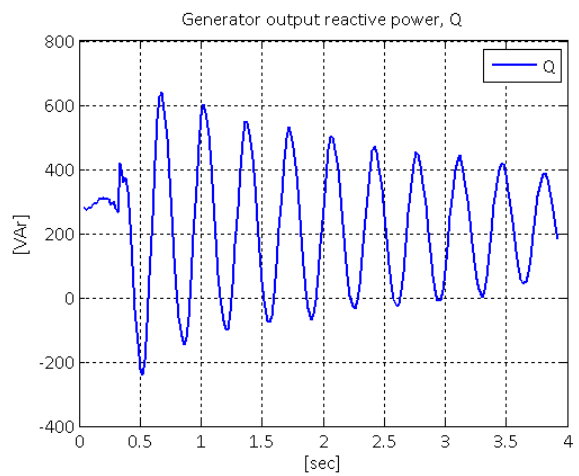
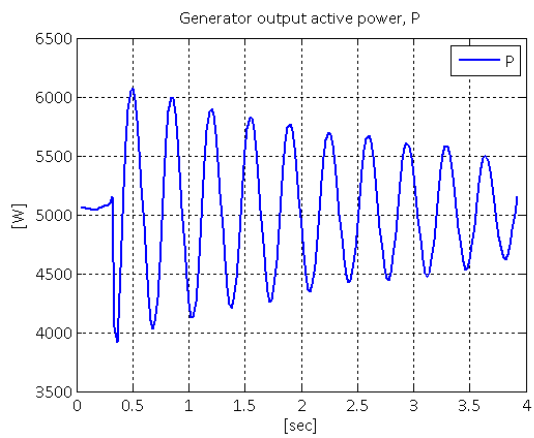
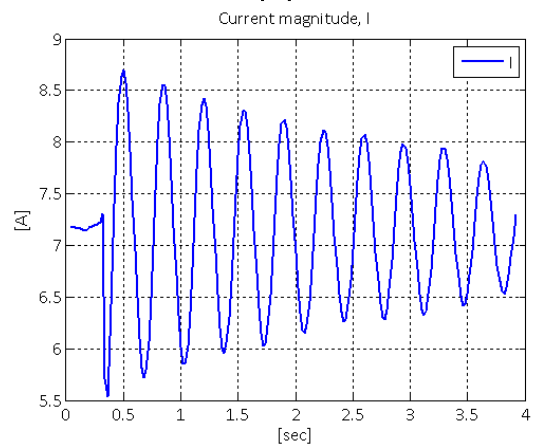
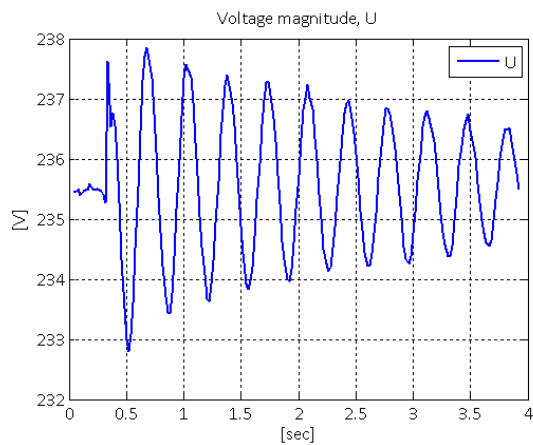
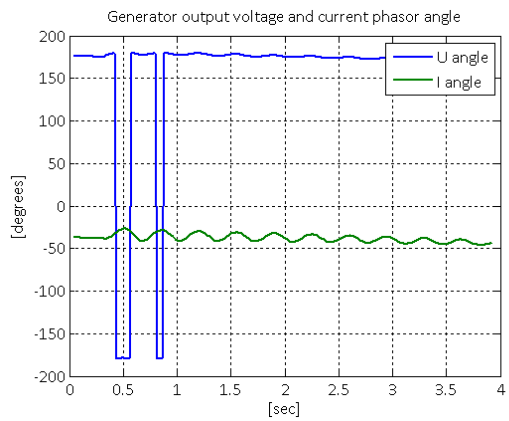
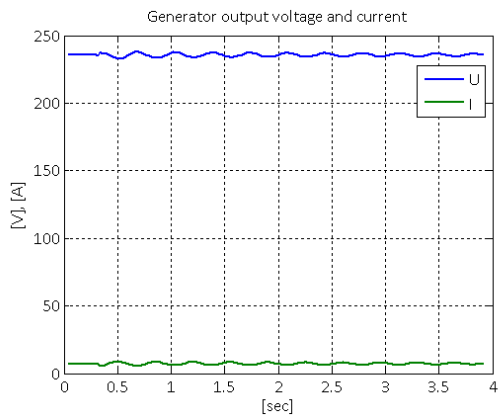
A8.9 Test scenario 9



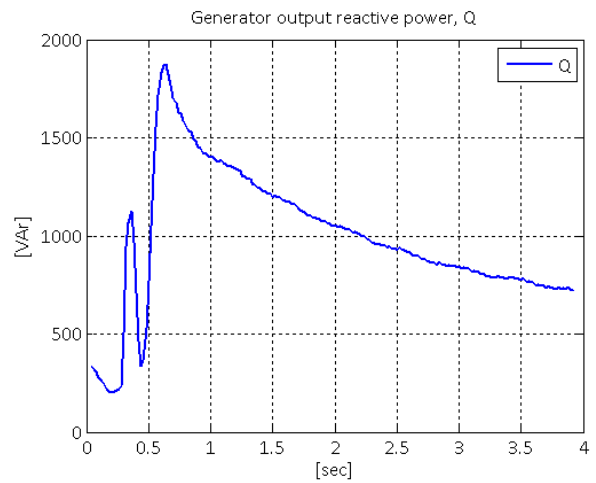
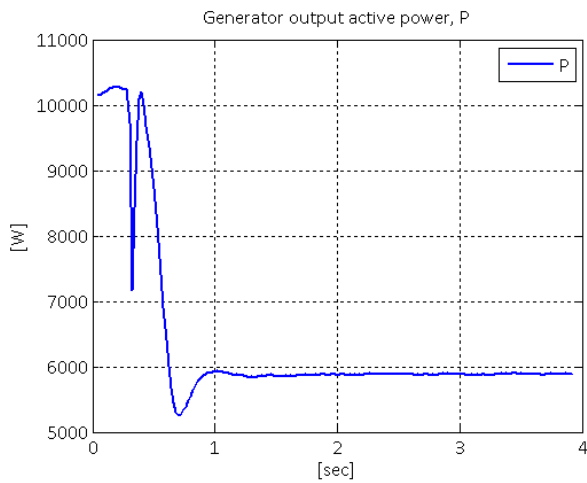
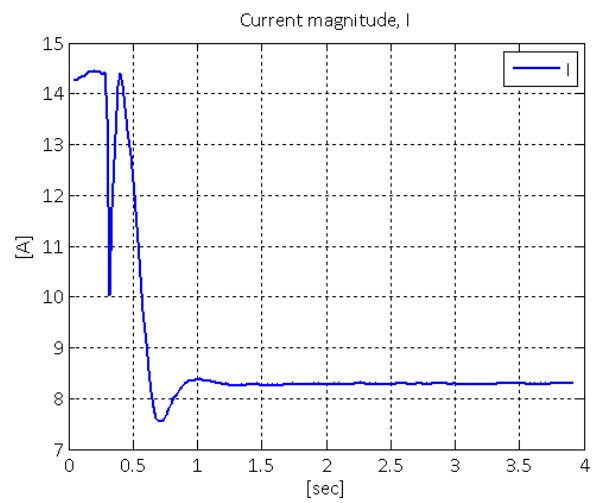
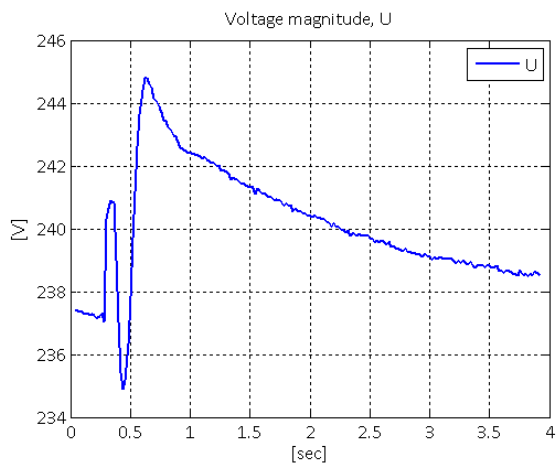
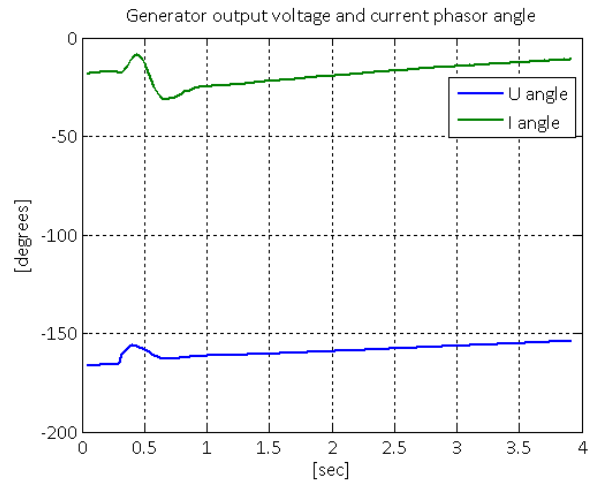
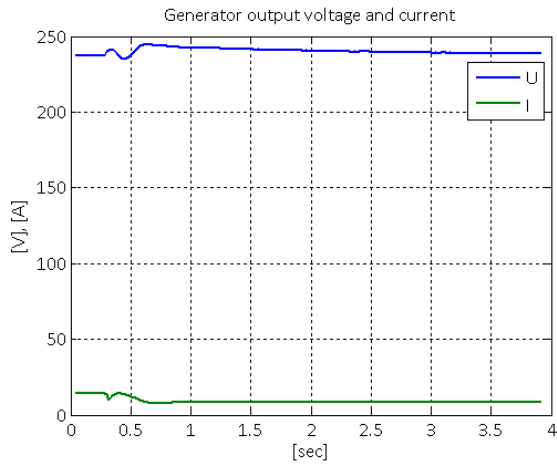
A8.10 Test scenario 10



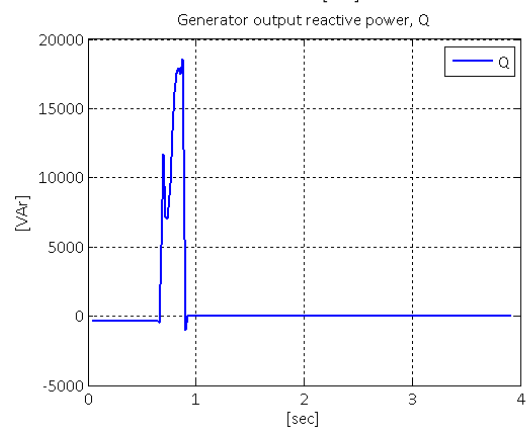
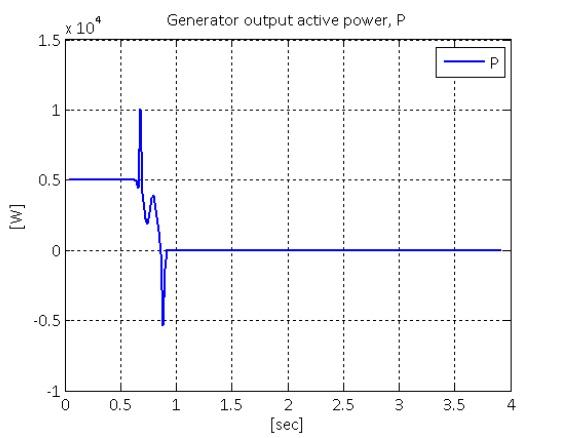
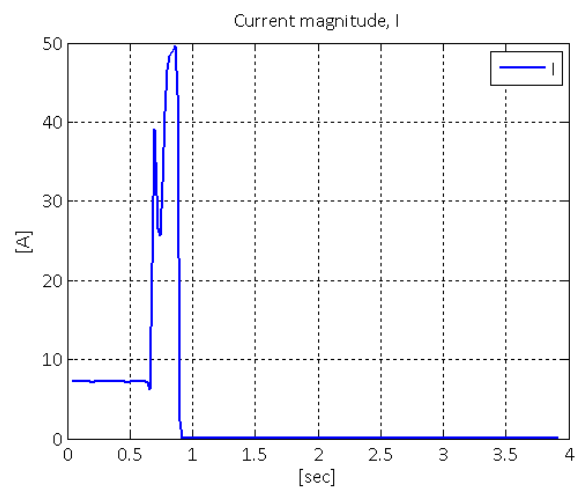
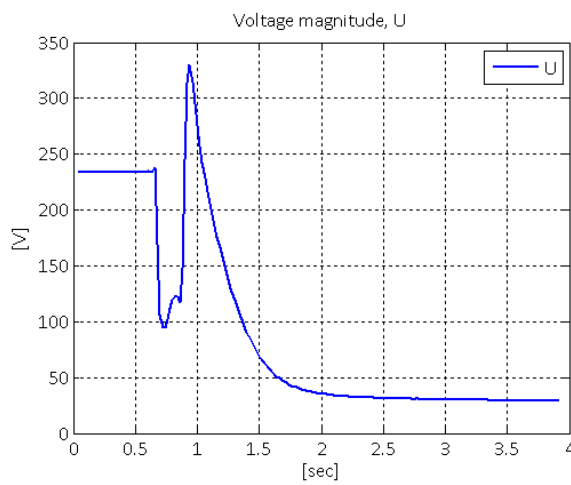
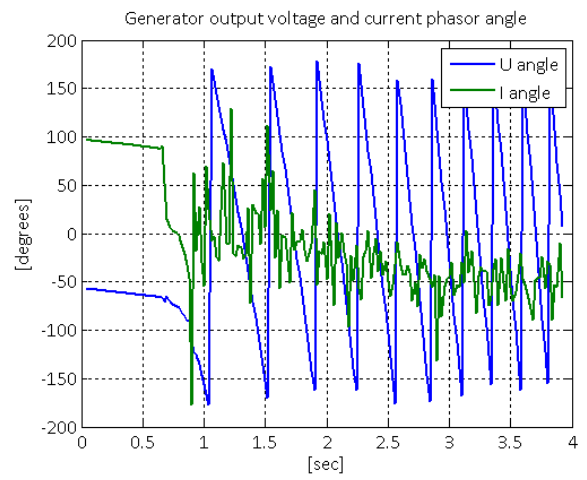
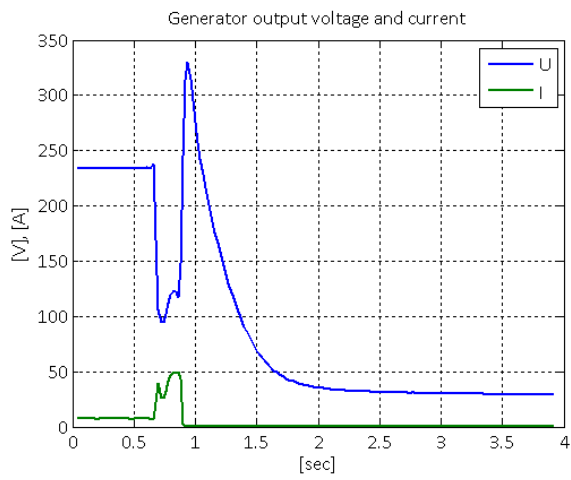
A8.11 Test scenario 11



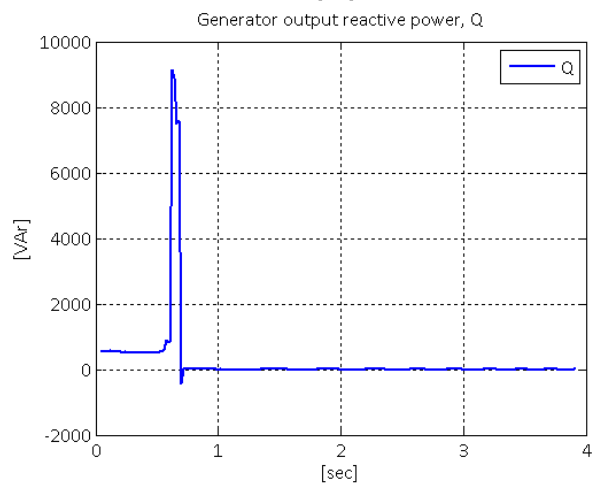
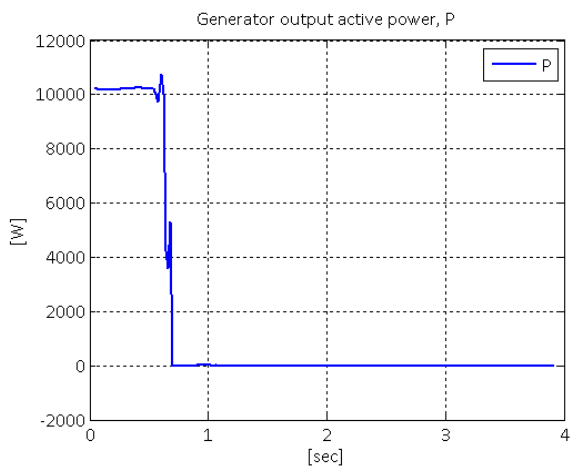
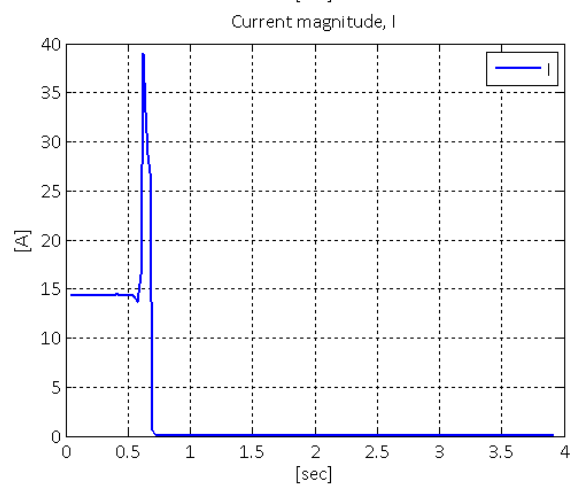
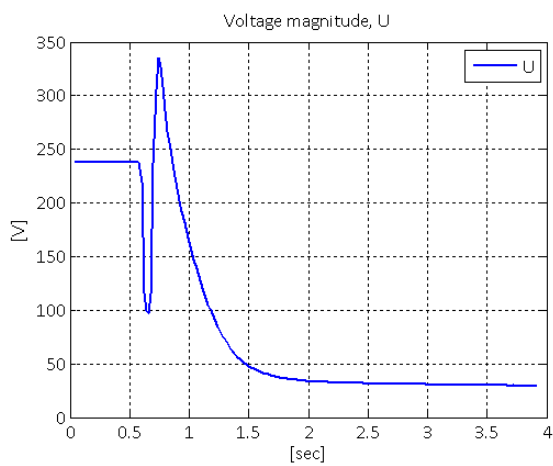
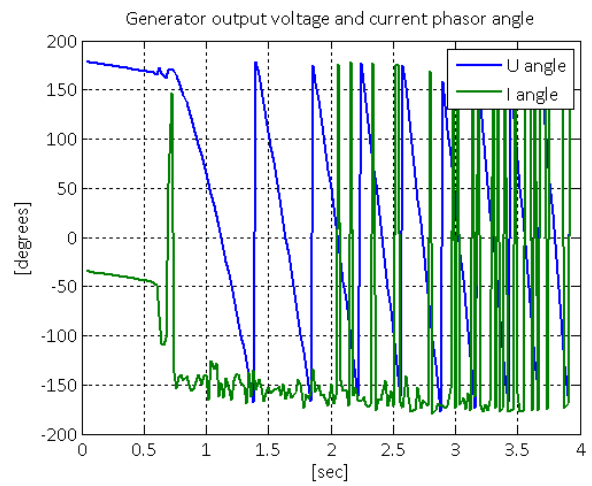
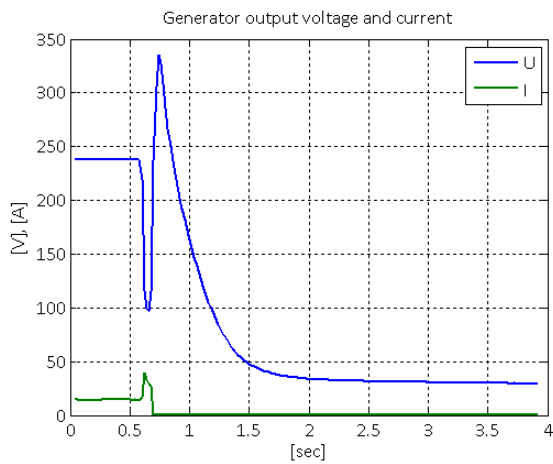
A8.12 Test scenario 12



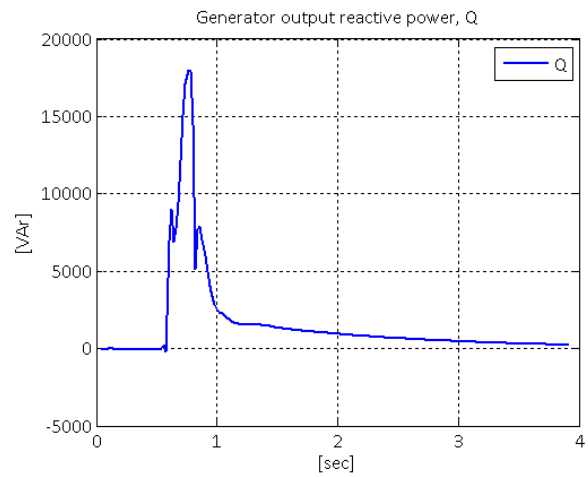
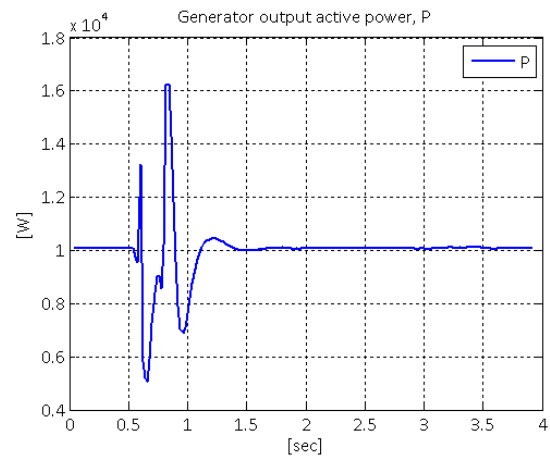
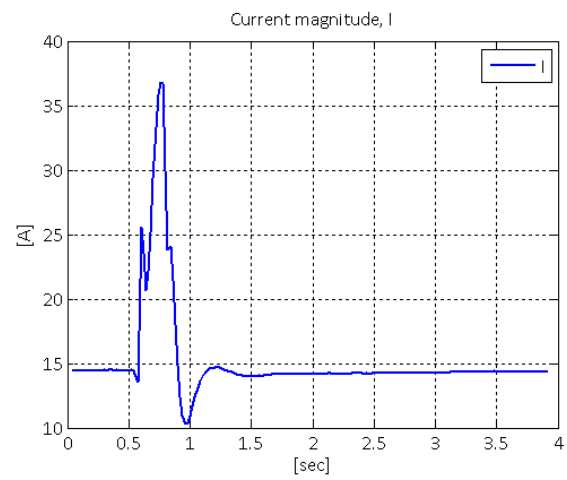
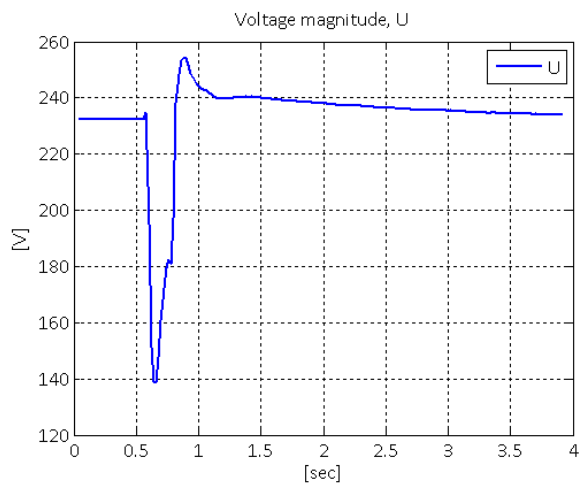
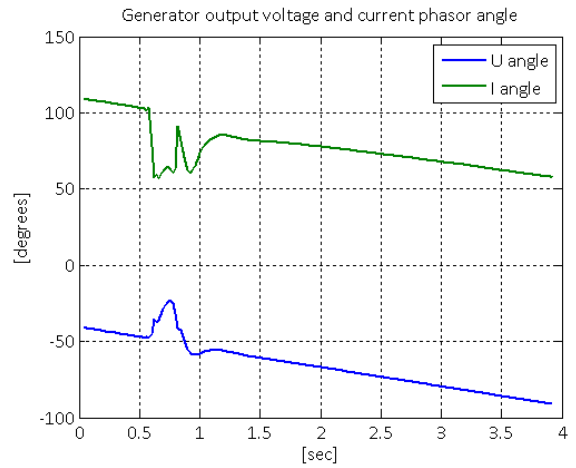
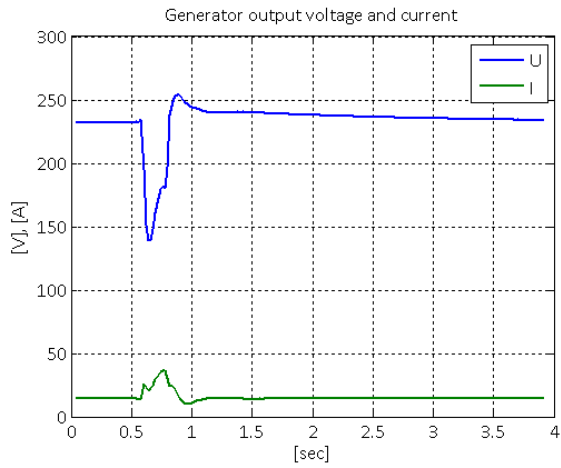
A8.13 Test scenario 13



A8.14 Test scenario 14



A8.15 Test scenario 15



A8.16 Test scenario 16

